Investigation of the applicability of polyHIPE materials in liquid chromatography

by

Sidratul Choudhury B.Sc. (Hons)

Thesis Submitted for the Degree of Doctor of Philosophy

School of Chemical Sciences

Supervisors:

Dr. Blánaid White

Dr. Damian Connolly (Waterford Institute of Technology)

Dublin City University **January 2016**

Declaration:

I hereby certify that this material, which I now submit for assessment on the programme of study leading to the award of PhD is entirely my own work, that I have exercised reasonable care to ensure that the work is original, and does not to the best of my knowledge breach any law of copyright, and has not been taken from the work of others save and to the extent that such work has been cited and acknowledged within the text of my work.

Signed: _____

(Candidate) ID No.: 58562938

Date: _____

Table of Contents

List of Abbreviations

A/O	Aqueous phase in organic phase
AAm	Acrylamide
ACN	Acetonitrile
AFM	Atomic force microscopy
AMT	Additive manufacturing technology
APS	Ammonium persulfate
A_s	Peak asymmetry
ATAL	2-aminothiazole
AuNPs	Gold nanoparticles
BDS	Beads
BET	Brauner Emmett Teller
CE	Capillary electrophoresis
CEC	Capillary electrochromatography
CIM	Convective Interaction Media
CMC	Critical micelle concentration
DAA	D-amino acid
DEA	Diethylamine
d_{hyd}	Hydrodynamic radius
DI	Deionised

D-tryp	D-tryptophan
DVB	Divinylbenzene
EDGMA	Ethylene glycol dimethacrylate
EHA	Ethylhexyl acrylate
EOF	Electroosmotic Flow
EtOH	Ethanol
FESEM	Field Emission Scanning Electron Microscope
FTIR	Fourier transform infrared spectroscopy
GMA	Glycidyl methacrylate
GO	Graphene oxide
GONPs	Graphene oxide nanoparticles
H or HETP	Height equivalent of theoretical plates
HEA	Hydroxy ethyl acrylate
HEMA	Hydroxyethyl methacrylate
HILIC	Hydrophilic interaction liquid chromatography
HIPE	High internal phase emulsions
HLB	Hydrophilic-lipophilic balance
HPAC	High performance affinity chromatography
HPLC	High performance liquid chromatography
HSA	Human serum albumin

ID	Inner diameter
IDA	Isodecylacrylate
IL-18	Interleukin-18
k	Permeability
k’	Retention/Capacity factor
K_d	Distribution coefficient
KPS	Potassium persulfate
L	Length of column
LC	Liquid chromatography
LLE	Liquid-liquid extraction
MeOH	Methanol
META	2-(Methacryloyloxy) ethyl trimethylammonium chloride
MIPs	Molecular imprinted polymers
MPa	Mega Pascal
N	Number of theoretical plates
n_c	Number of carbons
NPs	Nanoparticles
O/A	Organic phase in aqueous phase
OD	Outer diameter
OTCEC	Open tubular capillary electrochromatography

P	poly
PAHs	Polyaromatic hydrocarbons
PDI	Polydispersity index
PEEK	Poly ether ether ketone
PIAL	2-phenylimidazole
PolyHIPEs	polymeric high internal phase emulsions
PS	Polystyrene
PVA	poly vinyl alcohol
RP-HPLC	Reverse phase high performance liquid chromatography
R_s	Resolution
RSD	Relative standard deviation
SDS	Sodium dodecyl sulfate
SEC	Size-exclusion chromatography
SEM	Scanning electron microscopy
SMC	Short monolithic columns
SPE	Solid phase extraction
Sty	Styrene
TGA	Thermal gravimetric analysis
t_r	Retention time
UPR	Unsaturated polymer resin

UV	Ultraviolet
VBC	4-vinylbenzene chloride
VE	Vinyl ester
α	Selectivity

List of Publications

1. **"Supermacroporous polyHIPE and cryogel monolithic materials as stationary phases in separation science: A review"** Sidratul Choudhury, Damian Connolly and Blánaid White, *Analytical Methods, 2015, 7, 6967. Front cover of themed issue: "Emerging Investigators".*
2. **"Polystyrene-co-divinylbenzene polyHIPE monoliths in 1.0 mm column formats for the isocratic separation of alkylbenzenes."** Sidratul Choudhury, Damian Connolly and Blánaid White. Submitted in *Materials, 2015*.
3. **"Enhancing physical properties of low surface area PS-*co*-DVB polyHIPE materials with graphene oxide nanoparticles in HPLC applications"** Sidratul Choudhury, Damian Connolly and Blánaid White. To be submitted in *Applied Materials and Interfaces, 2016*.
4. **"Fabrication of novel polyHIPE coated columns for potential applications within CEC"** Sidratul Choudhury, Damian Connolly and Blánaid White. To be submitted in *Journal of Applied Polymer Science, 2016*.

List of Poster Presentations

1. **"Investigation of Graphene oxide inclusion on polyHIPE physical and chromatographic properties"** Sidratul Choudhury, Damian Connolly, Brett Paull and Blánaid White. *Virtual Symposium on Applied Separation Science (VSASS), June 2015.*
2. **"PolyHIPES (high internal phase emulsion) with tailored pore morphology as super-macroporous monolithic stationary phases in capillary chromatography"** Sidratul Choudhury, Laurence Fitzhenry, Mark Kelly, Damian Connolly and Blánaid White. *Analytical Research Forum, ARF, Burlington House London, UK, July 2014.*
3. **"Fabrication and characterisation of nano-structured super-macroporous polymer monoliths for applications in bio-separations"** Sidratul Choudhury, Laurence

Fitzhenry, Damian Connolly and Blánaid White. *Analytical Research Forum, ARF, GlaxoSmithKline & the University of Hertfordshire, UK, July 2013.*

List of Oral Presentations

1. **"Fabrication and characterisation of nano-structured super-macroporous polymer monoliths for applications in bio-separations"** Sidratul Choudhury, Laurence Fitzhenry, Damian Connolly and Blánaid White. *Conference of Analytical Science in Ireland, CASi, University College Cork, Cork, Ireland, June 2013.*
2. **"Graphene oxide modified polyHIPEs as stationary phase materials for liquid chromatography"** Sidratul Choudhury, Damian Connolly, Brett Paull and Blánaid White. *ACROSS monthly meeting, April 2015 and DCU Chemistry Day June 2015.*

List of Honours and Awards

1. Judge's choice poster award (VSASS, 2015).
2. Marie Curie MASK- IRSES travel exchange grant (2015).
3. Analytical Chemistry Trust Fund bursary for attendance to the RSC Analytical Research Forum (2013).
4. Analytical Chemistry Trust Fund bursary for attendance to the RSC Analytical Research Forum (2014).
5. Irish Research Council Embark initiative grant (2012).

Acknowledgments

Firstly, I would like to thank the Irish Research Council under the EMBARK initiative for funding my research. Next, I would like to extend my gratitude to my supervisors Blánaid and Damian for their patience and encouragement on this challenging journey and the corrections of this thesis. In particular, thank you to my primary supervisor, Blánaid, you have taught me how to be a confident researcher and have encouraged me through every success, but more importantly, every shortcoming I thought I had in this project. Thank you for adopting me, I would be lost without you. I would also like to extend my gratitude to Professor Dermot Diamond and Professor Brett Paull for giving me the opportunity to visit ACROSS. I thank Brett for all of his guidance during my stay in Tasmania; it truly was the highlight of my PhD.

My sincere gratitude goes to all of the technical staff in the School of Chemical Sciences, NCSR and ACROSS for all of their expertise and help. You are all such an invaluable resource especially to postgraduate students. I would like to thank in particular Dr. Brendan Twamley for FESEM analysis as well as Dr. Laurence Fitzhenry and Dr. Emer Duffy for the BET analysis carried out.

To all the members of S201 and X153 past and present for all of their help and friendship. Special thanks go to Orla, Brian, Nicky, Saorla, Keana, Andrew, Patrick, Dave, Liam, Finn, Jonathan, Donal, Laura and Katya for all of the tea, chats and advice! A special thanks to all my friends in UTAS and in particular Sara, Alain, Marina, Dario, Sinead, Chris, Amin, Jeremy and Emer for all of their help and friendship during my visit.

To my friends outside of DCU, Rebecca for being the best friend in the world and dragging me out of my PhD cave. Thanks to Sinead, Hadja, Laura and Emma for the endless laughter and yummy food. Many thanks to Annmarie and Richie for all the love and encouragement through the years.

I would like to thank my family who have always encouraged me throughout my years in education. Most of all, thanks to my parents. Thanks for all the lifts, help with moving, kind words and a place to come back to call home. In particular, I would like to thank my mom for always believing in me and encouraging me.

Last, but certainly not least, thanks to Chris for quite literally everything. I honestly do not think I could have finished this without you. Thank you for being a nurse, cook, editor, IT assistant, shrink and every other role that you have fulfilled. Most of all, thank you for being my best friend through all of this.

Dedication

For my late-grandfather, Shamsul Alam.

Abstract

Sidratul Choudhury

Investigation of the applicability of polyHIPE materials in liquid chromatography

Polymer monoliths have gained significant interest as stationary phase materials over the last 25 years. More recently, enthusiasm for polymer high internal phase emulsions (polyHIPEs) in chromatographic separations has grown, primarily due to their large pore sizes (greater than 10 µm), which make polyHIPEs highly permeable and ideal for high flow rate separations. In this study, the applicability of polyHIPE materials as stationary phase materials was investigated and novel methods to increase their surface area explored. A range of different polyHIPEs were prepared using monomers such as Sty, GMA and VBC to impart varying surface functionalities. The first instance of an OTCEC polyHIPE column was demonstrated and applied in a modest separation of alkylbenzenes.

Upon development of various polyHIPE materials, it was found that styrenic polyHIPEs gave an ideal morphology and were most appropriate for HPLC separations compared with VBC and GMA polyHIPEs. Previously, polyHIPEs have predominantly been utilised in gradient separations of protein standards. However, the applicability of these materials as stationary phase materials have not yet been investigated in isocratic separations. PS-*co*-DVB polyHIPEs within silcosteel columns (100 mm x 1.02 mm in I.D) were fabricated and chromatographic performance characteristics of the columns produced were established. The separation efficiency for alkylbenzenes investigated was lower than traditional polymer monoliths. However, the polyHIPEs of low surface area demonstrated a high separation capacity in comparison to traditional polymer monoliths produced in previous studies and presented the novel use of PS-*co*-DVB polyHIPEs for the separation of alkylbenzenes in HPLC. In addition the resolution, peak asymmetry, and high batch-to-batch reproducibility of %RSD of up to 3% were established of the polyHIPEs as stationary phases.

While separation capacity of the PS-*co*-DVB polyHIPEs were exceptional for such low surface area materials of 20 m^2 g^{-1}, surface area would become a major limitation upon developing the materials for more complex analytes. Methods such as inclusion of NPs during emulsion fabrication, agglomeration of NPs after amination and inclusion of additional porogens were utilised to enhance the surface area of the polyHIPEs. The inclusion of

additional porogen toluene and agglomeration of gold NPs were investigated; the polyHIPEs were unsuitable for downstream applications because of mechanical rigidity and permeability issues respectively. The inclusion of GONPs within the PS-*co*-DVB emulsion was found to decrease the surface area of the material by up to 40% (16 m^2 g^{-1}). Nonetheless, the GONP modified polyHIPEs were utilised in HPLC in their reduced and non-reduced states. The GONP modified polyHIPEs showed no difference in selectivity; however were found to give similar separation capacities when compared to the unmodified higher surface area polyHIPE. The significance of these results was that the GONP modified polyHIPEs demonstrated a superior method of adsorption for the RP-HPLC of alkylbenzenes.

Finally, the first instance of fabrication of a polyHIPE coated OTCEC column using a multiple layer polymerisation technique was investigated in an attempt to increase the separation efficiency of the polyHIPE materials. The successfully fabricated coated columns had an increased efficiency of up to 3460 plates. However, poor injection-to-injection reproducibility was observed with increasing injections resulting in co-eluted peaks and greater diffusion effects. In addition, effects on the polyimide coatings in OTCEC in general when using organic modifier ACN was also expected to be an attributing factor to the low injection-to-injection reproducibility. The latter, however, was deemed an issue in which OTCEC polyHIPE columns would not be able to overcome.

From this study, it was established that polyHIPE materials have potential as stationary phase materials; however, the issue of low surface area, mechanical rigidity and inherent concave void structure of polyHIPEs will ultimately need to be addressed to minimise low separation capacities and higher diffusion effects. Throughout this thesis, strategies have been explored to negate these issues, and additional strategies have been proposed for future work. It is certain that if these issues are addressed, polyHIPEs have the potential to not only be comparable to traditional polymer monoliths in terms of chromatographic performance, but to exceed these traditional formats in terms of fabrication reproducibility, ultimately increasing their application in real world applications.

Chapter One

Literature review of polyHIPE monolithic materials as stationary phases in separation science.

“If I have seen further... it is by standing upon the shoulders of giants.”- **Sir Isaac Newton.**

1. Aim

The aim of this review examines the success of polyHIPEs applied in separations and elucidates the successful strategies to improve their application as stationary phases for future chapters. Current applications, such as chelation resins demonstrate the diverse interaction modes and applications of polyHIPEs in analytical separations are considered in this review. PolyHIPEs have been shown to be ideal media for removal of environmental contaminants, separation of crude proteins and separation of small molecules. As well as reviewing the success of polyHIPEs in the literature, the potential limitations as well as strategies to overcome such limitations are explored.

1.1 Introduction

This literature review discusses the development of polymeric high internal phase emulsions (polyHIPEs) as stationary phase materials. The areas in which the materials have been shown to be particularly advantageous have been highlighted. With their unique supermacroporous architecture, polyHIPEs have huge potential as analytical separation stationary phases. Due to their fully interconnected pore structure, mass transfer occurs predominantly via convection, potentially allowing for enhanced chromatographic performance. Additionally their surface functionalities can be tailored by modification of substrates both during and post fabrication. The surface area of polyHIPEs are typically lower than comparable particulate stationary phases and problems with their rigidity persist. For these reasons, apart from their applications for large biomolecule analysis, the potential of polyHIPE materials as stationary phases in separation science have not been extensively realised. However, multiple strategies exist to overcome these limitations, potentially enabling the application of polyHIPEs for a diverse range of separations. The most noted increase in surface area has been using additional porogens and hypercrosslinking reactions. In this chapter, the limitations of modification techniques are explored, and strategies to overcome these limitations and further develop these monolithic phases for analytical separations are presented.

1.2 Introduction to polymer monoliths as stationary phases

Since the first instance of using monolithic columns in separations, almost 25 years ago, there has been a fast incline of research within this area [1]. Monoliths are highly porous materials, where the open pores form an interconnected channel network [2]. They are used for a wide range of applications from biological scaffolds for cell growth [3, 4], DNA purification [5], catalysis [6], separation media [7] and sample preparation media for uses such as solid phase extraction [8]. Although particulate stationary phases are predominantly used as separation media in modern chromatography, monoliths can withstand higher flow rates due to lower backpressure, resulting in shorter analysis time. While the resistance to mass transfer can be reduced in particulate columns by decreasing particle size, the accompanying increase in back pressure presents additional technical hurdles. In contrast to particulate stationary phases, monolithic stationary phases exhibit an enhanced mass transfer due to fully interconnected pores acting as direct channels where mobile phase can flow. Mass transfer in a monolithic column is therefore dominated by convection rather than diffusion [9]. Typical silica monolith morphology is demonstrated in Figure 1.1 (a) below with macrosized pores (50 nm-1000 nm) and nanosized pores (1-100 nm). In contrast, in polymer monoliths a “cauliflower like” skeleton is evident, as shown in Figure 1.1 (b).

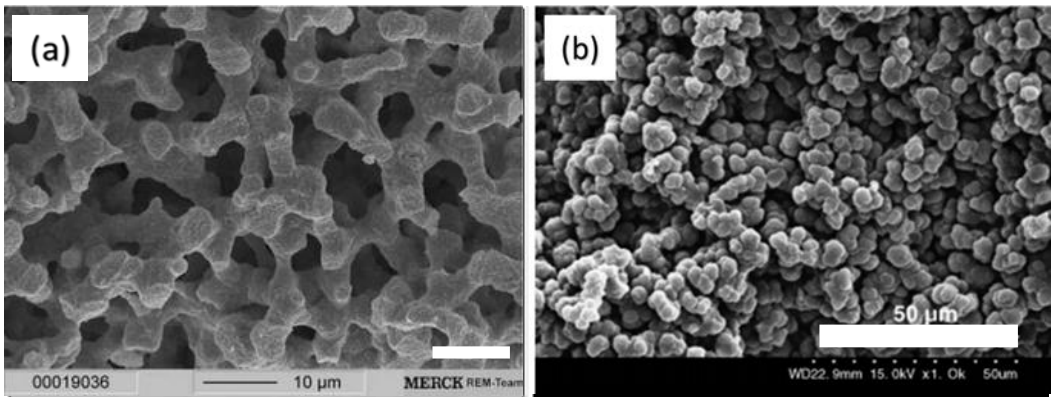

Figure 1.1: *Scanning electron microscope (SEM) image of (a) silica monolith (Magnification not specified, scale bar 10 µm) [10] and (b) glycerol dimethacrylate polymer monolith (Magnification 1,000x, scale bar 50 µm) pore architectures [11].*

While chromatographic performance can be improved by using monolithic stationary phases, like any other stationary phase, the material has its limitations. While silica based monoliths were initially found to be promising separation materials due to their high surface area (up to 300 $m^2 g^{-1}$) [12], a major limitation of the material is its narrow working pH range, typically pH 2-8. Below pH 2, bonded stationary phase ligands can be lost via hydrolysis of the silyl-ether linkage; above pH 8 the silica monolith itself dissolves[13]. By contrast, organic polymeric monolithic columns, despite having lower surface areas (3-20 $m^2 g^{-1}$) [1], have the advantage of a wider working pH range, typically of pH 1-14 [14]. In their mini review, Arrua *et al.* highlighted distinct performance characteristics of polymer monoliths which resulted from their morphology [15], polyHIPEs were highlighted as one of the most promising for separation science due to their unique morphology as well as their ability to be polymerised in standard bore housings [16]. Unlike traditional organic polymer monoliths which are known to have a “cauliflower” morphology, polyHIPEs comprise of supermacropores (pore sizes from 10-250 µm) resulting in unique pore architectures [17], as illustrated in Figure 1.2. In this particular chapter, the application

of these materials as chromatographic stationary phases will be explored to highlight the increasing potential of these materials in separation science.

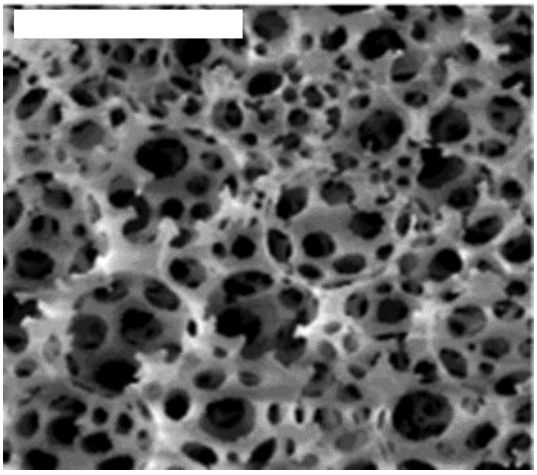

Figure 1.2: *SEM image of polyHIPE (Scale bar 50 µm) [17].*

1.3 PolyHIPEs

PolyHIPE materials, first studied in 1962, consist of an internal phase fraction dispersed in droplet form [18]. In a high internal phase emulsion, this internal phase constitutes greater than 74% of the total emulsion volume [19]. At this percentage a polyhedral structures are formed by the deformation of dispersed droplets, these polyhedrons are separated by thin layers of continuous phase [20]. Figure 1.3 (a) below demonstrates, where an organic phase in an aqueous phase (O/A) emulsion is formed. The organic phase (containing polymerisable monomers, crosslinker and surfactant) will act as the porogen and is dispersed within the discontinuous aqueous phase, and forms polymer particles upon polymerisation. In an aqueous phase in organic phase (A/O) emulsion (Figure 1.3 (b)), the aqueous phase (containing electrolyte and initiator) acts as the porogen and is dispersed in the organic phase (continuous phase) forming a continuous polymer network with interconnecting pores [21-23]. The macropores present due to the removal of porogen are known as voids

and the interconnecting pores within these voids are referred to as windows, illustrated in Figure 1.3 (c) [19]. Interest and research in these polyHIPE materials has increased significantly since the 1980s with terminologies such as porous polymers, open microcellular foams, polymer foams and polyHIPEs all being used to describe this particular material [24-27]. For clarity, throughout this thesis these fascinating materials will be referred to exclusively as polyHIPEs and the morphological features will be referred to as voids and windows.

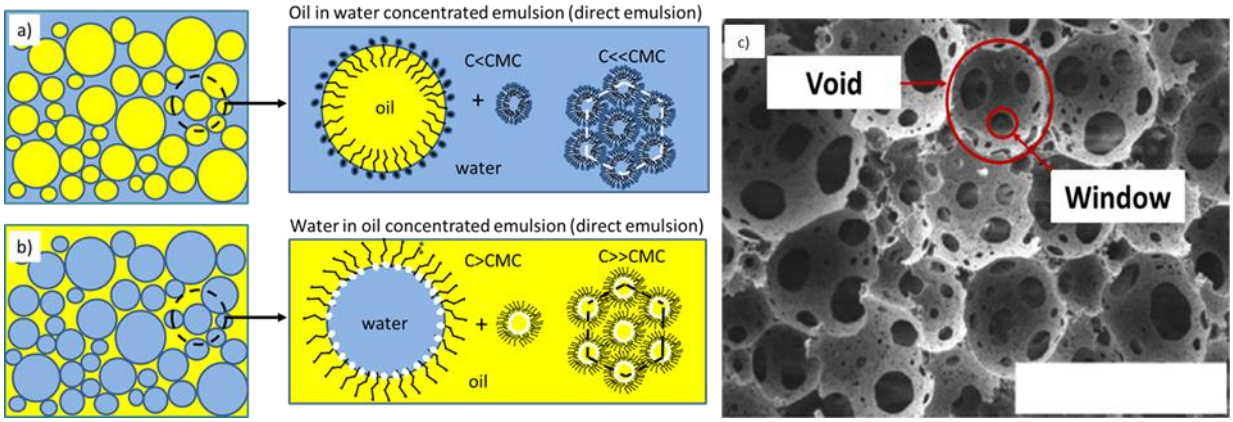

Figure 1.3: *(a) O/A (oil in water) and (b) A/O (water in oil) high internal phase emulsion [12] and (c) SEM image indicating morphological features that represent voids and windows in polyHIPE materials (Magnification not specified, scale bar 10 µm)[23].*

1.3.1 PolyHIPE preparation

1.3.1.1 Fabrication of polyHIPE materials

Emulsions of A/O polyHIPEs comprise functional monomer, crosslinker and surfactant within the organic phase. The aqueous phase consists of water, electrolyte and free radical initiator. Hydrophobic monomers used to fabricate nonpolar materials include styrene (Sty) and divinylbenzene (DVB) [26, 28, 29]. To fabricate more

hydrophilic materials monomers such as polyacrylamide (AAm), hydroxy ethyl acrylate (HEA), hydroxyethyl methacrylate (HEMA) and glycidyl methacrylate (GMA) are used [16, 30]. More complex systems can be achieved where monomers are present in both aqueous and organic phases [23]. In these cases, the removal of the internal phase will also leave behind a continuous phase consisting of polymerised monomers. Recently, hybrid silica-polymer polyHIPEs have also been fabricated, which incorporate the mechanical rigidity and surface area of silica monoliths, as well as increase permeability, working pH range and modify the general architecture of polymer monoliths [31]. However, there are few interconnecting pores present in hybrid silica polyHIPEs, which will lead to poor permeability for applications in separations. Hydrophobic and hydrophilic polyHIPEs commonly use DVB and ethylene glycol dimethacrylate (EGDMA) respectively as crosslinkers [28, 32]. More recently however a GMA polyHIPE was crosslinked using DVB illustrating that crosslinkers can be used to impart enhanced functionality to the final polyHIPE surface chemistry [33].

While the monomer and crosslinker mix is important in defining the morphological features of the resulting polyHIPE, amphiphilic surfactants (having both polar and non-polar components) are used to reduce the interfacial tension allowing the distinct voids and windows to form. Migration to the organic-aqueous phase interface must result in vertically positioned surfactant molecules packed along the interface between the two phases in order for the interfacial tension to be reduced and is known as the “condensed interfacial film”. The correct hydrophilic-lipophilic balance (HLB) relates to the number of hydrophilic and hydrophobic parts of the surfactant (typically between 0-40) to form a stable emulsion [34]. Generally A/O surfactants are within 4-8 on the HLB scale [34]. When the correct HLB of a surfactant proves difficult

to obtain [35], Pickering emulsions using nanoparticles are used and have also been found to impart an improved mechanical rigidity to the resulting polyHIPEs [36-38]. More recently, Pickering emulsions have been used to form unique HIPE-organogels using polymer latex particles and poly (N-isopropylacrylamide) particles by multiple hydrogen bond interactions, a self-assembly technique [39-41].

Once the emulsion components to fabricate the polyHIPE have been chosen, a free radical initiator is required to initiate the polymerisation reaction and is employed in the presence of a water-soluble salt to avoid Ostwald ripening. Ostwald ripening is the merging of one droplet into another. This water soluble salt increases the ionic strength of the aqueous phase. The initiator selected is dependent on the mode of polymerisation of the polyHIPE, typically thermal or photo-initiation. Commonly used thermal initiators are persulfates (KPS/APS) [16, 32, 42]. Photo-initiators are typically utilised when the emulsion is not stable enough to permit thermal polymerisation. Photo-initiation occurs at a much faster rate (order of seconds as opposed to hours) than thermal polymerisation. However, using photo-initiators the ability to obtain complete polymerisation is limited by the thickness of the polyHIPE that is to be produced, as there is only a certain UV penetration depth (µm-mm depending on UV source) to which the photo-initiator can function adequately, due to its opacity [43, 44]. Furthermore, non-absorbing monomers must be used to avoid self-screening of effects that can occur [19]. This chapter focuses on the application of polyHIPEs as a stationary phase material; for the sake of brevity, fabrication protocols will not be discussed in detail. A comprehensive review on formulation methods of polyHIPEs by Kimmins *et al.* is recommended for further reading of fabrication methods [19].

1.3.1.1.1 Strategies to tailor and increase surface area

The realisation of polyHIPE stationary phase application is largely dependent on overcoming their surface area limitations without compromising their structural rigidity. The tailoring of these morphological factors can be controlled during fabrication.

The simplest strategy to tailor pore morphology is to control the volume ratio of monomers to porogen. In a formulation where the percentage of aqueous phase is increased, the percentage porosity of the resulting polyHIPE is also increased. Therefore, a polyHIPE prepared using an 80% internal phase should be more open than one which used 75% [25, 42, 45], is illustrated in Figure 1.4.

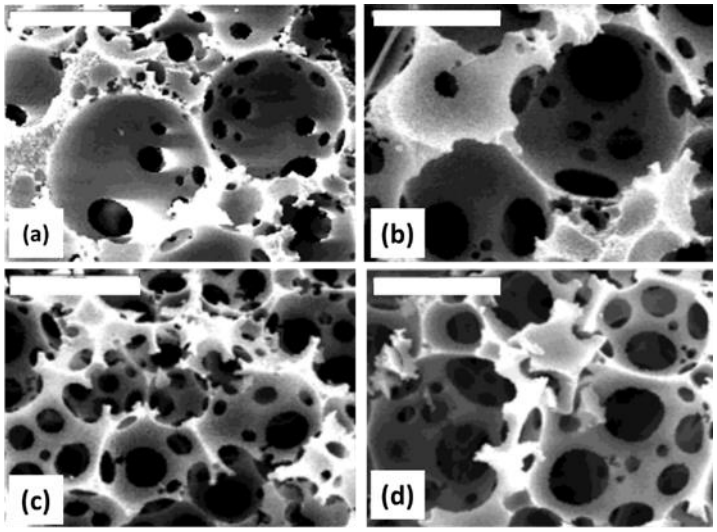

Figure 1.4: *PolyHIPEs fabricated by varying aqueous phase ratios with chlorobenzene as additional porogen where percentage aqueous phase is (a) 75% (b) 80% (c) 85% and (d) 92% (Scale bars 20 µm, magnification not specified) [17].*

A second strategy to increase the openness of the polyHIPE is to increase the temperature of the aqueous phase. The increased temperature gives rise to larger

voids and windows in the polyHIPE structure. Figure 1.5 below the increase of temperature to 80°C increased the void size observed [46, 47].

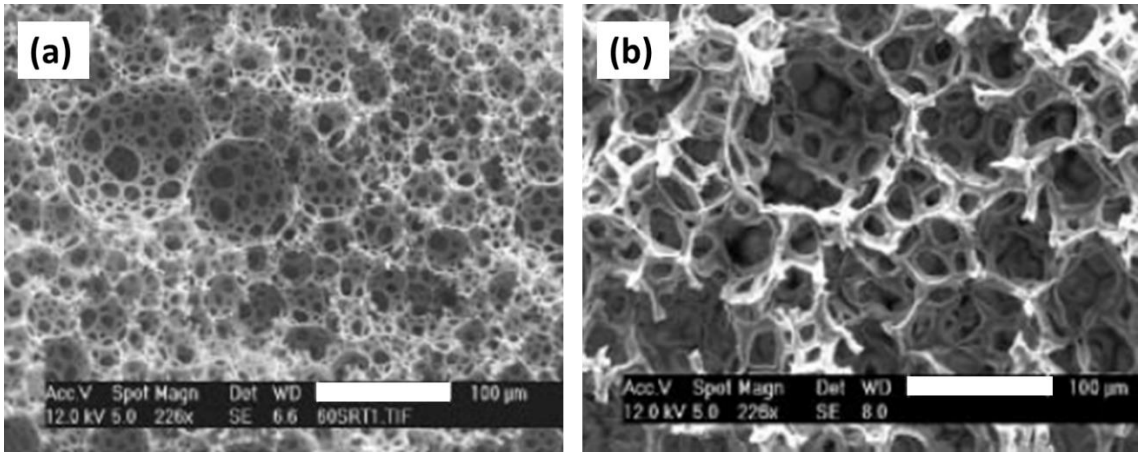

Figure 1.5: *PolyHIPEs demonstrating the effect aqueous phase temperature in emulsions where Polystyrene (PS)-co-DVB polyHIPEs were prepared at aqueous phase temperature (a) room temperature (Scale bar 100 µm, magnification 226x) and (b) 80°C (Scale bar 100 µm, magnification 226x [46]*.

The initial concentration of crosslinker also alters the resulting polyHIPE morphology. In general, for most polyHIPE emulsions 2 to 4% crosslinker is employed. As expected it has been shown that when the percentage crosslinker in the formulation is increased, the average void size decreases [23, 28]. When decreasing the percentage crosslinker the opposite is true and larger void sizes are present. Smaller voids would intuitively indicate a greater surface area; however, the polyHIPEs structural rigidity would also be affected. It has been demonstrated that incorporation of an excessive percentage crosslinker has resulted in the fabrication of a significantly brittle polyHIPE with an elasticity modulus as low as 31 MPa [28, 48]. As commercial liquid chromatography (LC) stationary phases typically operate at much higher pressures, up to 110 MPa [28], a highly crosslinked polyHIPE is incompatible for high

pressure separations. However elasticity may be increased using polybutadiene as an additive to increase the mechanical rigidity of the polymer [49].

1.3.1.1.2 Increasing polyHIPE surface area

PolyHIPEs typically have a low surface area (ranging from 3-20 $m^2 g^{-1}$) [17], relative to that of packed bed stationary phases (surface area of 150-400 $m^2 g^{-1}$) [50] and silica monoliths (surface area ~300 $m^2 g^{-1}$) [50]. However, there are multiple strategies to increase polyHIPEs surface area.

In addition to using percentage crosslinkers and aqueous phase ratios to control the morphology of polyHIPEs, using additional porogens is also a commonly used strategy to increase their surface area. The number of interconnecting windows present in a polyHIPE is increased by introducing additional porogens into the continuous phase during the polyHIPE fabrication. This also results in the formation of micropores (pore less than 2 nm), increasing the surface area of the otherwise non-porous polyHIPE skeleton. To maintain a polyHIPE's structural rigidity the correct porogen ratio must be chosen for the appropriate formulation. Incorporation of porogens such as 1-chloro-3-phenyl-propane, chlorobenzene and 2-chloroethylbenzene has been reported to increase surface area up to 829 $m^2 g^{-1}$ [17]. Higher surface areas have been reported, but structural rigidity has been compromised [51-53]. Introducing additional porogens into the organic phase increases the number of interconnecting windows present in the resulting polyHIPE, with incorporation of monomers such as AAm in the aqueous phase reducing window diameter tenfold [45]. While this reduction of window diameter would be expected to result in an increase in surface area, the overall structural rigidity would also have to be assessed. Indeed porogen incorporation usually impacts structural rigidity, and to

date physical inspection of such modified polyHIPEs has resulted in high surface areas, but increasingly brittle material.

PolyHIPE surface area can also be increased by hypercrosslinking via Friedel-Crafts alkylation, which allows neighbouring polymer chains to crosslink. This results in a microporous pore structure upon the removal of the porogen and increases the surface area dramatically, with surface areas ranging from 50-1210 $m^2 g^{-1}$ reported [54]. Typically, the polyHIPE is subjected to a multiple alkylation where it becomes swollen by internal electrophiles already present in the network or by the introduction of external electrophiles. Unfortunately, the Friedel-Crafts catalyst can hinder purification of the monolith which could contribute to poor chromatography, as the metal cations (especially iron) can interact directly with certain chelating solutes, resulting in poor peak shape for these analytes. If purification problems could be overcome however, these polyHIPEs could be amenable to chromatography. The backpressure measured on a chromatographic system using hypercrosslinked monoliths (column length 4.1x260 mm) was 20.5 MPa at a flow rate of 0.5 $\mu L.min^{-1}$, which is acceptable for a capillary LC instrument [54, 55]. Recently, successful post-polymerisation without a Friedel-Crafts catalyst has been reported with styrene and co-polymer DVB. The formation of micropores ultimately resulted in a 7.2 fold increase in surface area in comparison to unmodified polyHIPEs [56]. While the resulting surface area was lower than that obtained by the using a Friedel-Crafts catalyst, there was no requirement to remove any metal impurities from the final monolith. More recently, by coupling the technique of high internal phase emulsion templating with lithography [57], additive manufacturing technology (AMT) has been used to decrease the size of the pores within polyHIPE materials using an acrylate/thiol based polymer network. Here emulsions of over 80% porosity have been achieved. Unfortunately,

despite being mechanically stable at 60 MPa, an overall low surface area still resulted from these materials (26.7-53.7 $m^2 g^{-1}$).

An increase in surface area of polyHIPE materials is most certainly attainable, and significant advances by tailoring the polyHIPE morphology have been made to improve the specific surface area. However, it is important to realise that a polyHIPE exhibiting both high surface area and high mechanical stability remains elusive.

1.3.2 PolyHIPE application for specific analyte class analysis

One of the most attractive features of polyHIPEs and of growing interest for specific chromatographic applications is the ability to tailor the morphology and surface chemistry of polyHIPEs. The possibilities for application of polyHIPEs for separations are both broad and diverse given the extent to which their surface chemistry can be varied. These possibilities are only beginning to be explored, with the main areas of application to date emerging in the removal of water impurities, [32, 58] and in separations of large biomolecules as well as small molecules, [16, 59-62] all of which demonstrate the separation capability of these potential stationary phases

1.3.2.1 Small molecule separations using polyHIPEs

Heavy metals are prevalent in groundwater of countries around the world, including Bangladesh, Hungary, Finland and Greece [58]. The removal of heavy metals by use of polymeric bead resins has been extensively researched and has resulted in successful commercial resins [63-67]. However, particulate resins when housed in column format, are limited by high backpressures resulting in poor quality separations. PolyHIPE materials are currently being investigated to overcome this issue due to their unique pore structure. Typical polymeric anion exchange resins use the addition of pyridine groups to remove heavy metals, with 2-methyl-5-vinylpyridine

and 4-vinylpyridine co-polymerised with DVB is most common. As 4-vinylpyridine is commercially available, it serves as a benchmark for polymeric resins and many other modified polyHIPEs that will be discussed in this chapter [68].

DVB polyHIPEs have formed the polymer backbone for a number of successful heavy metal analyses. Benicewicz *et al.* reported the use of a PS-*co*-(4-vinyl benzene chloride) VBC-*co*-DVB polyHIPE with UV addition of 4-vinylpyridine enabling its use for adsorption of analytes such as iron and plutonium [69]. The polyHIPEs (void size distribution 2-100 µm) displayed promising extraction performance, with a 10% higher adsorption capacity reported when compared 4-vinylpyridine functionalised commercially available beads (Relliex^{TM}). The distribution coefficient (K_d) value for iron removal was 362 for the commercial beads, significantly less than the polyHIPE material K_d of 842 [69]. Similarly, the comparison of commercial PS beads to iron hydroxide coated PS-*co*-DVB polyHIPE granules was investigated for the adsorption of arsenate and arsenide in water [32]. Katsoyiannis *et al*. compared these two materials although this comparison was somewhat compromised by the differences in material dimension. In contrast to the previous study, the polyHIPE granules were used in batch format overlooking polyHIPE permeability, which is the material's most notable advantage. The greatest adsorption of the arsenic compounds reported was using a polyHIPE with a pore diameter of 12.7 µm. Although adsorption of the arsenates and arsenites was dependent on pH, at pH 7 both ion species were readily removed. With the optimised parameters investigated, the uptake of the analytes was 20% greater with the polyHIPE material which was attributed to macroporous nature [58]. A more recent study by the group compared the iron hydroxide modified polyHIPE granules and calcium alginate granules [32]. A closer comparison was achieved as all the materials were in granular form. In agreement to the study by Benjamin *et al.*, the

unique morphology of the polyHIPE granules resulted in higher As uptake with an adsorption capacity of 93 mg g^{-1} of polyHIPE material [67].

Removal of metal analytes can also be achieved with non-DVB polyHIPEs. The binding of metal analytes Ag, Cu and Cr was achieved using a GMA polyHIPE formulated using unsaturated polymer resin (UPR) with amine ligand functionality. GMA contains a reactive epoxy group allowing desired functionalisation of the resulting polyHIPE material [59]. Amine functionalised GMA polyHIPEs typically resulted in craters present throughout the monolith (Figure 1.6) [42, 59, 70, 71]. These craters in this context are voids with little to no interconnecting pores and are irregular in shape and size. Unfortunately, the adsorption results were not compared to a commercial resin as in previous studies. From the aminated ligands investigated on one such GMA, 2-aminothiazole (ATAL) and 2-phenylimidazole (PIAL) gave the highest adsorption of Ag (9.05 mmol g^{-1}), Cu(II) was best adsorbed with a 1,4-ethylenediamine modified (4.99 mmol g^{-1}) polyHIPE and Cr(III) was best adsorbed with the 2-phenylimidazole functionality (2.92 mmol g^{-1}). This emphasises the versatility of polyHIPE materials and the ability to tailor them according to the final application [59].

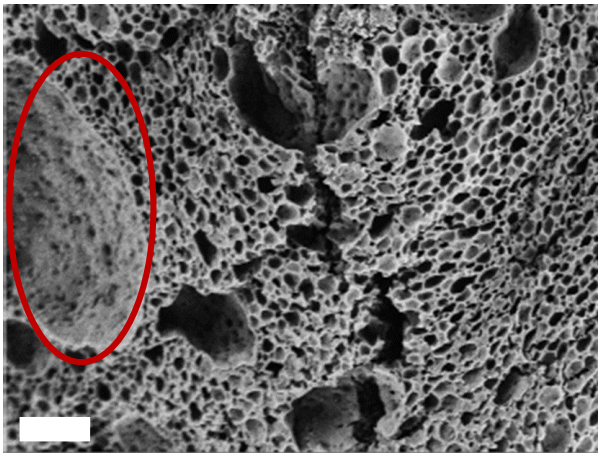

Figure 1.6: SEM of *UPR/GMA/Sty polyHIPE where region highlighted in red shows an example of a crater (Scale bar 2 µm, magnification not specified) [59].*

Environmental contaminants other than heavy metals can also be removed using modified polyHIPEs [72]. I. Pulko *et al.* investigated the removal of atrazine in water by comparing uptake using crushed 4-nitrophenolacrylate piperazine functionalized polyHIPE (PS-*co*-VBC-*co*-DVB-*co*-4-nitrophenolacrylate) and piperazine functionalised Sty-*co*-4-nitrophenylacrylate beads (abbreviated to BDS by the authors) [72]. As piperazine forms covalent bonds with atrazine, it provides an attractive alternative to using carbon as adsorbents [73]. The polyHIPEs investigated were in powder form, which, similar to Katsoyiannis *et al.* overlooks the advantage as a highly porous flow through media upon using a polyHIPE. However, the polyHIPE showed a faster uptake over time when compared to the BDS, with almost complete removal of atrazine within 48 h while near complete removal was observed in the BDS at 144 h. The increased uptake was attributed to the higher porosity of the polyHIPE compared to the polymer beads indicating that polyHIPE materials have a distinct advantage over beads and ultimately over generic carbon adsorbent methods [72].

The previous studies show the use of polyHIPEs to be utilised once cut up and packed into columns instead of as a complete single unit [58, 61, 69, 74]. This is likely

to be because where modifications of the materials are required bulk material is used as it is less challenging. However, when translated to a column format modification protocols are less efficient and increasingly challenging. Recently an on column modification for removal of acid chlorides has been demonstrated using A VBC-*co*-DVB-PS polyHIPE. The column was fabricated within an 8 mL Convective Interaction Media (CIM) monolithic column housing (15 mm x 45 mm I.D.) and was aminated in situ to recover a selected acid chloride [75]. The polyHIPE removed 98% of the analyte with a flow rate of 4 mL min^{-1}, resulting in a backpressure of 1 bar.

The potential of polyHIPEs as ion exchange resins has also been investigated, most notably by Inoue *et al.* A PS-*co*-DVB polyHIPE functionalised with sulphonic acid groups [76]. The resulting polyHIPE was cut in 3 mm cubes and packed into a column of 8 mm x 180 mm I.D. with a volume of 9.04 mL. The cation exchange capacity was 3.4-4.8 milliequivilents g^{-1} and the polyHIPE ion exchanger was shown to have an electric conductivity five times greater than the commercial beads studied. Despite the ion exchange capacities of the two materials being similar, the fact that ions were present uniformly along the polyHIPE resulted in a higher contact area and therefore, better electric conductivity [76]. While this polyHIPE was presented in a packed bed format, the ion exchange attributes of the material as a stationary phase could be improved by using the whole material within a column, formed as a single unit within a column housing.

A subsequent development in the realisation of polyHIPEs as a stationary phase involved their application in Capillary Electro-Chromatography (CEC). Tunç *et.al.* produced a relatively hydrophobic isodecylacrylate (IDA)-*co*-divinylbenzene (DVB) polyHIPE of 90% porosity within polyimide fused silica capillary housings of 100 µm I.D. and 360 µm O.D. Figure 1.7 (c) shows the polyHIPE applied in CEC separation

of alkylbenzenes with high reproducibility (%RSD values of 4.02-4.68). The resulting plate count and plate height was 200,000 and 5µm respectively for thiourea and was comparable to polymer monoliths produced by other groups [77-79]. SEM was used to confirm a highly permeable supermacroporous morphology with secure bonding of the polyHIPE to the capillary wall via silanisation, shown in Figure 1.7 (a) and 1.7 (b) below. Compression tests demonstrated high-pressure tolerance of 1 MPa, lower than previous studies but nevertheless, demonstrated the suitability of the material for high-pressure applications as well as CEC mode [74, 80]. In later studies, the separation of alkylbenzenes was further investigated by Tunç *et. al.* using a PS-*co*-DVB polyHIPE of 90% porosity prepared in 100 µm fused silica capillary with the Electroosmotic flow (EOF) generated by the adsorption of buffer molecules on excess free radical initiator $K_2S_2O_8$ [81]. The theoretical plate number resulting was 142,000 with a minimum plate height of 7 µm for the thiourea peak, lower than previously reported [79]. The %RSD values were within a range of 0.36-2.86% indicating improved reproducibility of the polyHIPE material for separations relative to that previously reported as well as a significantly increased surface area of 20 $m^2 g^{-1}$ [79]. However, the baseline resolution of the analytes decreased significantly when using the polystyrene polyHIPEs as shown in Figure 1.7 (d), indicating the importance of the polyHIPE surface chemistry on the separation capacity of the material.

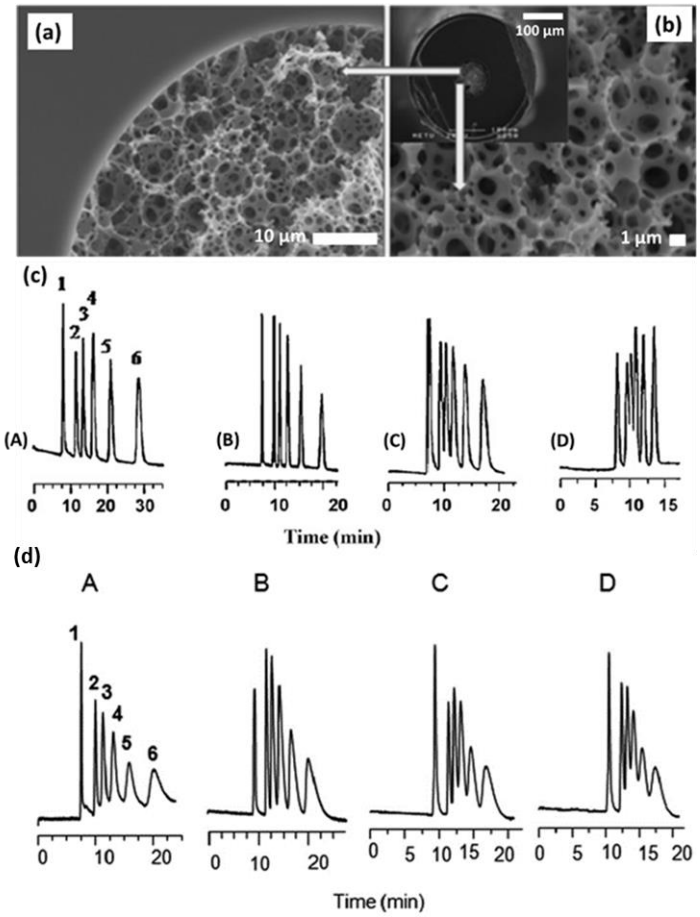

Figure 1.7: (IDA)-*co*-divinylbenzene (DVB) polyHIPE: (a) SEM image of the polyHIPE *bound to the capillary wall (Magnification 2,000x), (b) SEM image of the morphology of the polyHIPE produced (Magnification 4,000x) and (c) CEC separation of alkylbenzenes with the elution order; thiourea, benzene, toluene, ethylbenzene, propylbenzene, and butylbenzene respectively under accelerating voltage of 10, 15, 20, 25 and 30 kv respectively [79] and (d) PS-co-DVB polyHIPE CEC separation of alkylbenzenes (1-6) thiourea, benzene, toluene, ethylbenzene, propylbenzene, and butylbenzene respectively, varying ACN ratio (v/v): (A): 60/40, (B): 65/35, (C): 70/30, (D): 75/25* [81].

PolyHIPEs have also been successfully demonstrated as separation media in flow through format. Recently, a novel application of polyHIPE materials has investigated the separation of nanoparticles (NPs) by size [82]. The authors of this

study suggested that the separation method would be similar to that of size exclusion chromatography (SEC) where larger NPs would elute more readily than smaller particles. Upon investigation on both PS-*co*-DVB and EDGMA polyHIPEs within 150x4.6 mm I.D. columns it was found that the predicted order of separation was not as expected. For PS-*co*-DVB columns gold NPs of 5 nm and 10 nm in diameter were retained, exhibiting average retention times of 5.88 and 8.13 min respectively at a flow rate of 0.5 mL min^{-1}. The separation of larger gold nanoparticles (20 nm) was also attempted, however, these blocked the column. Similarly, the separation of dysprosium doped PS latex particles of 52 and 155 nm on the EDGMA column gave retention times of 1.75 min and 2.21 min respectively. Both instances show that smaller the particles size had lower retention times. While resolution was poor, this separation could be improved by tailoring the polyHIPE morphology and surface chemistry.

From the above studies, polyHIPEs have repeatedly shown superior efficiencies to polymer resin beads and carbon adsorbents for specific contaminant removal, primarily through tailored surface modifications. Given this, incorporation of the supermacroporous polyHIPE scaffold with judicious choice of surface modification has exciting potential for application in chromatographic separation of a wide range of analyte class.

1.3.2.2 Biomolecule separations using polyHIPEs

Analysis of large biomolecules such as proteins is the most extensively developed application using polyHIPEs. Biological fluids and cell culture/fermentation media are extremely complex samples and so most separation methods require a sample preparation step in order to first isolate highly abundant proteins present in cell

cultures. [83] After filtration/isolation steps are complete, the biological sample is then suitable for downstream analysis such as LC. Where most commercial columns available for protein separations are silica based and have a pH working range constraint. The typical polymer monolith will have a wider working pH range for protein separation but will consist mainly of micropores. The microporous morphology of a typical polymer monolith can limit the flow of large biomolecules such as proteins. Macroporous polyHIPEs provide the potential to reduce complex sample preparation steps involved in processing biological samples.

Protein separations using commercial CIM disks were compared to diethylamine (DEA) modified glycidyl methacrylate (GMA)-*co*- EGDMA polyHIPEs in CIM disk format were studied by Krajnç *et al.* The polyHIPE was fabricated using more hydrophilic monomers in order to impart a similar functionality to the commercial CIM disk [42]. Where typical LC separations of proteins are carried out using gradient reverse phase chromatography, the functionality of this polyHIPE allowed use of only binding and elution buffers. Porosities of 60%, 75%, 80% and 90% were prepared with the latter two used for HPLC analysis, presumably for increased flow rates. The greater porosity polyHIPE should decrease in surface area; but unfortunately, a Brauner Emmet Teller (BET) value was not reported. The morphology of the polyHIPE was found to have a porous structure with large craters present as shown in Figure 1.8 (a) and 1.8 (b). These craters gave rise to higher rates of dispersion in comparison to the CIM disk separation as significant co-elution of myoglobin, conalbumin and soybean trypsin inhibitor was observed as shown in Figure 1.8 (c). Despite this, the 90% porosity material achieved an improved run time of ~0.6 min highlighting the advantages of the macroporous material. Subsequently ethylhexyl acrylate (EHA) was added to the GMA polyHIPE formulation to investigate its effect on mechanical rigidity

and the chromatographic performance on a standard protein mix [84]. Promisingly, addition of EHA polyHIPEs significantly increased the mechanical rigidity of the resulting materials. The material's chromatographic performance was expected to be compromised as the addition of EHA decreased the number of available surface groups for analyte interaction. The study found that upon addition of HEA however, no significant change was observed in analyte retention time. It was hypothesised that, mechanical rigidity increased the access of the analyte molecules to the binding sites.

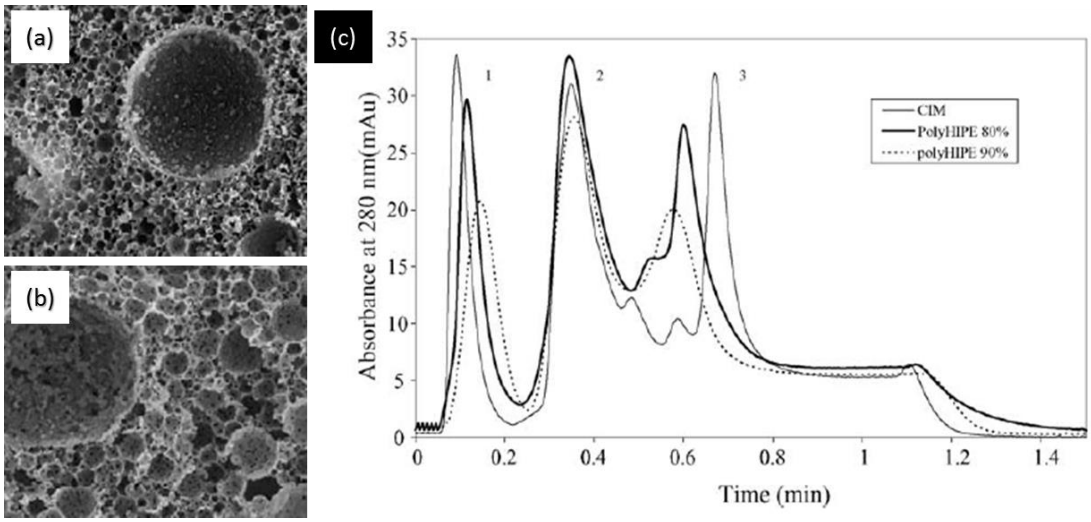

Figure 1.8: *(a) 80% GMA-co-DVB polyHIPE (b) 90% (c) Gradient separation of a protein mixture on PolyHIPE and CIM methacrylate monolithic columns. With the conditions of: mobile phase A: 20 mM Tris–HCl buffers, pH 7.4 and mobile phase B: 20 mM Tris–HCl buffer+1 M NaCl, pH 7.4. A flow rate: 4 mL* min^{-1}*, gradient of 0–70% buffer B in 53 s were applied. The samples consisted of: 1 mg* mL^{-1} *of myoglobin (peak 1), 3 mg* mL^{-1} *of conalbumin (peak 2) and 4 mg* mL^{-1} *of soybean trypsin inhibitor (peak 3) dissolved in buffer A with an injection volume of: 20 µl; and UV detection at 280 nm [42]. Magnification (a) and (b) 1,000x, no scale bars specified.*

This highlights that the issue of mechanical rigidity could be overcome without reducing the separation efficiency of these materials, indicating a potential strategy for overcoming structural rigidity limitations of polyHIPEs.

While the previous studies demonstrated fast protein separations using polyHIPEs within CIM disk format. Yao *et al.* separated proteins using GMA-*co*-EGDMA polyHIPEs in a normal bore HPLC column, a more sophisticated flow through format. The study found that the surfactant, Pluronic™ F127 (PF127) gave unique submicron morphology as the percentage of surfactant in the emulsion increased as observed in Figure 1.9 (a). In comparison to the studies by Krajnç. *et al.*, it was observed that there were no craters present in the polyHIPE morphology, which, reduced unwanted dispersion during analysis.

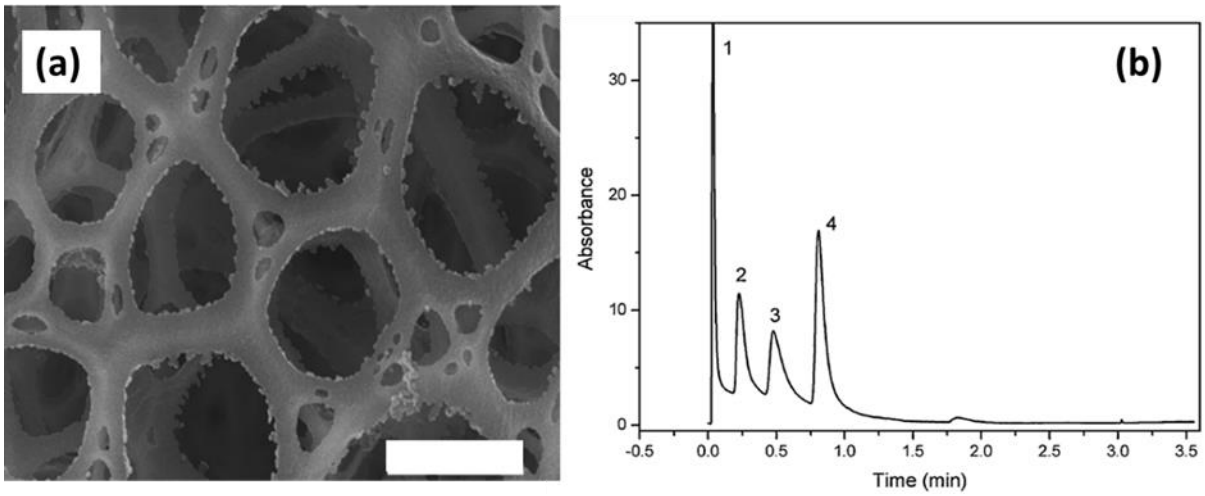

Figure 1.9: *(a) SEM image of 5.5% v/v surfactant to water HIPE (b) Separation of lysozome (1), Bovine Serum Albumin (2), ovalbumin (3) and pepsin (4) at 6 mL* min^{-1} *flow rate with mobile phase consisting of buffer A: 10 mM Tris-HCl buffer, pH 7.6 and buffer B: 10 mM Tris-HCl buffer, pH 7.6 [16]. Magnification (a) 15,000x.*

The surface area was reported at 161 $m^2\ g^{-1}$, much higher than polyHIPE materials with no surface modification, which was attributed to the type and relative

percentage of surfactant used [16]. In addition, a high thermal stability up to 240°C was demonstrated, and pressure drop tests carried out reported permeability to be 30 times higher than that of packed 10 µm particle packed columns Mechanical tests resulted in crush strength 3.1 MPa and Young's modulus of 48.3 MPa, typical for polyHIPEs [85]. When analysed as a stationary phase for protein separation as observed in Figure 1.9 (b), a high flow rate of 6 mL min^{-1} gave a near to complete separation within 1 min [16]. In later studies Yao *et al.* compared a conventional GMA polymer monoliths to a GMA polyHIPE where separation of cytochrome c, myoglobin, ribonuclease A, lysozyme and BSA within 4 min at a high flow rate (1440 cm h^{-1}) was achieved [61]. The polyHIPE material surpassed standard commercial organic monoliths in fast biological separations with a difference of 188.2 $m^2 g^{-1}$ in surface area observed. In addition, compared to CIM columns, the direct binding capacity was increased by 12.5 mg mL^{-1} using 80% porosity polyHIPEs [61]. In a subsequent study, these columns were immobilised with HSA via pendent epoxy groups on the polyHIPE surface. The most interesting application of this column was the chiral separation of L and D form amino acids by high performance affinity chromatography (HPAC) after the samples were incubated with D-amino acid (D-AA) oxidase. D-AA-oxidase hydrolyses D amino acids into α-ketoacids and ammonium, thus decreasing the concentration of D-amino acids such as D-tryptophan (D-tryp). The material allowed the quantification of D-tryp from 12 µM to 979 µM with correlation greater than 0.99 [60].

Protein separation has also been demonstrated in biological samples. The separation of immunoglobulins from human plasma and egg yolk was reported using a hydrolysed GMA-*co*-EGDMA polyHIPE [74]. Upon characterisation using SEM (Figure 1.10 (a)) it was found that the material had typical polyHIPE morphology,

however, had small through pores (less than 10 µm). Exact measurements of pore volume, surface area and porosity were not reported, however. The polyHIPE was found to be able to withstand pressure of 3 MPa In this study, only two analytes were separated at varying flow rates as shown in Figure 1.10 (b). With only one protein, lysozyme, appearing to be retained at all on the column, its efficiency was low, especially when compared to previous studies where protein separation was possible in less than 1 minute with at least three analytes [16, 61, 74]. A vinyl ester VE-*co*-EGDMA polyHIPE column (50 x 4.6 mm I.D.) prepared by Yang *et al.* resulted in a similar separation of immunoglobulins [80].

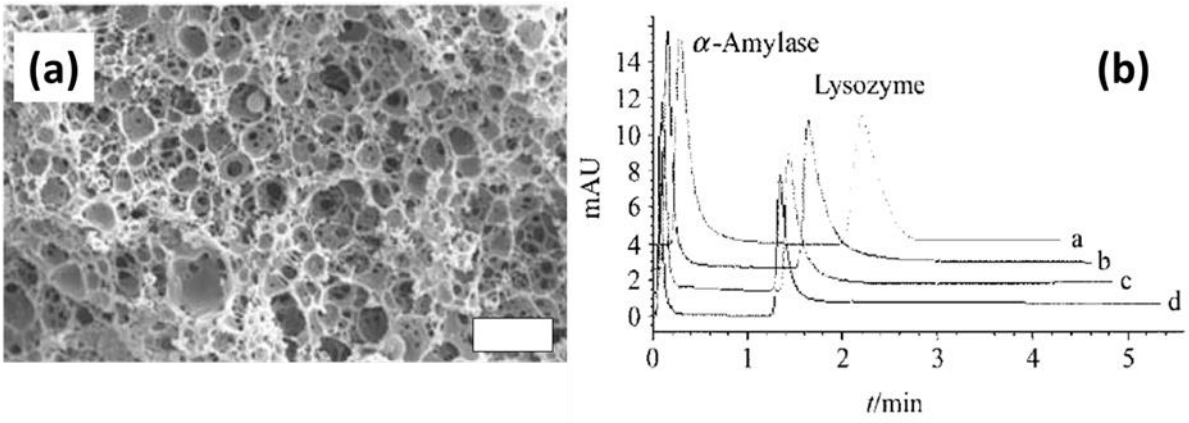

Figure 1.10: *(a) SEM image of the GMA-co-EGDMA polyHIPE (Scale bar 10 µm, magnification 1,000x) and (b) fast separation of α-amylase and lysozyme on PolyHIPE monolith. The LC conditions were: gradient, 0-1.5 min, 100% A (0.001 M, phosphate buffer, pH 7.8), 1.51-2.5 min, from 30% B to 100% B (in which 1 M NaCl was added into the buffer A); gradient elution at flow rates of (a, b, c and d 361 cm h^{-1}, 722 cm h^{-1}, 1083 cm h^{-1} and 1445 cm h^{-1} respectively). The sample injection volume of the autosampler was 5.0 µL [74].*

The role of VE was to induce stability at higher working temperatures and alkali pH range, along with enhancing mechanical rigidity of the polyHIPE [80].

Characterisation of the resulting stationary phase material via SEM and mercury intrusion porosimetry highlighted small voids and windows with an average pore diameter of 0.85 µm. Additionally, the surface area of the polyHIPE was found to be 121.96 $m^2 g^{-1}$, confirming that smaller morphological features in polyHIPEs typically result in higher surface areas. While it was claimed that the VE used resulted in an increased mechanical rigidity, the polyHIPE was found to have a lower pressure capacity (1 MPa lower than the previous column) [74]. Nevertheless, a high operational flow rate of 1445 cm h^{-1} (4 mL min^{-1}) resulted in the successful baseline resolved separation of Immunoglobulin Y and G from egg yolk and human plasma within 4 min (Figure 1.11), illustrating an absorption capacity of 1.579 mg g^{-1} [80]. The role of VE was to tailor the polyHIPE to have higher working temperatures, mechanical rigidity and alkali pH range [80]. Characterisation of the resulting stationary phase material via SEM (Figure 1.11 (a)) and mercury intrusion porosimetry reported small voids and windows with an average pore diameter was 0.85 µm. Additionally, the surface area of the polyHIPE was found to be 121.96 $m^2 g^{-1}$, confirming that smaller morphological features in polyHIPEs typically result in higher surface areas. The inclusion of VE was suggested to increase mechanical rigidity, but was found to have a lower pressure capacity (1 MPa lower than the previous study) [74], however, the operational flow rate was still 1445 cm h^{-1} (4 mL min^{-1}) for the chromatographic separations [80]. The loading capacity of lysozyme was investigated and was found to have an absorption capacity of 1.579 mg g^{-1}. Immunoglobulin Y and G were successfully separated from egg yolk and human plasma and resulted in a separation within 4 minutes. Though the analysis time increased in comparison to the previous separation and the first analyte (IL-18) again appeared to be unretained the biological analytes were baseline resolved. This highlights the potential of using such highly

porous materials for protein separations with no sample preparation steps before analysis (Figure 1.11 (b)) [80].

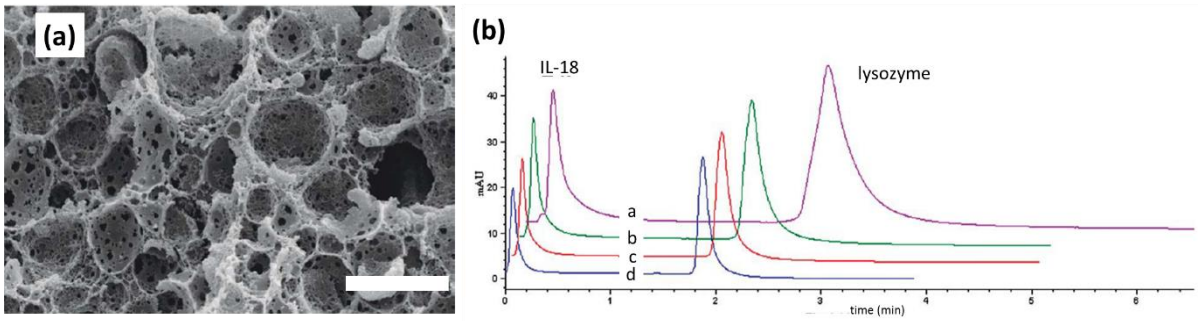

Figure 1.11: *(a) SEM image of poly(VE)-co-EGDMA polyHIPE (Scale bar 10 µm, magnification 3,000x) and (b) Separation of Lysozyme and Interleukin 18 (IL-18) with chromatographic conditions at gradient elution of mobile phase A (0.001 mol/L phosphate buffer at pH 7.8 at 1.5 min), (0.001 mol/L phosphate buffer at pH 7.8 at 1.5 min), mobile phase B (buffer A), mobile phase B (buffer A with 1 mol/L of NaCl added from 30-100% over 1.51 -2.5 min). The different flow rates investigated were (a) 361, (b) 722, (c) 1083, (d) 1445 cm h^{-1} [80].*

As illustrated in the above studies optimising polyHIPE morphologies of has the potential to decrease dispersion effects and increase column efficiency. This would further advance the potential of these materials in protein separations, with high operating flow rates resulting in no mechanical deficiencies and the analysis of direct biological samples successfully demonstrated. The robustness of the materials for long-term analysis also makes the material desirable as a stationary phase. Additionally the functionality of polyHIPE materials has the potential to tailor its selectivity for a particular analyte.

1.4 Conclusion

PolyHIPE materials have promising qualities such as excellent permeabilities, low operating backpressures, higher tolerance of both extreme pH and temperatures and various methods available for tailoring. Surface chemistry of these materials can be modified both prior to and post polymerisation. An area of concern for the application of polyHIPEs are the low surface areas they present. Surface area more importantly should be improved without compromising the material's mechanical rigidity to allow for the materials use as stationary phase materials. Methods such as hypercrosslinking and incorporation of additional porogens is prevalent throughout the literature. However, until recently hypercrosslinking methods could cause Friedel Crafts catalyst to remain on the resulting monolith. Introduction of micropores via additional porogens have to date compromised the rigidity of the final polyHIPE.

It is clear that polyHIPEs have yet to result in superior analytical separations for a range of analyte classes, recent advances in their application are extremely promising in terms of highlighting the separation potential of these materials. To date GMA polyHIPEs have been shown to have successful separations in the literature, however they have also been found to contain craters. Defects in surface morphologies such as craters must be removed to eliminate dispersive effects that many of the polyHIPE materials have demonstrated thus far. Multiple strategies have the potential to ameliorate or even completely alleviate these issues which have not yet been explored. If these issues can be overcome, polyHIPE materials can be successfully applied as stationary phases in separation science. These stationary phases potential can then begin to be fully realised, with their supermacroporous

structure and tailored surface chemistry enabling a superior chromatographic efficiency.

1.4.1 Thesis outline

The purpose of this work was to address and investigate the current limitations of polyHIPE materials as stationary phases in separation science. Limitations investigated include improving surface area of polyHIPE materials and novel modifications of surface chemistry to allow use of polyHIPEs in a wide range of applications. Initially a model polyHIPE that contains minimal surface defects must be fabricated in a suitable housing. Once this is achieved tailoring of the surface area and final surface chemistry of the materials can be investigated.

In *Chapter 2* the fabrication and characterisation of different polyHIPEs using various different monomers in various housings will be investigated. Surface modifications using nanoparticles post and prior to polymerisation will is reported in attempt to improve surface area as well as monolith selectivity. While more hydrophilic monomers produced a greater degree of surface morphology defects such as craters. The PS polyHIPEs fabricated although having low surface areas demonstrated ideal morphologies, and were modified with additional porogen toluene and graphene oxide nanoparticles as a strategy to improve surface areas and selectivity.

PS polyHIPEs fabricated within silcosteel and fused silica housings in *Chapter 2* are subjected to chromatographic separations of the small molecules, alkylbenzenes. In *Chapter 3*, the reproducibility of polymerisation will be characterised using backpressure profiles and van Deemter plots, while their permeabilities will be determined using pressure drop experiments. Chromatographic performance will be

investigated in order to establish the extent of dispersion experienced by the polyHIPE materials.

Chapter 2 demonstrated the fabrication of graphene oxide nanoparticle (GONP) modified polyHIPEs and the unique surface coverage observed. The GONPs are suspected to change the retention factor of the alkylbenzene separation after reduction using ascorbic acid, which is investigated in *Chapter 4*. The preliminary change in physical properties with the inclusion of GONPs outlined in *Chapter 2* were found to give superior absorption properties which are expected to have arisen due to GONP modification.

Chapter 5 investigated the use of unmodified PS polyHIPEs in CEC separations. This study attempted to produce polyHIPE coated columns which would be interesting in the area of food separations, where complex sample matrices are commonplace. However, the coated columns were found to give poor injection-to-injection reproducibility and subsequent blockages resulted from the deterioration of the polyimide coating from ACN.

Finally, conclusions and strategies for future work for polyHIPE materials are outlined in *Chapter 6.*

1.5 References

[1] F. Svec, Journal of Chromatography A, 1217 (2010) 902.

[2] G. Guiochon, Journal of Chromatography A, 1168 (2007) 101.

[3] M.W. Hayman, K.H. Smith, N.R. Cameron, S.A. Przyborski, Journal of Biochemical and Biophysical Methods, 62 (2005) 231.

[4] J. Krenkova, F. Foret, F. Svec, Journal of Separation Science, 35 (2012) 1266.

[5] M. Bencina, A. Podgornik, A. Strancar, Journal of Separation Science, 27 (2004) 801.

[6] A. Zampieri, H. Sieber, T. Selvam, G.T.P. Mabande, W. Schwieger, F. Scheffler, M. Scheffler, P. Greil, Advanced Materials, 17 (2005) 344.

[7] F. Svec, Journal of Separation Science, 27 (2004) 1419.

[8] F. Svec, Journal of Chromatography B-Analytical Technologies in the Biomedical and Life Sciences, 841 (2006) 52.

[9] S. Miller, Analytical Chemistry, 76 (2004) 99 A.

[10] K. Cabrera, Journal of Separation Science, 27 (2004) 843.

[11] D. Lubda, W. Lindner, M. Quaglia, C.D. von Hohenesche, K.K. Unger, Journal of Chromatography A, 1083 (2005) 14.

[12] X. Ma, H. Sun, P. Yu, Journal of Materials Science, 43 (2008) 887.

[13] D. Josic, A. Buchacher, A. Jungbauer, Journal of Chromatography B, 752 (2001) 191.

[14] P.G. Wang, ILM Publications, 2010.

[15] R.D. Arrua, T.J. Causon, E.F. Hilder, Analyst, 137 (2012) 5179.

[16] C.H. Yao, L. Qi, H.Y. Jia, P.Y. Xin, G.L. Yang, Y. Chen, Journal of Materials Chemistry, 19 (2009) 767.

[17] A. Barbetta, N.R. Cameron, Macromolecules, 37 (2004) 3188.

[18] H. Bartl, W. Von Bonin, Makromol. Chem., 57 (1962) 74.

[19] S.D. Kimmins, N.R. Cameron, Advanced Functional Materials, 21 (2011) 211.

[20] N.R. Cameron, D.C. Sherrington, Biopolymers Liquid Crystalline Polymers Phase Emulsion, 126 (1996) 163.

[21] L.L. Schramm, Emulsion, foams and suspensions: Fundamentals and applications, Wiley, Weinheim, 2005.

[22] N. Brun, S. Ungureanu, H. Deleuze, R. Backov, Chemical Society Reviews, 40 (2011) 771.

[23] M.S. Silverstein, Polymer, 55 (2014) 304.

[24] E. Ruckenstein, J.-H. Chen, Journal of Applied Polymer Science, 43 (1991) 1209.

[25] J.M. Williams, Langmuir, 4 (1988) 44.

[26] J.M. Williams, D.A. Wrobleski, Langmuir, 4 (1988) 656.

[27] H. Maekawa, J. Esquena, S. Bishop, C. Solans, B.F. Chmelka, Advanced Materials, 15 (2003) 591.

[28] J.M. Williams, A.J. Gray, M.H. Wilkerson, Langmuir, 6 (1990) 437.

[29] J.M. Williams, Langmuir, 7 (1991) 1370.

[30] R. Butler, I. Hopkinson, A.I. Cooper, Journal of the American Chemical Society, 125 (2003) 14473.

[31] F. Audouin, A. Heise, Polymer, 55 (2014) 403.

[32] P.M. Solozhenkin, A.I. Zouboulis, I.A. Katsoyiannis, Journal of Mining Science, 43 (2007) 212.

[33] S. Yang, L. Zeng, Z. Li, X. Zhang, H. Liu, C. Nie, H. Liu, European Polymer Journal, 57 (2014) 127.

[34] W.C. Griffin, J Soc Cosmetic Chemists, 1 (1946) 311.

[35] S.U. Pickering, Journal of the Chemical Society, Transactions, 91 (1907) 2001.

[36] S. Aland, A. Voigt, Colloids and Surfaces A: Physicochemical and Engineering Aspects, 413 (2012) 298.

[37] B.P. Binks, S.O. Lumsdon, Langmuir, 17 (2001) 4540.

[38] E. Vignati, R. Piazza, T.P. Lockhart, Langmuir, 19 (2003) 6650.

[39] P.J. Colver, S.A.F. Bon, Chemistry of Materials, 19 (2007) 1537.

[40] Y.H. Chen, N. Ballard, F. Gayet, S.A.F. Bon, Chemical Communications, 48 (2012) 1117.

[41] Y.H. Chen, N. Ballard, S.A.F. Bon, Chemical Communications, 49 (2013) 1524.

[42] P. Krajnc, N. Leber, D. Stefanec, S. Kontrec, A. Podgornik, Journal of Chromatography A, 1065 (2005) 69.

[43] S.M. Mousavinasab, I. Meyers, European journal of dentistry, 5 (2011) 299.

[44] T. Scherzer, Applied Spectroscopy, 56 (2002) 1403.

[45] I. Pulko, P. Krajnc, Macromolecular Rapid Communications, 33 (2012) 1731.

[46] R.J. Carnachan, M. Bokhari, S.A. Przyborski, N.R. Cameron, Soft Matter, 2 (2006) 608.

[47] N.R. Cameron, D.C. Sherrington, L. Albiston, D.P. Gregory, Colloid and Polymer Science, 274 (1996) 592.

[48] Phenomonex, 2013.

[49] S.M. Lai, Y.C. Liao, T.W. Chen, Polymer Engineering and Science, 45 (2005) 1461.

[50] J. Urban, F. Svec, J.M.J. Frechet, Analytical Chemistry, 82 (2010) 1621.

[51] A.Y. Sergienko, H.W. Tai, M. Narkis, M.S. Silverstein, Journal of Applied Polymer Science, 94 (2004) 2233.

[52] K. Jeřábek, I. Pulko, K. Soukupova, D. Štefanec, P. Krajnc, Macromolecules, 41 (2008) 3543.

[53] N.R. Cameron, A. Barbetta, Journal of Materials Chemistry, 10 (2000) 2466.

[54] M.G. Schwab, I. Senkovska, M. Rose, N. Klein, M. Koch, J. Pahnke, G. Jonschker, B. Schmitz, M. Hirscher, S. Kaskel, Soft Matter, 5 (2009) 1055.

[55] J. Urban, F. Svec, J.M.J. Frechet, Journal of Chromatography A, 1217 (2010) 8212.

[56] U. Sevšek, J. Brus, K. Jeřabek, P. Krajnc, Polymer, 55 (2014) 410.

[57] M. Susec, S.C. Ligon, J. Stampfl, R. Liska, P. Krajnc, Macromolecular Rapid Communications, 34 (2013) 938.

[58] I.A. Katsoyiannis, A.I. Zouboulis, Water Research, 36 (2002) 5141.

[59] E.H. Mert, M.A. Kaya, H. Yildirim, Designed Monomers and Polymers, 15 (2012) 113.

[60] C.H. Yao, L. Qi, J.A. Qiao, H.Z. Zhang, F.Y. Wang, Y. Chen, G.L. Yang, Talanta, 82 (2010) 1332.

[61] C.H. Yao, L. Qi, G.L. Yang, F.Y. Wang, Journal of Separation Science, 33 (2010) 475.

[62] Y. Tunc, C. Golgelioglu, N. Hasirci, K. Ulubayram, A. Tuncel, Journal of Chromatography A, 1217 (2010) 1654.

[63] S.T. Beatty, R.J. Fischer, D.L. Hagers, E. Rosenberg, Industrial & Engineering Chemistry Research, 38 (1999) 4402.

[64] C. Xiong, C. Yao, Chemical Engineering Journal, 155 (2009) 844.

[65] R. Say, N. Satiroolu, E. Piskin, S. Bektas, O. Genc, Analytical Letters, 31 (1998) 511.

[66] A.R. Reddy, K.H. Reddy, Proceedings of the Indian Academy of Sciences-Chemical Sciences, 115 (2003) 155.

[67] M.M. Benjamin, R.S. Sletten, R.P. Bailey, T. Bennett, Water Research, 30 (1996) 2609.

[68] H. Nishide, E. Tsuchida, Makromolekulare Chemie-Macromolecular Chemistry and Physics, 177 (1976) 2295.

[69] B.C. Benicewicz, G.D. Jarvinen, D.J. Kathios, B.S. Jorgensen, Journal of Radioanalytical and Nuclear Chemistry, 235 (1998) 31.

[70] I. Pulko, V. Smrekar, A. Podgornik, P. Krajnc, Journal of Chromatography A, 1218 (2011) 2396.

[71] U. Sevsek, P. Krajnc, Reactive & Functional Polymers, 72 (2012) 221.

[72] I. Pulko, M. Kolar, P. Krajnc, Science of the Total Environment, 386 (2007) 114.

[73] E. Hollink, S.E. Tichy, E.E. Simanek, Industrial & Engineering Chemistry Research, 44 (2005) 1634.

[74] J. Yang, G.L. Yang, H.Y. Liu, L.G. Bai, Q.X. Zhang, Chinese Journal of Chemistry, 28 (2010) 229.

[75] S. Kovacic, P. Krajnc, Journal of Polymer Science Part a-Polymer Chemistry, 47 (2009) 6726.

[76] H. Inoue, K. Yamanaka, A. Yoshida, T. Aoki, M. Teraguchi, T. Kaneko, Polymer, 45 (2004) 3.

[77] C. Yu, F. Svec, J.M.J. Frechet, Electrophoresis, 21 (2000) 120.

[78] G.C. Ping, L.H. Zhang, L. Zhang, W.B. Zhang, P. Schmitt-Kopplin, A. Kettrup, Y.K. Zhang, Journal of Chromatography A, 1035 (2004) 265.

[79] Y. Tunç, Ç. Gölgelioğlu, N. Hasirci, K. Ulubayram, A. Tuncel, Journal of Chromatography A, 1217 (2010) 1654.

[80] J. Yang, G. Yang, H. Liu, L. Bai, Q. Zhang, (2011).

[81] Y. Tunc, C. Golgelioglu, A. Tuncel, K. Ulubayram, Separation Science and Technology, 47 (2012) 2444.

[82] J.M. Hughes, P.M. Budd, K. Tiede, J. Lewis, Journal of Applied Polymer Science, 132 (2015).

[83] A.J. Atkinson, W.A. Colburn, V.G. DeGruttola, D.L. DeMets, G.J. Downing, D.F. Hoth, J.A. Oates, C.C. Peck, R.T. Schooley, B.A. Spilker, J. Woodcock, S.L. Zeger, G. Biomarkers Definitions Working, Clinical Pharmacology & Therapeutics, 69 (2001) 89.

[84] S. Jerenec, M. Simic, A. Savnik, A. Podgornik, M. Kolar, M. Turnsek, P. Krajnc, Reactive & Functional Polymers, 78 (2014) 32.

[85] C. Martin, J. Coyne, G. Carta, Journal of Chromatography A, 1069 (2005) 43.

Chapter Two

The fabrication and characterisation of polyHIPE materials for application in liquid chromatography

*“One never notices what has been done; one can only see what remains to be done.”***-**

Marie Curie.

2. Aim

This chapter details the fabrication of numerous polyHIPEs comprising of different functional monomers. PolyHIPE modifications both during and post fabrication were investigated. In addition, morphologies and surface areas of the materials were varied to determine their applicability as a chromatographic stationary phase. The materials developed in this chapter include an aminated GMA-*co*-EGDMA polyHIPE agglomerated with gold NPs, VBC-*co*-DVB polyHIPEs and PS-*co*-DVB polyHIPEs of varying porosity, addition of porogen toluene and addition of GONPs.

2.1 Introduction to polyHIPE modification strategies

PolyHIPE materials have significant potential as analytical stationary phases. They typically exhibit a pore size ranging from 10-100 µm in diameter [1]. This large pore size facilitates higher permeability, low backpressures and analysis of complex matrices without purification [2-6]. However, a major disadvantage of these materials is the issue of low surface area, typically in the range of 20 m^2 g^{-1} [7]. To successfully apply these materials as separation media, the problem of low surface area must be overcome. Methods of surface modification can be carried out either prior to polymerisation or after polymerisation has occurred. This chapter will detail modification strategies undertaken in order to obtain a high surface area polyHIPE. All fabricated materials were characterised visually using Atomic force microscopy (AFM), FESEM and SEM, while surface areas were determined using BET and thermal stabilities were measured by Thermal gravimetric analysis (TGA).

2.1.1 Modifications prior to polymerisation

2.1.1.1 Tailoring the surface chemistry

Hydrophobic materials such as C18 bonded stationary phases are the most commonly used in reverse phase chromatography. PolyHIPE materials can be fabricated out of hydrophobic monomers such as Sty and VBC with hydrophobic crosslinkers such as DVB and alkylmaleimide. Increasing their applicability as stationary phases, more hydrophilic monomers such as GMA, AAm, HEA and HEMA generally incorporated with crosslinkers such as EGDMA and PVA (polyvinyl alcohol) can be used to impart a polar functionality [8-10]. While the aforementioned types of polyHIPEs are the most commonly fabricated, polyHIPEs have also been formed using inorganic oxides such as silica, titania, zirconia and alumina [11-14]. In addition,

polyHIPEs using gold [15], nickel [16] and carbon [17] can be fabricated. Such exotic polyHIPEs could be applied in alternative modes of separations due to their change in surface chemistry. In this chapter, reactive groups present in the functional monomers were used to tailor the polyHIPE surface chemistry. As two main classes of analytical stationary phase identified were polar and hydrophobic, polyHIPEs with polar groups such as GMA-*co*-EDGMA and VBC-*co*-DVB and hydrophobic PS-*co*-DVB polyHIPEs were fabricated.

2.1.1.2 Increasing surface area by porogen addition

A popular method to alter polyHIPE morphology is to introduce additional porogens into the organic phase of the polyHIPE. A change in morphology is observed as an increase of the number of interconnecting windows present in a polyHIPE as well as the introduction of micropores (pore size less than 2 nm) [18]. The production of micropores introduces a surface roughness increasing surface area; however, an optimal porogen ratio is required for an appropriate formulation to maintain a polyHIPE's structural rigidity. Most studies of this nature have included the addition of toluene, 1-chloro-3-phenyl-propane, chlorobenzene and 2-chloroethylbenzene in A/O emulsions as they are soluble within the organic phase [18]. The incorporation of such porogens have been extensively studied with DVB based polyHIPEs. Early studies show an increase in surface area when using PS-*co*-DVB polyHIPEs however no pressure measurements have been carried out on these materials [19]. Recent studies also show incorporation of toluene as a porogen in GMA-*co*-DVB polyHIPE materials, again resulting in high surface area materials. Despite the high surface area reported, to date the mechanical rigidity of the final polyHIPEs have not been explored [20]. In this study, the inclusion of toluene in PS-*co*-DVB polyHIPEs was investigated. The porogen, toluene, was incorporated prior to polymerisation to determine its effect on

surface area and its mechanical rigidity as a stationary phase material before assessing the separation capacity of these materials in Chapter 3.

2.1.1.3 Increasing surface area by Nanoparticle (NP) addition

In most cases, NPs are included in polyHIPE emulsions as an emulsion stabiliser, however, they also have the potential to increase surface area and alter surface chemistry [21-23]. NP-stabilised emulsions are referred to as Pickering emulsions. As well as acting as an emulsion stabiliser, Pickering emulsions are used to impart a greater mechanical stability to polyHIPEs [24-26]. The exploration of NPs as a method to both increase surface area and alter selectivity of polyHIPE materials has not yet been developed for separations. Generally, NPs are added in place of a surfactant and coagulate around the organic-aqueous interface in an emulsion, subsequently reducing surface tension. The dominating morphology visualised in such materials is a closed pore structure. In closed pore structures, there are little to no interconnecting pores, which leads to poor permeability [22, 27, 28]. In addition to poor permeability, the closed pore morphology would hinder a separation process by adding a high level of dispersive effects. However, open pore structures using Pickering emulsions have also been studied. One method used to fabricate open pore structures involves the use of NPs to form HIPE gels [29, 30]. The presence of NPs on the surface of the final material has been demonstrated using MnO_2 NPs [31], Fe_2O_3/Fe_3O_4 and ZnO NPs [28, 32]. These recent advances highlight the potential of NP incorporated polyHIPEs to increase surface area and modify selectivity of the materials as a stationary phase. In this chapter, a detailed study using graphene oxide NPs to alter physical properties of polyHIPE materials for separations is discussed.

2.1.2 Modifications post polymerisation

While modification during polymerisation can negatively impact pore morphology and structural rigidity as this involves altering an emulsion formulation, nonetheless, these limitations can be overcome by modifying the material post polymerisation. Specifically, when using supermacroporous materials as a stationary phase it is important that the morphology is consistent with little or no evidence of extremely large pores or craters. This is to ensure high permeability and reduced dispersive effects to minimise band broadening when employed as stationary phase. In the following sections, the most common post polymerisation techniques are discussed briefly.

2.1.2.1 Increasing surface area by hypercrosslinking via Friedel-Crafts reaction

Friedel-Crafts hypercrosslinking reactions are among the most widely utilised mechanisms to increase surface area post polymerisation. They have previously been found to increase the surface area of polyHIPEs by up to 1210 m^2 g^{-1} [33]. While external electrophiles can be included, typically it is easier to use an electrophile already present within the polymeric network [33-35]. VBC polyHIPEs which contain an internal electrophile have therefore been most commonly utilised in this strategy of surface modification. Although high surface areas result from this method of modification, there are still disadvantages with respect to final material purity. The excess catalyst present on the surface of the polyHIPEs, if used as a stationary phase, can potentially hinder the separation process. This could happen where the excess catalyst desorbs from the material, passes through the column with the sample analytes or causes unspecific adsorption of sample molecules. Recently, hypercrosslinking studies without using an iron catalyst resulted in cleaner final

polyHIPE material. In such studies, the polyHIPE materials are swollen with solvent and crosslinked again before washing, enabling crosslinks to form between polymer chains in the material [36].

2.1.2.2 Surface treatment of polyHIPEs post polymerisation

In addition to hypercrosslinking, polyHIPE materials have undergone surface treatments such as sulfonation and amination extensively in the literature as a method to increase surface area [37-39]. In particular, hydrophobic supports have previously been used for ion exchange after sulphonation or as reverse phase stationary phases [40]. Addition of sulfonate groups and amine groups to the final material renders the polyHIPE positively or negatively charged respectively. Once modified, the potential attachment of many types of ligands and NPs can be achieved. Throughout the literature, polyHIPEs have had various types of ligand modification [37-39]. However, there are no reports of adsorption of NPs to polyHIPEs in the literature. In this chapter, the fabrication of polyHIPEs that were aminated and modified using NPs is discussed, and their applications as stationary phases is explored in Chapter 4.

2.2 Materials

Millipore ultrapure water purified to a resistance of >18 MΩcm was used throughout. Calcium dihydrochloride >99% and Span ®80 were purchased from Fluka (Sigma Aldrich, Tallaght Ireland). Toluene anhydrous ≥99.8% and anhydrous iron (iii) chloride were purchased from Riedel de Haën (Sigma Aldrich, Tallaght Ireland). 3-Glycidoxypropyl-trimethoxysilane ≥98%, glycidyl methacrylate (GMA), potassium persulphate (KPS), Sty ≥99%, DVB 80% isomeric mix, 4-vinylbenzyl chloride (VBC) 90%, 1, 2-dichloroethane, ethylene glycol dimethacrylate (EGDMA) 98%, pluronic® L-121, and gold (iii) chloride trihydrate ≥99.9% were all purchased from Sigma Aldrich

(Tallaght Ireland). All other chemicals were of analytical grade and were used as received. All solvents used were analytical HPLC grade. All fused silica tubing (100 and 250 µm in I.D.) was supplied by CM Scientific (West Yorkshire UK) and silcosteel tubing (1.02 mm and 2.16 mm in I.D.) was supplied by RESTEK (Belfast, Northern Ireland). An aqueous solution of graphene oxide nanoparticles (GONPs) at quoted 450 nm in size and of 2 mg mL^{-1} in concentration was donated by the University of Wollongong and was used as received.

2.2.1 Instrumentation

All morphological characterisation was carried out using a Hitachi S-3400N scanning electron microscope and all samples were gold sputtered using a 750T sputter coater, Quorum Technologies (UK). All Field emission electron microscope (FESEM) samples were examined using Hitachi S-5500 (DCU) and Hitachi S-7000 (University of Tasmania). All surface area measurements were obtained using a Micrometrics surface area analyser (Gemini 2360). TGA was carried out using a Setaram LabSys Evo with aluminium crucibles, samples were held at 60°C for 20 minutes before applying a temperature ramp of 10°C min^{-1}. A Knauer Smartline 100 pump was used for washing the prepared monoliths within silcosteel and fused silica tubing and a KD scientific syringe pump was used for all flow-through operations. Malvern Zetasizer (NanoZS) was used for particle size analysis at 0.01 absorption and refractive index of 1.33 for graphene oxide.

2.2.2 Methods

2.2.2.1 Tubing modifications

2.2.2.1.1 Silanisation of fused silica capillary

Fused silica capillary of I.D. 100 µm and 250 µm was prepared by washing with acetone for 5 minutes and then dried using a stream of nitrogen gas for 10 minutes. The dried capillary was then treated using 0.2 *M* NaOH for 30 minutes, and then rinsed with water for 5 minutes before treating with 0.2 *M* HCl for 5 minutes. Finally, the capillary was washed with water and then acetone for 5 minutes each before drying with nitrogen for 10 minutes. The procedures above were carried out at a flow rate of 1 µL min^{-1} using a syringe pump. The capillary was filled with 50% v/v solution of 3-(trimethoxysilyl) propyl methacrylate in acetone until all air was expelled. The capillary was end capped using silicone septa. Polymerisation was carried out in a water bath at 60°C for 20 hours. After polymerisation was complete, the silanised fused silica capillary was rinsed with acetone for 5 minutes at 1 µL min^{-1} before drying with nitrogen.

2.2.2.1.2 Silanisation of silcosteel tubing

Silcosteel tubing of I.D. 1.02 mm and 3.18 mm was prepared by washing with acetone for 10 minutes and then dried using a stream nitrogen gas for 20 minutes. The dried tubing was then treated using 0.2 *M* NaOH for 1 hour and rinsed with water for 10 minutes before treating with 0.2 *M* HCl for 10 minutes. Finally, the capillary was washed with water and then acetone for 10 minutes each before drying with nitrogen for 20 minutes. The above procedures were carried out at a flow rate of 3 µL min^{-1} using a syringe pump. The tubing was attached to sacrificial pieces of PEEK tubing (Figure 2.1) at each end and was filled with a 50% v/v solution of 3-

(trimethoxysilyl)propyl methacrylate in acetone until all air was expelled. The capillary was end capped using a union endcap. Polymerisation was carried out in a water bath at 60°C for 20 hours. After polymerisation was complete, the silanised fused silica capillary was rinsed with acetone for 5 minutes at 3 µL min^{-1} before drying with nitrogen.

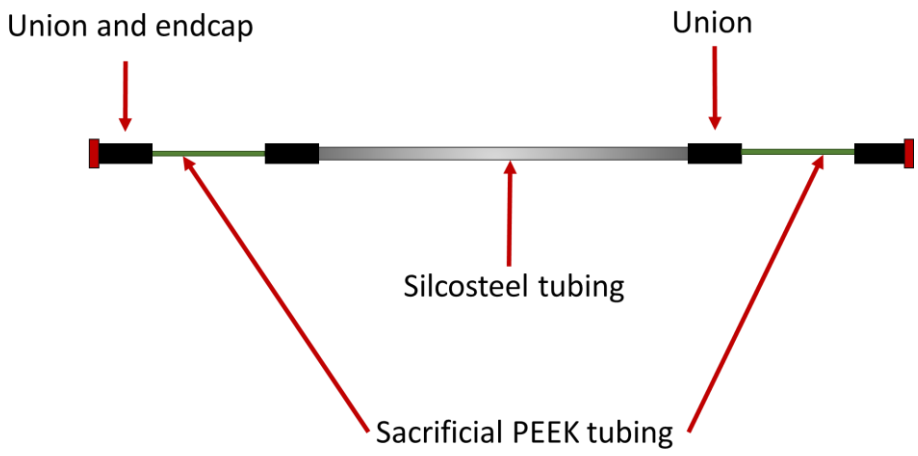

Figure 2.1: *Diagram of the 100 mm x 1.02 mm column after silanising agent is added to the housing.*

2.2.2.1.3 Modification of PEEK tubing for monolith attachment

The internal walls of the PEEK tubing were modified via sulphonation and reacted with GMA as previously described [41]. Briefly, 1/16" I.D. PEEK tubing was filled with 50% sulphuric acid, encapped and left to stand for 6 hours. The PEEK tubing was then washed with water before filling the tubing with 1 *M* GMA in acetone followed by endcapping and held at room temperature for 4 hours. The tubing was then rinsed with acetone and dried under a stream of nitrogen gas.

2.2.3 Material preparation

2.2.3.1 Preparation of 90% porosity GMA-co-EDGMA polyHIPEs

The formulation and procedure for the GMA-*co*-EDGMA polyHIPE was adapted from the literature [42]. The organic phase was prepared by adding 2.32 mL glycidyl methacrylate, 1.07 mL EDGMA and 0.715g pluronic PL21 into a sample vial and homogenised with a vortex. The aqueous phase was prepared by dissolving 0.0744 g of potassium persulphate with 0.5130 g of calcium dihydrogen chloride in 15 mL water in a sample vial. The organic phase was transferred into a 3 neck round bottomed flask where the central neck was attached to an overhead stirrer including a d-paddle. One of the two remaining necks was attached to a N_2 line and the other was sealed using a rubber septa. The aqueous phase was added dropwise to the organic phase with a stirring rate of 350 rpm. After the aqueous phase was added, the emulsion was left stirring for 30 minutes and then transferred into a suitable container for polymerisation (HPLC vials or PEEK tubing) and polymerised for 48 hours at 60°C. After polymerisation, the polyHIPE was washed with water and then EtOH in batch format before storing in a sample vial.

2.2.3.2 Modification of GMA-co-EDGMA polyHIPE with diethylamine and subsequent attachment of gold NPs

The resulting polyHIPEs were aminated by immersing the polyHIPEs in 1 *M* DEA solution and heating to 60°C for 16 hours. After the amination step, the polyHIPEs were washed with copious amounts of DI water until neutralised. To enable gold NP attachment the polyHIPEs were dried overnight in a 60°C oven before being added to a stirring solution of gold NPs in a beaker. The colour change of the polyHIPE from

white to red/purple indicated successful attachment of gold NPs. The gold NPs used were of 20 nm in size.

2.2.3.3 Preparation of 90% porosity VBC-co-DVB polyHIPEs and incorporation of styrene

The organic phase was prepared by adding 2 mL VBC, 1.332 mL DVB and 0.656 g Span 80® into a sample vial followed by homogenisation with a vortex. The aqueous phase was prepared by dissolving 0.0666 g of potassium persulphate with 0.3332 g calcium dihydrogen chloride in 30 mL of water in a sample vial. The monomers used were purified via liquid-liquid extraction (LLE) using 6% NaOH aqueous solution to remove any inhibitors present that would result in impurities in the resulting polyHIPE. Both the organic phase and aqueous phase were purged with N_2 gas for ten minutes. The organic phase was transferred into a 3 neck round bottomed flask where the central neck was attached to an overhead stirrer including a d-paddle. One of the two remaining necks was attached to a N_2 line and the other was sealed using a rubber septa. The emulsion preparation was carried out as outlined in the previous Section ***2.2.3.1*** above in 1.5 mL centrifuge tubes and 100 µm I.D. fused silica capillary. After polymerisation, the polyHIPE was washed with MeOH and the bulk material was Soxhlet extracted for 48 hours with MeOH. The resulting capillary columns were washed with ACN (24 hours). When Sty monomer was incorporated, the VBC volume decreased e.g. 50:50 Sty: VBC was 1 mL Sty and 1 mL VBC while the remaining emulsion components remained the same.

2.2.3.4 Preparation of varying porosities of (PS-co-DVB) polyHIPEs

The emulsion preparation of the PS-*co*-DVB polyHIPE was adapted as per procedure outlined [43]. Briefly, for a 90% polyHIPE the emulsion consisted of two

phases, the aqueous phase (15 mL ultrapure DI water, KPS 0.03 g and calcium chloride dihydrate 0.10 g) and the organic phase (Sty 1.333 mL, DVB 0.333 mL and Span 80® 0.329 g). Porosities of 75%, 80% and 90% were also investigated. The aqueous and organic phase ratios were adjusted according to the previous procedure. Both phases were prepared separately and homogenised by vortex. The organic phase was placed into a 250 mL round bottomed flask that was connected to the overhead stirrer and a nitrogen supply. The overhead stirrer was set to 350 rpm and the aqueous phase was added drop-wise using a hypodermic syringe. The white emulsion that formed upon addition of the aqueous phase was left to stir for 20 minutes. The emulsion was transferred into a suitable column housing (fused silica capillary or silcosteel) and the remaining emulsion transferred into 1.5 mL centrifuge tubes for characterisation. After polymerisation was complete, the resulting polyHIPE was washed with MeOH for 48 hours using a Soxhlet apparatus.

2.2.3.5 Preparation of polystyrene-co-divinylbenzene (PS-co-DVB) polyHIPEs in fused silica capillaries and silcosteel tubing

The emulsion was prepared as outlined in Section ***2.2.3.4***. The capillary was filled using a syringe containing the emulsion until all air had been expelled and the emulsion began to exit from the outlet side of the capillary. The capillary was sealed using silicone septa and polymerised at 60°C for 48 hours.

To polymerise the emulsion in a 1.02 mm I.D. silcosteel column, sacrificial PEEK tubing was added to each end of the column in order to reduce any voids that could occur along the column (Figure 2.1). The column was filled using a syringe vertically positioned so any air that was present could rise to the top into the tubing to avoid formation of voids. The PEEK tubing was sealed using a union and endcap

fitting, whereby the end unions were filled with emulsion to reduce any void developments. The emulsion was polymerised as per previous polymerisation conditions.

To fill the larger bore silcosteel tubing (2.16 mm) teflon tubing was attached in lieu of PEEK to each end of the column. The tubing was not sealed but the flow of emulsion was intercepted by mechanical clamping. The emulsion in this housing format required polymerisation at a higher temperature of 75ºC for 48 hours.

2.2.3.6 Preparation of PS-co-DVB polyHIPEs with additional porogens

PolyHIPEs were made in bulk and capillary format by adapting the procedure for PS-*co*-DVB materials of lower toluene addition from 2 to 12% and higher toluene additions of 25, 50 and 75%. The materials varied in degree of porogen added, where 100% additional porogen would be equal to the quantity of crosslinker in the organic phase [18]. For a 90% polyHIPE with 100% toluene addition the aqueous phase comprised of 15 mL ultrapure DI water, KPS 0.03g and calcium chloride dehydrate 0.10 g and the organic phase included DVB 0.333 mL, toluene 0.333 mL and Span 80® 0.329 g. The emulsion preparation and Soxhlet extraction methods were carried out as outlined in Section ***2.2.3.4*** in 1.5 mL centrifuge tubes.

2.2.3.7 Preparation of GONP modified PS-co-DVB polyHIPEs

The emulsion was prepared as outlined in Section ***2.2.3.4*** with some exceptions including the time of stirring and the addition of graphene oxide nanoparticles were added. The emulsion was left stirring for 10 minutes after complete aqueous phase addition. Then the addition of GONPs at concentrations of 13, 20, 33 and 66 ppm relative to the aqueous phase were added to the emulsion under mechanical stirring and left to stir for 5 minutes. The emulsions produced were polymerised in batch and

capillary format (250 µm I.D.) as per Section ***2.2.3.5*** a polyHIPE with 20 ppm GONPs was labelled as GOPSDVB as the prefix and 20 as the suffix resulting in GOPSDVB20. This is the naming convention used throughout this work.

2.3 Results and discussion

2.3.1 Characterisation of GMA-*co*-EGDMA monolith fabricated within PEEK tubing

As discussed in Section ***2.1.1.1***, GMA-*co*-EDGMA polyHIPEs have been shown to be successful polyHIPE skeletons for surface modifications. Using sulphonated PEEK tubing as a mould, GMA-*co*-EGDMA polyHIPEs were prepared in accordance with Section ***2.2.3.1*** and imaged via SEM as shown in Figure 2.2. The SEM images below illustrate the unique morphology obtained, which was similar to morphology reported by Krajnç *et al.* [42]. In the polyHIPEs prepared in our research, a number of voids were prominent within the polyHIPE morphology, however, few if any interconnecting windows were present. It was observed that the polyHIPE within the PEEK tubing did not bind to the inner walls of the tubing.

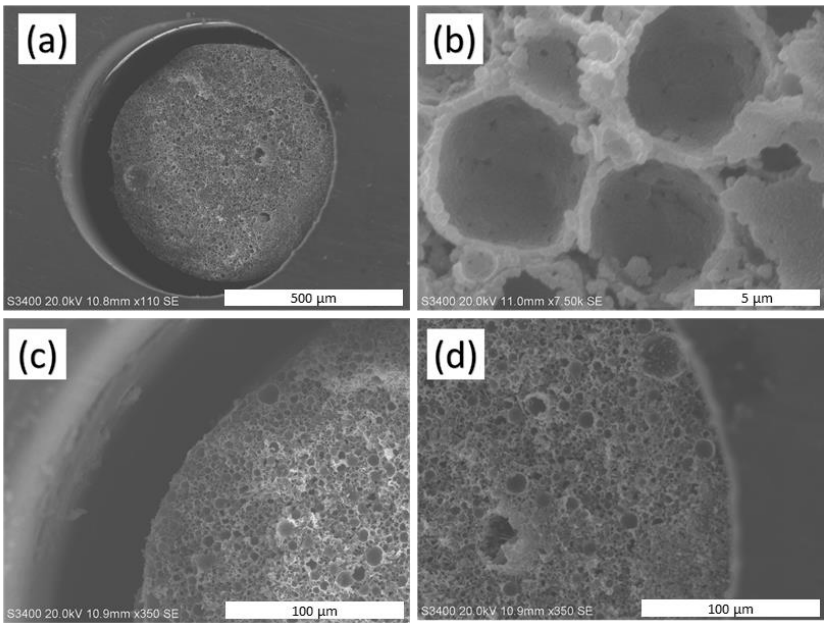

Figure 2.2: *SEM images of GMA-co-EGDMA polyHIPE showing (a) polyHIPE within PEEK tubing of 50 mm x 1.02 mm I.D., (b) morphology of the resulting polyHIPE, indicating the lack of flow through pores (c) polyHIPE unattached to PEEK interior wall and (d) area where the polyHIPE appears to have attached to the interior wall of PEEK tubing. Magnification: (a) 110x, (b) 7,500x, (c) 350x and (d) 350x.*

In Figure 2.2 (a) and 2.2 (c) presented below it could be seen that the polyHIPE contracted away from the tubing wall. This contraction was most likely due to shrinkage induced by polymerisation [44]. This was confirmed by the application of pressure while washing the resultant polyHIPE in PEEK tubing (50 mm x 1.02 mm I.D.) with MeOH, which resulted in emergence of the polyHIPE from the column before finally, complete detachment from the column housing due to insufficient binding to the housing walls. Moreover, as shown in Figure 2.2 (b) and (d) the low occurrence of interconnecting pores indicates the likelihood of a low permeability polyHIPE, reducing the material's suitability as a stationary phase.

As the polyHIPE prepared in PEEK tubing exhibited unfavourable morphologies (e.g. lack of interconnecting pores), the corresponding polyHIPEs prepared in the more facile bulk format were employed to determine of their potential for surface modification. Upon processing the bulk monolith for surface modification with DEA (Figure 2.3) and the subsequent addition to a gold NP suspension (20 nm in size) as per Section ***2.2.3.2***, the external surface of the polyHIPE appeared to be modified (Figure 2.4). This was confirmed by the change in colour of the monolith exterior from white to purple (Figure 2.4 (a)). The gold solution did not permeate into the interior region of the polyHIPE, however, as evidenced by the absence of colour changes, Figure 2.4 (b). It was hypothesised that this was due to the absence of an applied pressure during modification, meaning the polyHIPE did not absorb the amination solution. Additionally the bulk material suffered from a lack of interconnecting pores within the polyHIPE that restricted amination to the exterior surface. Without amination of the interior section of the polyHIPE material, no functional groups were present to enable gold NP attachment.

Fundamentally, the lack of interconnecting pores within the polyHIPE would severely inhibit interaction of analytes flowing through the material as well as restrict their surface modification. Thus, there was little potential of the material resulting in a successful stationary phase for liquid chromatography. For these reasons, this material was not pursued any further.

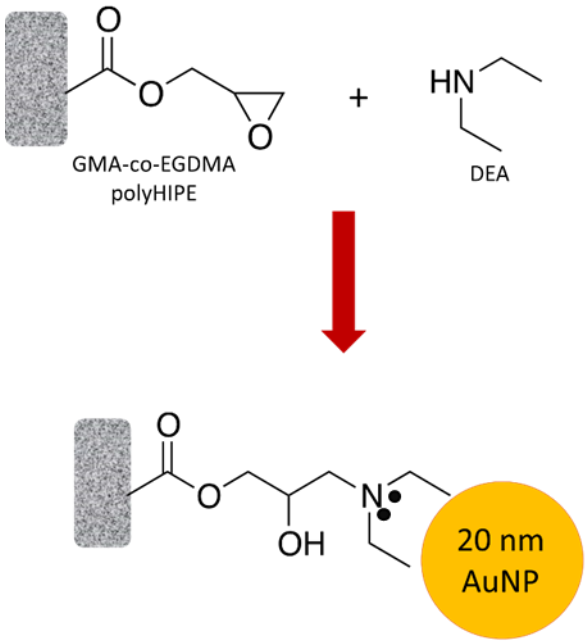

Figure 2.3: *Reaction scheme for the amination of GMA-co-EGDMA polyHIPE and subsequent gold NP attachment.*

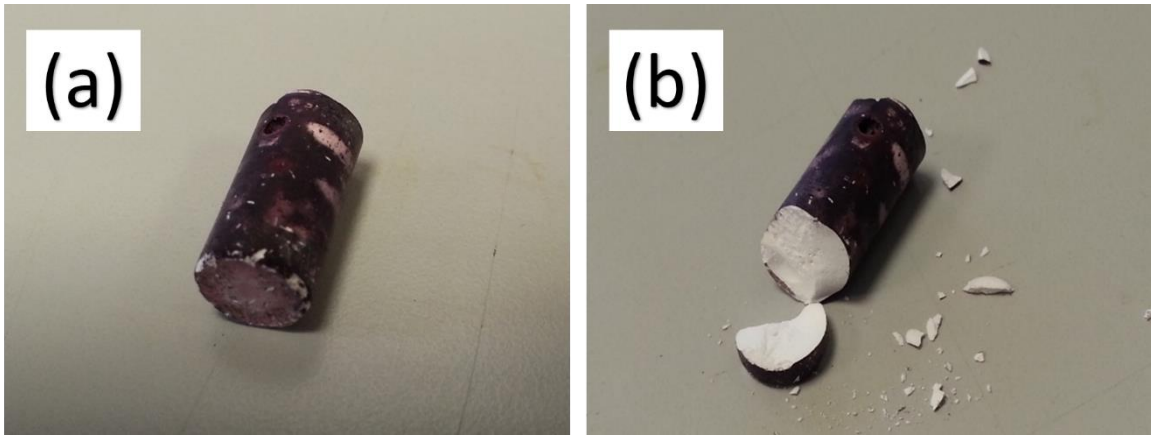

Figure 2.4: *Digital image of (a) exterior of GMA-co-EDGMA polyHIPE aminated and modified with gold NPs (b) white interior of polyHIPE where amination and gold NP attachment was not successful.*

2.3.2 VBC monoliths fabricated within fused silica capillary

2.3.2.1 SEM characterisation of VBC monoliths fabricated within fused silica capillary

VBC monoliths are hydrophobic in nature and therefore, have potential application in reversed phase chromatography. The preparation of a VBC-*co*-DVB polyHIPE according to Section ***2.2.3.3*** resulted in the morphology shown in SEM images in Figure 2.5. This morphology was reproducibly obtained with successive fabrications despite purifying and deoxygenating the monomers prior to use. The VBC polyHIPE was fabricated within fused silica capillary (250 µm I.D.) and as illustrated, large craters (voids with little or no interconnecting pores) were present in the material. These craters were thought to be resultant of bubbling of the emulsion during the polymerisation process. In addition, many of the craters formed did not appear to contain any interconnecting windows. In contrast, SEM images of VBC polyHIPEs in the literature did not contain comparable craters and comprised of a homogenous pore distribution [33, 35, 45, 46]. Despite no mention of these craters within any studies involving VBC polyHIPEs, it was noted that none of the SEM images were taken at a low magnification as in Figure 2.5. It is possible that the authors could have overlooked areas with craters, as the polyHIPEs were not used for chromatographic separations.

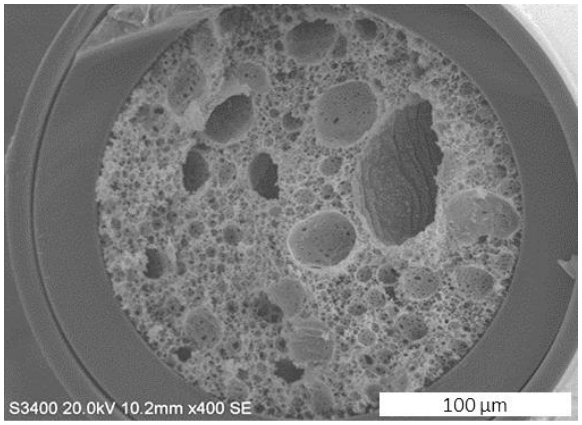

Figure 2.5: *SEM image of craters representative of those present in all similar polyHIPEs fabricated in a 90% porosity VBC-co-DVB polyHIPE in a 250 µm fused silica capillary. Magnification: 400x.*

In an attempt to overcome the crater formation, the Sty monomer was added to the emulsion. Sty has been used throughout the literature detailing high internal phase emulsions; styrenic polyHIPEs previously reported have a homogenous structure with few if any craters present in the material skeleton [18, 43, 47]. For this reason, it was hypothesised that the addition of Sty to the VBC polyHIPE would improve the surface morphology of the polyHIPE (prepared as per Section ***2.2.3.3***). Unfortunately, this was not the case. Encouragingly, as can be seen from Figure 2.6 (a)-(c), as the percentage of Sty was increased, both the size and frequency of the craters decreased. While at 25% Sty, numerous craters were still evident, at 75% Sty in some areas craters were no longer observed. Unfortunately, at 75% Sty, in some areas Sty aggregates were also seen, as illustrated in Figure 2.6 (d). In a similar manner to craters, this could have an adverse effect of the separation efficiencies of a polyHIPE and perhaps encourage undesired alternative retention mechanisms when applied as a stationary phase. As polyHIPE materials could not be fabricated using VBC which did not contain either craters or aggregates, this monomer was therefore no longer investigated.

However, further investigation into the use of polystyrene polyHIPEs was undertaken due to the open void and interconnecting window morphology that was observed to exist in the literature [18, 43, 47].

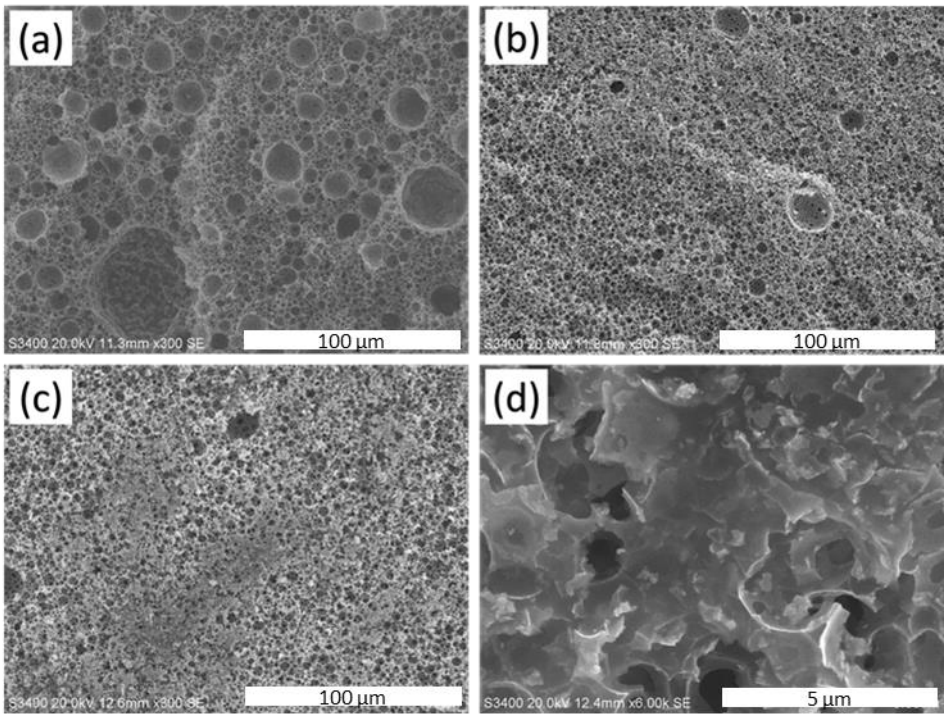

Figure 2.6: *SEM images of 90% porosity of PS-VBC-co-DVB polyHIPEs at different percentages of Sty where (a) 25% (b) 50% (c) 75% and (d)75% aggregates of Sty in resulting polyHIPE. Magnification (a)-(c) 300x and (d) 6,000x.*

2.3.3 Polystyrene polyHIPEs

2.3.3.1 SEM characterisation of PS-co-DVB polyHIPE with various aqueous phase percentages

PS polyHIPEs are hydrophobic and typically possess an open void and interconnecting window morphology and so have great potential as chromatographic stationary phases. In this study, in addition to examining the typical 90% PS-*co*-DVB polyHIPEs that are observed throughout the literature, the aqueous phase ratios of the

materials were varied. Emulsions were fabricated to produce 75%, 80% and 90% porosities of PS-*co*-DVB polyHIPEs as shown in SEM and AFM images in Figure 2.7. Here, the dependencies of the polyHIPE morphology on the aqueous phase ratios during fabrication was explored. It was expected that when the aqueous phase percentage was decreased, the voids and interconnecting windows also decreased in size. From the SEM images, it was noted that as expected, decreasing aqueous phase porosities resulting in a significant difference in morphology. Firstly, a lower occurrence of the interconnecting windows was observed as the concentration of the monomers were increased. The formation of these windows is a topic highly debated within the field of polyHIPEs, with two main hypothesises emerging. Menner and Bismarck speculated that the formation of the pores occurred post polymerisation, during the washing and drying steps [48]. In contrast, Cameron proposed that the interconnecting windows were formed during polymerisation, arising due to the difference in densities between the organic and aqueous phases. Cameron later proved his hypothesis using cryo-SEM images where he demonstrated that as the aqueous phase ratio was decreased, a significant difference between the densities of the organic and aqueous phases existed [18, 49-51]. This phenomenon could possibly explain the lower number of windows present within the voids of the polyHIPEs. Similar results were reported where the only difference in the polyHIPE formulation was that chlorobenzene was used as an organic phase porogen [18]. However, the aforementioned study using chlorobenzene as a porogen resulted in a decrease of window size as the aqueous phase decreased.

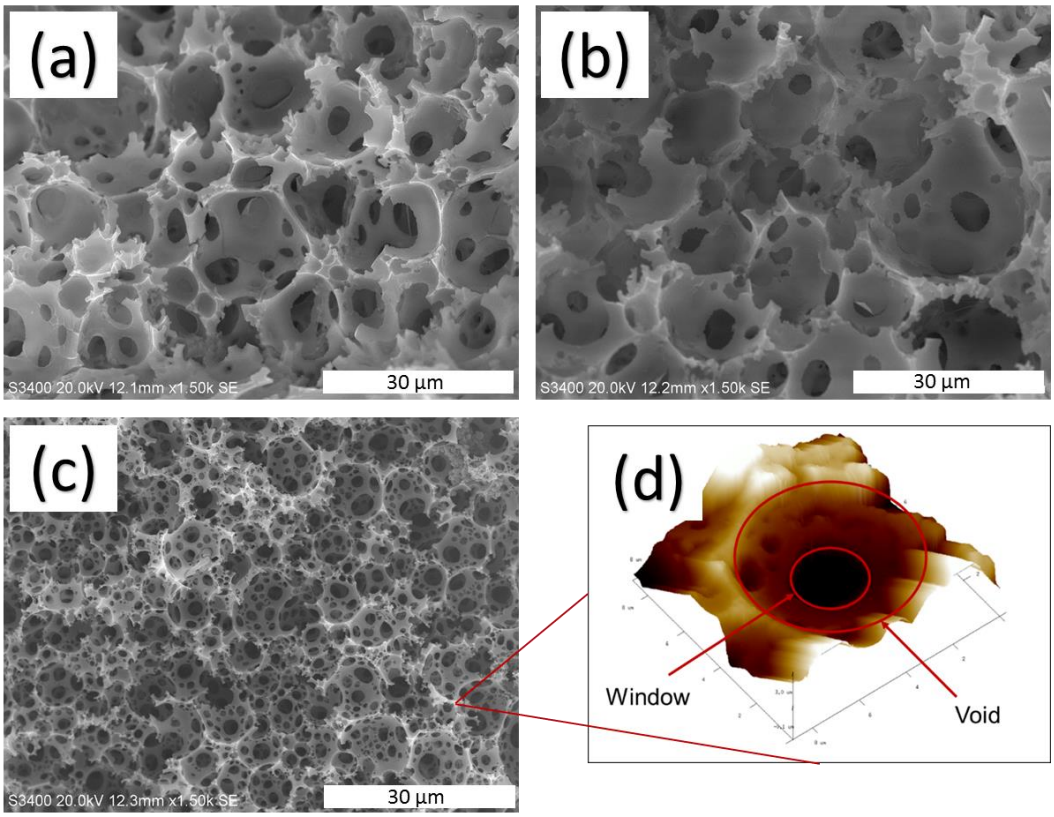

Figure 2.7: *SEM images of varied aqueous phase porosities of (a) 75% (b) 80% (c) 90% PS-co-DVB polyHIPEs and (d) an AFM image of morphological characteristics of a PS-co-DVB polyHIPE that typically contains voids with windows. Magnification: (a)-(d) 1,500x.*

The results produced in this study when varying the porosity of the polyHIPEs suggests these results are in agreement with Cameron's findings. In addition to the difference in the number of windows present within the voids of the polyHIPE structure, a difference in pore size diameter was also observed. It was noted that as the aqueous phase ratio decreased, the voids decreased in size (Table 2.1). The window diameter increased as the ratio of the aqueous phase was decreased for 80% and 75% polyHIPEs. The decrease in this study could be due to the density difference between the organic and aqueous phases where additional porogen is incorporated. It was expected that as the aqueous phase ratio decreased, the openness or porosity of the

polyHIPE also decreased. This was found to be true in the case of the voids but not the interconnecting windows [18, 50, 51]. Any differences between the void and window sizes resulting may be an effect attributed to the transfer of heat through the silcosteel column as a change in temperature would also cause a change in void and window formation due to change in density [52]. In addition, it was noted that the average pore size distribution for the 90% polyHIPE was 12.90 µm for the voids and 2.05 µm for the windows. In comparison to the study that the emulsion formulation was adapted from, the void and window size distribution found appeared to be similar when the standard deviation was taken into account [43].

Table 2.1: *Effect of aqueous phase percentage on void and window sizes (n=90)*

Porosity of PS-*co*-DVB polyHIPE (%)	Voids (µm)	Windows (µm)
90	12.90 ± 1.85	2.05 ± 0.23
80	10.44 ± 2.46	2.46 ± 0.39
75	7.48 ± 1.04	2.28 ± 0.17

In general the trend with the polyHIPE was that the voids were not monodisperse as shown in Figure 2.8 below. This shows the representation of the different areas imaged at each porosity and the recorded voids. It can be observed that the void size range can vary from as small as 2 µm to as large as 45 µm. Typically monodispersity of voids in polyHIPEs is associated with stirring rate. In general, the higher the stirring rate the more uniform void formation is. However, for the

applications required from these emulsions a high stirring rates in turn increases the viscosity making the emulsion more challenging to enter a column housing for curing.

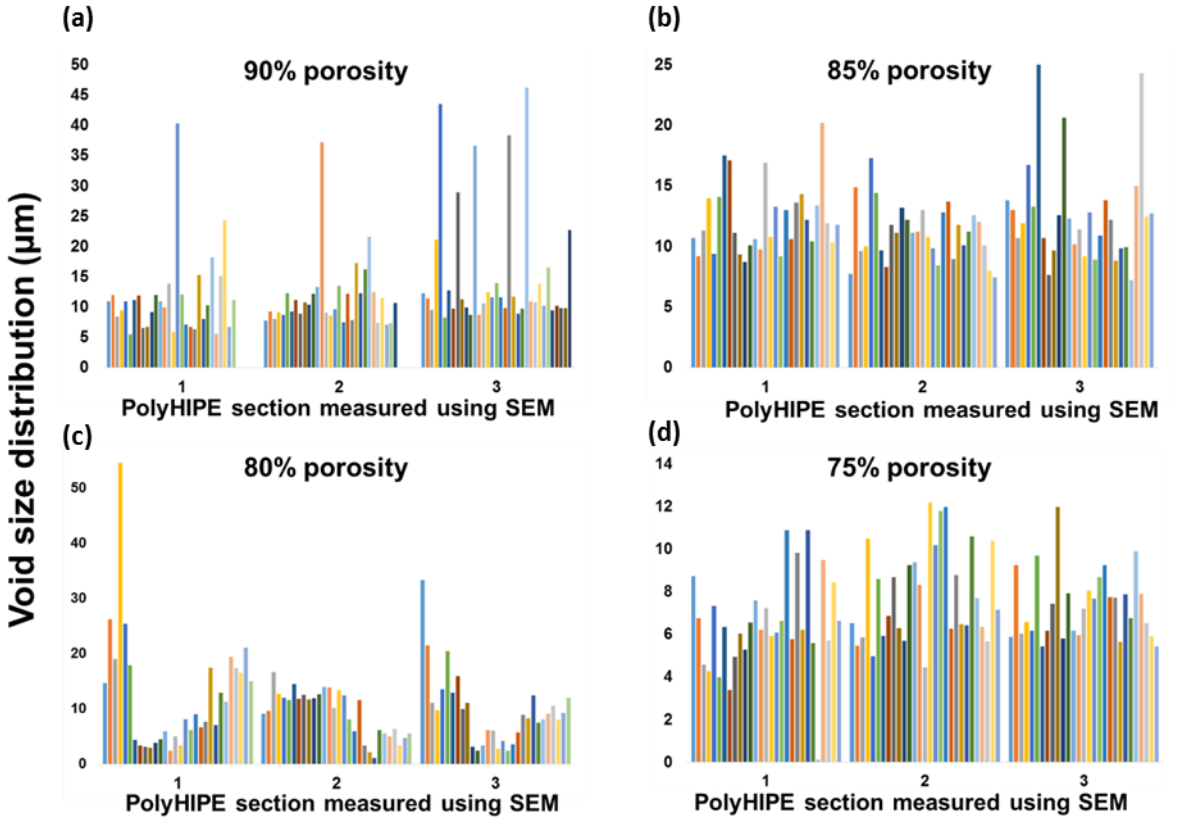

Figure 2.8: Pore size distributions of the voids of three different areas of each porosity (a) 90% (b) 85% (c) 80% and (d) 75% porosity.

2.3.3.2 SEM characterisation of 90% porosity PS-co-DVB polyHIPEs within 100 µm I.D. fused silica tubing and silcosteel tubing of 1.02 mm I.D. and 2.16 mm I.D.

Based on the characterisation of the bulk polyHIPEs in Section ***2.2.3.4***, a 75% polyHIPE should give a higher surface area, the larger pore size of the 90% polyHIPE would facilitate a higher flow rate though the material before the backpressure generated became inhibitive. For this reason a 90% polyHIPE was selected for initial chromatographic evaluation. The 90% PS-*co*-DVB polyHIPE shown in Figure 2.9 (a) was fabricated in 100 µm fused silica capillary columns as per Section ***2.2.3.5***. This

polyHIPE was successfully attached to the capillary wall as shown in Figure 2.9 (i). This was expected due to the silanol groups present on the inner capillary surface, which should form covalent bonds with the PS polyHIPE.

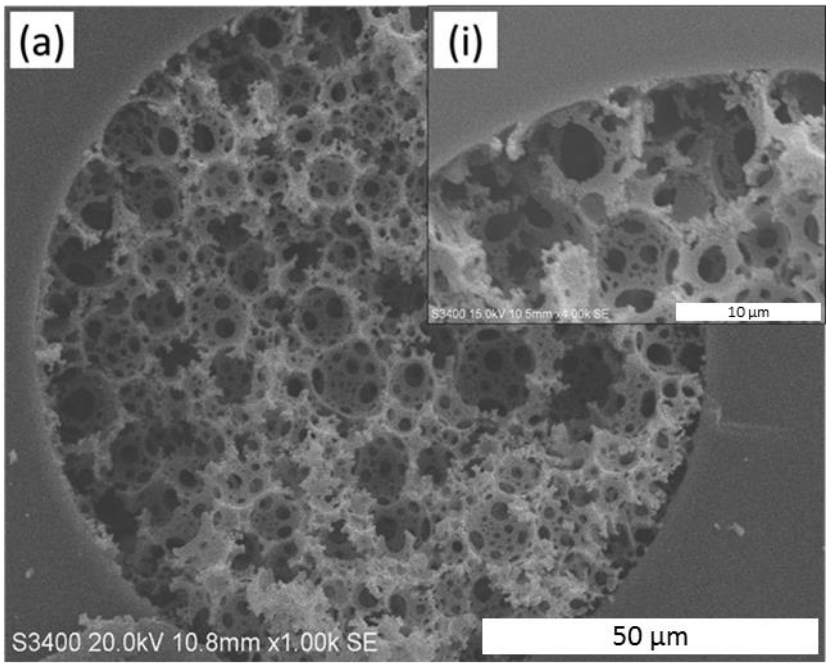

Figure 2.9: *SEM image of (a) 90% PS-co-DVB polyHIPE within 100 µm I.D. fused silica capillary and (i) SEM image showing attachment of polyHIPE to the inner walls of the housing.*

Unfortunately, polymerisation within the 2.16 mm I.D. silcosteel tubing was unsuccessful. A column of such diameter required a higher polymerisation temperature of 75°C, which, resulted in poor radial homogeneity, leading to areas where gaps (i.e. areas with no polyHIPE evident) were present in the monolithic column. For this reason, the polyHIPEs were fabricated within the confines of the narrower silcosteel tubing (100 mm x 1.02 mm I.D.). As shown in Figure 2.10, due to the nature of preparing the column for SEM imaging the quality of the resultant imaged material within silcosteel was relatively poor. This occurred despite having a flow of

liquid during the cutting step. The extensive mechanical sawing that was required to cut the tubing caused the polyHIPE material to crumble at the exposed surface.

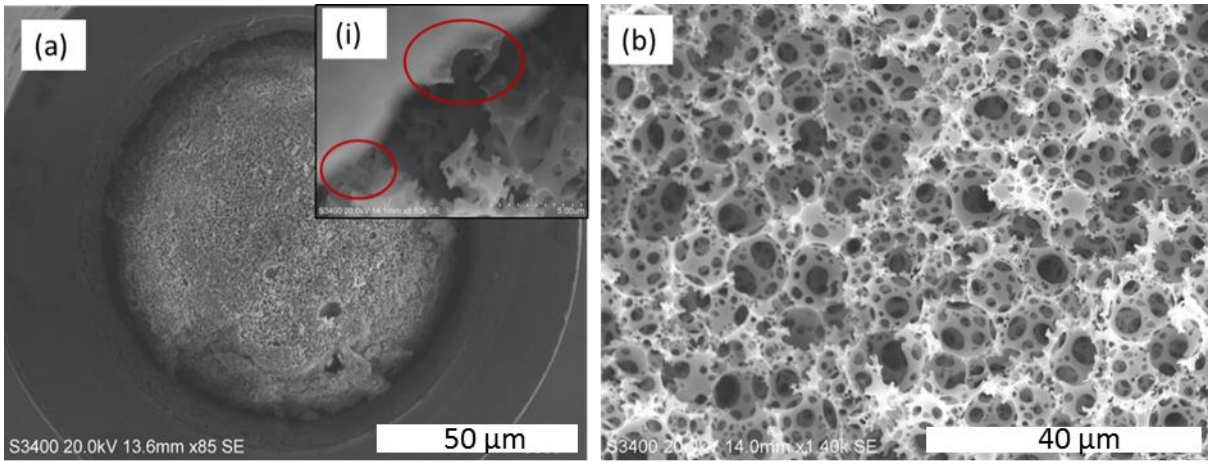

Figure 2.10: *SEM image of (a) 90% PS-co-DVB polyHIPE within 1.02 mm I.D. silcosteel tubing, (i) SEM image showing attachment of polyHIPE to the inner walls of the housing and (b) SEM image showing the void and window structure characteristic to polyHIPE materials Magnification: (a) 85x and (i) 8,500x and (b) 1,400 x.*

Figure 2.10 (a) indicates a darker area, which surrounds the interior wall of the housing suggesting that there are gaps along the housing to polyHIPE interface. Initially, it was thought that this was due to poor attachment of the polyHIPE to the housing wall. However, the high magnification image 2.10 (a) (i) illustrated that the material did bind to the inner walls of the tubing. It was therefore hypothesised that any gaps imaged were possibly artefacts of SEM preparation, resulting from the material being broken upon cutting. Figure 2.10 (b) clearly shows the characteristic voids and windows of polyHIPE materials, indicating successful polymerisation within the silcosteel tubing. Further investigations of these materials as stationary phases in Chapter 3 used van Deemter plots to illustrate the differences in the extent to which polymerisation of the material was successful.

2.3.4 BET surface area analysis of PS-*co*-DVB polyHIPEs with varied aqueous phase percentages

The surface areas of the 75%, 80%, and 90% polyHIPEs were determined to be 23.3 m^2 g^{-1}, 24.3 m^2 g^{-1} and 20.1 m^2 g^{-1} respectively. There was an increase in surface area of approximately 16% from the 90% polyHIPE to the 75% polyHIPE, which was expected and correlates well with the SEM data that showed a decrease in void size which would result in an increase of surface area. A decrease in aqueous phase meant more organic phase was present and accordingly a low percentage of voids were expected. This would allow the polyHIPE to have a more dense structure and in turn, a lower percentage of porogen resulting in a higher surface area overall. The 75% and 80% polyHIPEs had slightly higher surface areas then the 90% material. However, there was a decrease in surface area between the 80% and 75% polyHIPEs. The Brunauer Emmett Teller (BET) model in Figure 2.11 shows the adsorption/desorption isotherm for the 90% porosity polyHIPE. The blue line indicates the adsorption and the red line indicates desorption of gas. A type two isotherm was observed confirming that the pore size of the material was macroporous. Slight hysteresis noted can be attributed to mesoporous materials or N_2 gas being trapped

during desorption [53]. The surface area we obtained is typical for this type of polyHIPE [43].

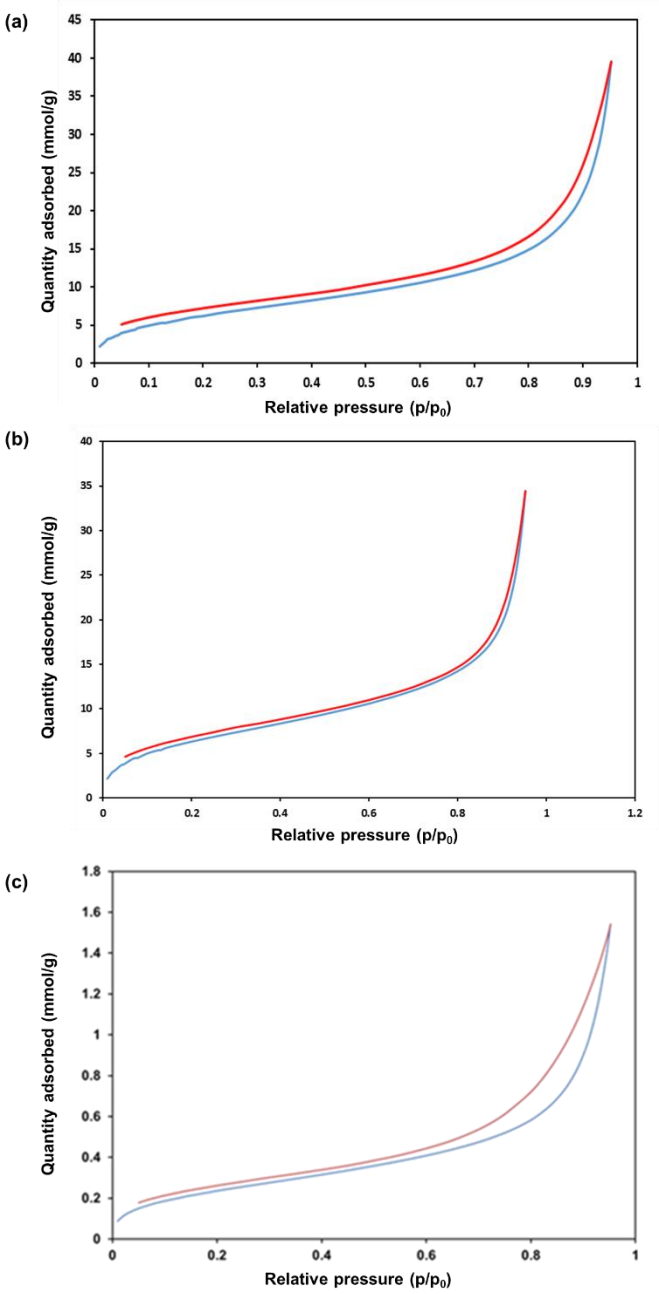

Figure 2.11: *BET isotherms of PS-co-DVB polyHIPEs at porosities (a) 75% (b) 80% and (c) 90% where the blue plot represents the adsorption isotherm and the red plot represents the desorption isotherm (b) 90% PS-co-DVB polyHIPE where the blue line indicates the adsorption isotherm and the red line indicates the desorption isotherm.*

All isotherms presented in Figure 2.11 are similar in adsorption and desorption and show evidence of hysteresis. Typically the path in which the gas adsorbs should be equal to the path it desorbs, thus the adsorption and desorption profiles would overlap. However, when gas molecules are trapped this path is not equal, leading to no overlap caused by hysteresis. This in conclusive as the lowest and highest porosity polyHIPEs showed little difference in surface area.

2.3.5 SEM and BET characterisation of PS-*co*-DVB polyHIPE with toluene as additional porogen

Typically, most styrenic polyHIPEs do not demonstrate particularly high surface areas. However, the incorporation of the porogens to the organic phase during fabrication stages has been commonly observed to increase surface area. In a previous report by Cameron *et al*., it was found that toluene addition resulted in a high surface area while retaining the morphological characteristics of voids and interconnecting windows of the polyHIPEs [18, 54]. In the current research presented, PS-*co*-DVB polyHIPEs were fabricated according to Section ***2.2.3.6***. The toluene was gradually increased by 2% in volume within the emulsion process in order to maintain structurally rigid materials. The main material attributes investigated include changes in morphology, thermal stability and surface area.

The inclusion of toluene by increasing the volume added in small increments (2 to 12% toluene) with respect to crosslinker was carried out as per Section ***2.2.3.6*** to investigate the effects on general polyHIPE morphology [18]. SEM imaging illustrated the occurrence of voids and windows within these materials. The change in morphology can be seen in Figure 2.12 below. However, visual analysis SEM images

were insufficient for an in depth analysis of void and window sizes upon gradual toluene addition.

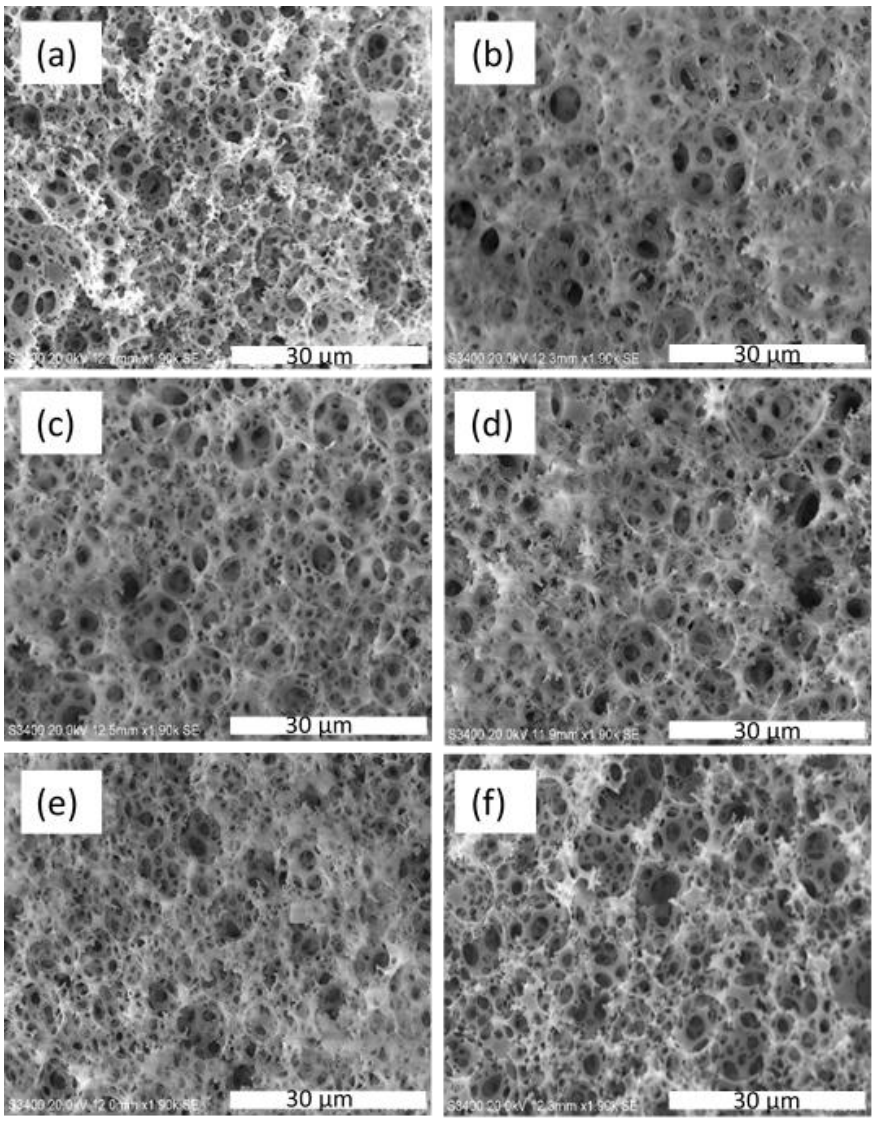

Figure 2.12: *Gradual increase of percentage toluene in 90% PS-co-DVB polyHIPE where (a)-(f) are 2, 4, 6, 8, 10 and 12% added toluene with respect to crosslinker volume (0.333 mL). Magnification at 1,900x and scale bar 30 µm.*

Using Image J software to analyse the SEM images of the polyHIPEs, the void and window size distribution upon toluene addition was determined as shown in Table 2.2. It was found that the void diameter of the materials predominantly increased with

addition of 2 to 4% toluene and then decreased further with the addition of 6 to 10% toluene before increasing slightly again at 12%. However, similar to this study, Carnachan *et al.* studied the effect of increasing porogen quantities of MeOH and THF in polyHIPEs and found increasing and decreasing pore sizes with no specific trend [55].

Table 2.2: *Void and window distribution and BET surface area on increasing toluene percentage*

Toluene (%)	Voids (μm)	Windows (μm)	Surface area (m^2 g^{-1})
2	5.38± 0.75	1.69± 0.40	50.58± 0.49
4	7.67± 0.39	2.06± 0.21	16.08± 0.08
6	7.23± 0.08	1.83± 0.08	19.29± 0.07
8	6.94± 0.43	1.88± 0.05	23.23± 0.19
10	6.52± 0.57	1.52± 0.06	17.41± 0.18
12	6.63± 0.80	1.79± 0.19	13.39± 0.05
25	6.96± 2.38	2.24± 1.24	35.78± 0.08
50	8.28± 2.80	1.47± 0.97	25.00 ± 0.50
75	7.71± 2.13	2.11± 0.73	31.56± 0.10

The studies within the literature show that by adding porogens to the organic phase, an accompanying increase in surface area should result. However, from the BET results reported in Table 2.2 above, a fluctuation in surface area values was

obtained. With close inspection of the polyHIPE void and window diameters, the surface area results show a trend that when both void and window size decreases the surface area of the material increases. When both the void size and window sizes decrease, the surface area tends to increase. This trend is most prominent moving from 2% and 4% toluene. It was hypothesised that perhaps a change in surface tension upon the addition of toluene could have an impact on the window formation [49]. However, with such a low porogen percentage added this was difficult to determine. To investigate the effect of porogen over a wider range, in terms of surface area and morphology, greater volumes of toluene were added to the organic phase [18]. The BET surface area results obtained for the 25-75% addition of toluene were outsourced. A decrease in surface area was observed from addition of 25% to 50% of toluene (Table 2.2), possibly due to an increase in pore size of the 50% addition of toluene. The 75% toluene addition resulted in an intermediate value for surface area. Overall, the surface area did not increase higher than 35 m^2 g^{-1} which would indicate that the lower addition of toluene did not have the desired effects to achieve materials with both greater mechanical rigidity and higher surface area. SEM images illustrated in Figure 2.13 show that it was nonetheless still difficult to decipher a general trend in void and window sizes. From these images, it was shown that the polyHIPEs fabricated were uniform, homogenous, and contained dense networks of interconnecting windows with no major craters. However, upon measuring the voids and windows as shown in Table 2.2 above, no linear relationships between toluene percentage and window/void sizes were observed. This was not unexpected as similar studies also reported sporadic results [18]. BET surface area analysis typically requires up to 100 mg of material which was the amount used in the materials produced here. It is a possibility that being such low surface area materials, perhaps

more material should have been used for analysis. In addition, it is observed amongst polymer materials in particular that N_2 molecules can occupy a greater area, giving a lower representation of the true surface area, which could be a likely explanation to the phenomena observed here. Overall, the pore sizes obtained in this study were smaller than similar studies on polydivinylbenzene (pDVB) polyHIPEs [55]. It was hypothesised that window formations were due to the different densities between the monomer aqueous phase and the organic external phase upon thermal polymerisation [49]. Temperature has previously been shown to have an effect on the void and window formation as the increase in temperature changes the density of the polymers within the emulsion [55]. In this study, this change in density could easily occur when the emulsion was housed within its mould. Once placed into a water bath for polymerisations to occur, the emulsion (~25°C) had to equilibrate with the temperature of the water bath, which is at 60°C. Therefore this heat transfer gradient present could have influenced the occurrence of a density differential, which, could have resulted in the window formations observed.

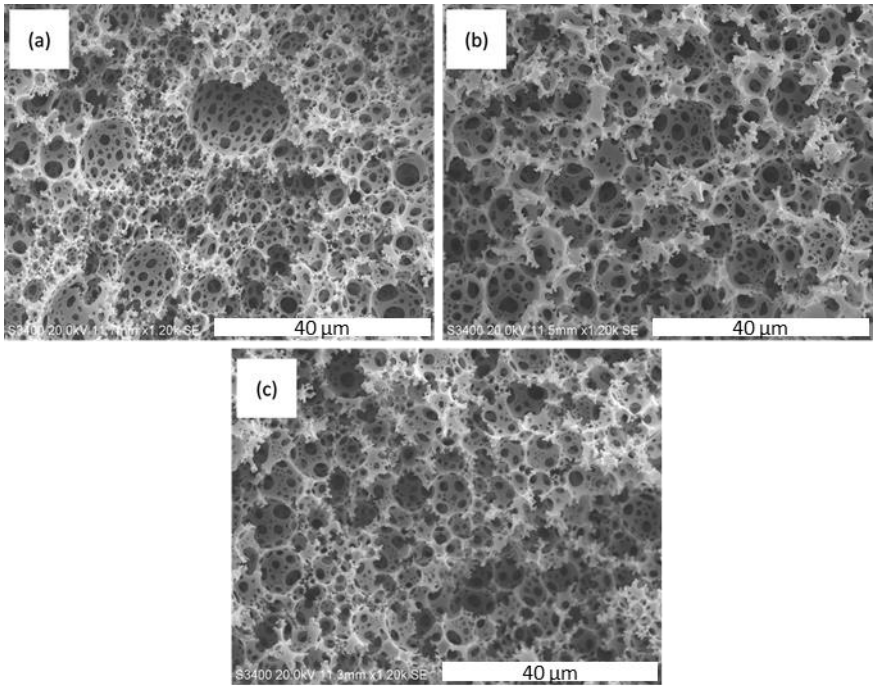

Figure 2.13: *SEM images of PS-co-DVB polyHIPE where additional porogen (toluene) was added at (a) 25% (b) 50% and (c) 75% of crosslinker ratio. Magnification (a)-(c) 1,200x.*

2.3.5.1 TGA of PS-co-DVB polyHIPE with toluene as additional porogen

Thermal stability profiles were analysed using TGA to determine if the addition of toluene decreased or increased the material's thermal resistance limits. In comparison to the literature, values for the thermal stability of PS-*co*-DVB materials was observed to be within a range of 300 to 450°C [56].

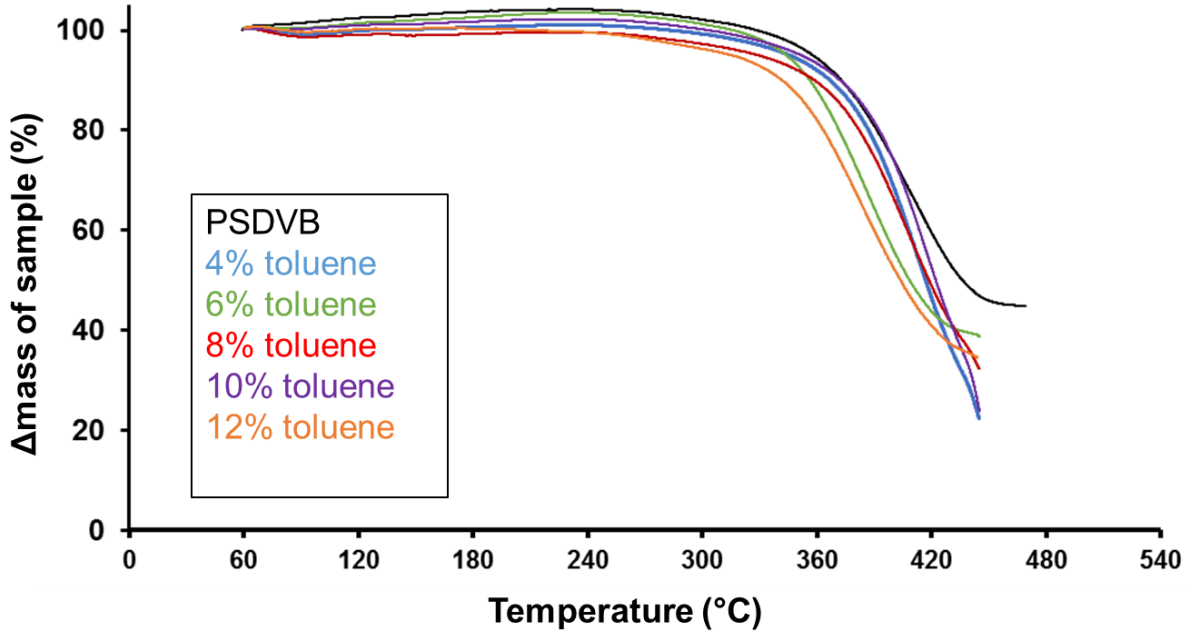

Figure 2.14: *TGA showing the decrease in percentage mass of polyHIPEs with increasing temperature. Here, polyHIPEs with increasing volumes of toluene were analysed.*

In this study, it was noted that the temperature profiles of materials with increasing toluene are very similar to each other, as shown in the TGA curve in Figure 2.14 above. A loss of mass of the materials was observed at roughly 280 to 450°C which is 20°C lower than that observed for PS materials in the literature, most likely due to the final morphology of the materials [57]. Complete sample loss was not observed as when the crucible was removed from the oven carbonised polyHIPE materials remained, however it was not necessary to obtain complete pyrolysis of

samples analysed. As the percentage of toluene increased, the rate of decomposition also increased and is signified by the steeper downward slope on the TGA curve. This increased rate of decomposition could be due to the toluene compromising the mechanical rigidity of the materials, making them more susceptible to thermal degradation.

2.3.6 PS-*co*-DVB polyHIPEs modified with GONP addition

2.3.6.1 FESEM characterisation of PS-co-DVB polyHIPEs modified with GONPs

2.3.6.1.1 Bulk polymerised PS polyHIPEs modified with GONP

Due to their amphiphilic nature, GONPs (single to a few layers of graphene) have been used as a Pickering agents in the past and the morphology of the resulting polymers fabricated have exhibited morphologies where a layer of GO coating the particles is observed [58]. In this study, an emulsion using 33 ppm of GO was fabricated in bulk format to investigate whether the addition of GONP had an impact on the PS-*co*-DVB polyHIPE's morphology using FESEM imaging. From the images presented in Figure 2.15 below, it is suspected that there are areas on the polyHIPE coated with GONPs and areas that remain free from GONPs. However, it is noted that a "popcorn" effect could also give the observed morphology. Nonetheless similar rough coating have been observed where GONP modified polymers have been investigated in the past [58].

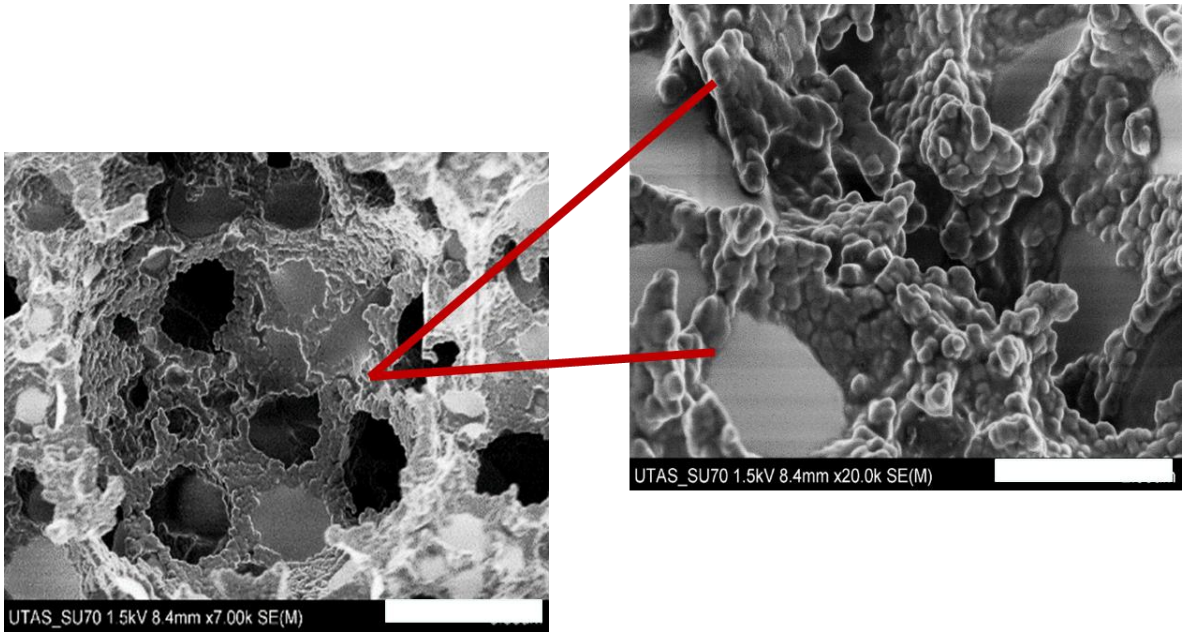

Figure 2.15: *FESEM images of (a) GONP (at 33 ppm) PS-co-DVB polyHIPE polymerised in bulk at magnification of 7,000 x (scale bar 5 µm) to show GONP coated morphology and (b) GONP coverage at 20,000 x (scale bar 2 µm).*

The promising results obtained above showed high potential that the surface of the polyHIPE materials changed in bulk polymerisation. Thus, polymerisation of the material with increasing concentrations of GONPs were pursued within capillary in the following section.

2.3.6.1.2 PS polyHIPEs modified with GONP polymerised within capillary format

PolyHIPEs fabricated within capillary housing were imaged as shown in Figure 2.16 which shows the effect of increasing concentration of GONPs on the resulting polyHIPE surface roughness.

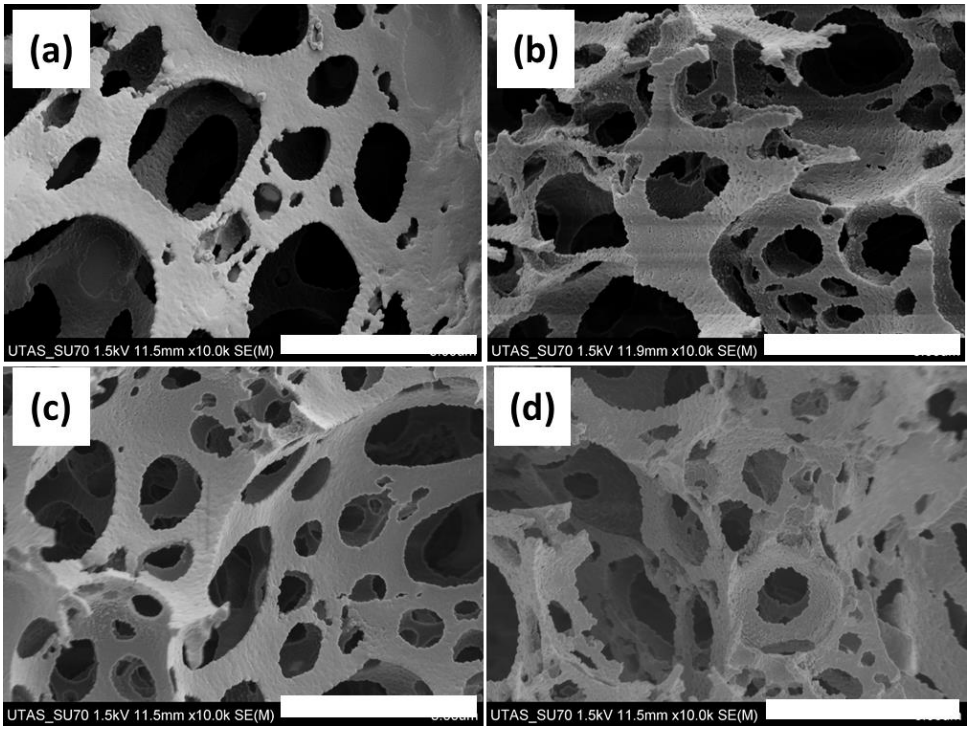

Figure 2.16: *FESEM images where no change in surface roughness was observed upon increasing GONP concentrations of (a) 0 ppm, (b) 13 ppm, (c) 33 ppm and (d) 66 ppm. Magnification of 10,000x and scale bar of 5 µm.*

Figure 2.16 (a) shows a blank PS-*co*-DVB polyHIPE polymerised within 250 µm fused silica capillary. The following images 2.16 (b)-(d) show that although the concentration of GONP added increased, there was no change in the surface roughness of the polymers. It was observed that although the addition of 0, 13, 33 and 66 ppm of GONP did not increase the surface roughness of the material, the 20 ppm concentration added showed the opposite effect. Figure 2.17 shows an increase in surface roughness of this material, possibly due to the addition of GONPs.

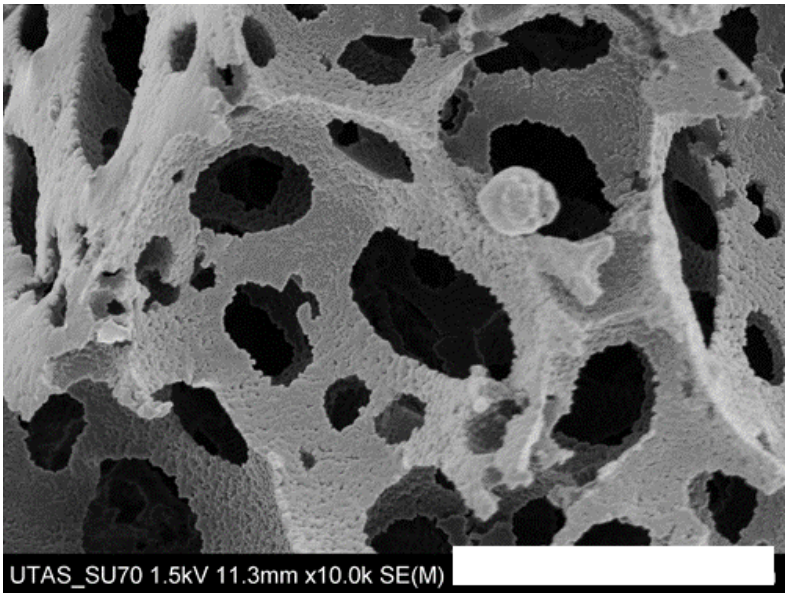

Figure 2.17: *FESEM showing the of 20 ppm addition of GONP into PS-co-DVB polyHIPE. Magnification of 10,000x and scale bar of 5 µm.*

Table 2.3: *Void and window distribution on increasing GONP concentration*

PolyHIPE	Voids (µm)	Windows (µm)
GOPSDVB0 (blank)	15.59±13.62	4.29±1.73
GOPSDVB13	13.97±8.15	3.54±0.91
GOPSDVB20	10.92±5.81	2.48±0.75
GOPSDVB33	17.48±10.20	4.87±2.26
GOPSDVB66	15.46±8.63	3.56±2.09

In Table 2.3, the increase of GONP concentration decreased the void and window sizes from 0 ppm to 33 ppm of GONP added. However, from 33 ppm concentration

this linear trend was no longer observed. From the FESEM it was still uncertain whether GONPs were present on the surface of the polyHIPE materials as hypothesised in the previous section. However, the FESEM data below would suggest a higher indication of an increased surface roughness resulting upon the addition of 20 ppm GONP to the emulsion.

2.3.6.2 BET surface area analysis of PS-co-DVB polyHIPEs modified with GONPs

The BET results reported the surface areas of the GONP modified materials as shown in Table 2.4. A decrease in surface area was observed with increasing concentration of GONPs from 0 to 33 ppm. The surface area increased again at 66 ppm of GONPs. This may be because at 66 ppm, the emulsion stability was compromised and the emulsion itself was in the process of phase inversion. The latter emulsion required to be transferred to a mould as soon as all GONP was incorporated.

Table 2.4: *BET surface area upon increasing GONP concentration*

PolyHIPE	Surface area ($m^2 g^{-1}$)
GOPSDVB0 (blank)	25±0.27
GOPSDVB13	24±0.28
GOPSDVB20	16±0.09
GOPSDVB33	12±0.04
GOPSDVB66	15±0.06

This would explain the change in the linear trend of the BET results. It was hypothesised that at higher concentrations, the GONPs formed aggregates, which ultimately disrupted the emulsion process and could have been the major cause of phase inversion.

2.3.6.3 FTIR analysis of PS-co-DVB polyHIPEs modified with GONPs

FTIR analysis was utilised to determine the presence of functional groups present in GONP modified polyHIPEs. The key functional groups that should have indicated the presence of GONPs would be OH groups and C=O groups. A PS-*co*-DVB polyHIPE would be expected to have a different absorption spectrum than a GONP containing PS-*co*-DVB polyHIPE. In Figure 2.18 below, the FTIR spectra shows an unmodified PSDVB polyHIPE. Figure 2.19 (i) shows the region where the hydroxyl absorption was expected on the modified polyHIPE. The results indicate a broad OH absorption observed for the blank polyHIPE. This broad OH group would not be expected on the polyHIPE surface but could be due to residual solvent present. The 66 ppm GONP polyHIPE was expected to have the greatest OH absorption, however, no absorption in the OH region (3200 to 3600 cm^{-1}) for this polyHIPE was observed. More interestingly, the 20 ppm GONP polyHIPE had an absorption profile where two distinct absorption peaks resulted in the OH region [59]. The two peaks observed are typically common when OH groups are on the surface of a molecule and no hydrogen bonding can occur. This resulted in a strong possibility that GONPs could be present on the surface of 20 ppm GONP polyHIPE. This also correlates with the FESEM results that showed the 20 ppm GONP polyHIPE to be the only polyHIPE to have change in surface morphology. It was also noted that no carbonyl absorption was present in the FTIR results. This is unexpected as for the polyHIPEs containing GONPs a substantial absorbance signal should be present at the region of 1720 cm^{-1} as graphene oxide contains multiple C=O groups. This absorption peak was not observed in either of the GONP containing polyHIPEs.

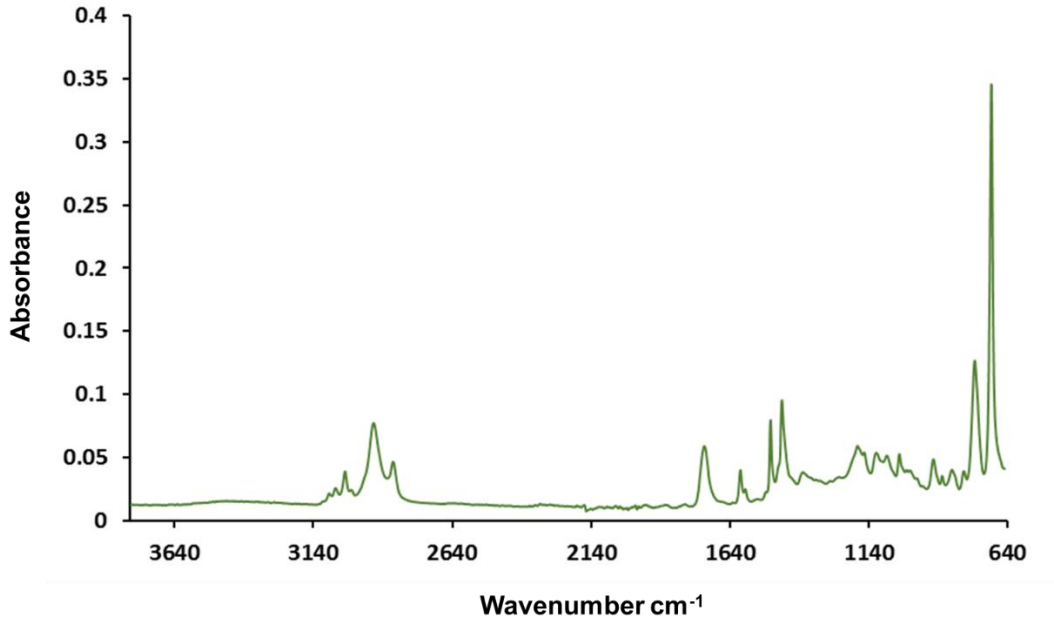

Figure 2.18: *FTIR absorption spectra of PSDVB polyHIPE with no GONP included.*

The FTIR spectra in Figure 2.19 (purple) was of another 20 ppm GONP polyHIPE from a different parent emulsion to see if the OH absorption peak was present again. Figure 2.19 (i) shows similar results where the two peaks in the OH region were observed again (purple). These results indicated a strong possibility of GONPs present in the GOPSDVB20 polyHIPEs, however, further analysis would be required to confirm their presence.

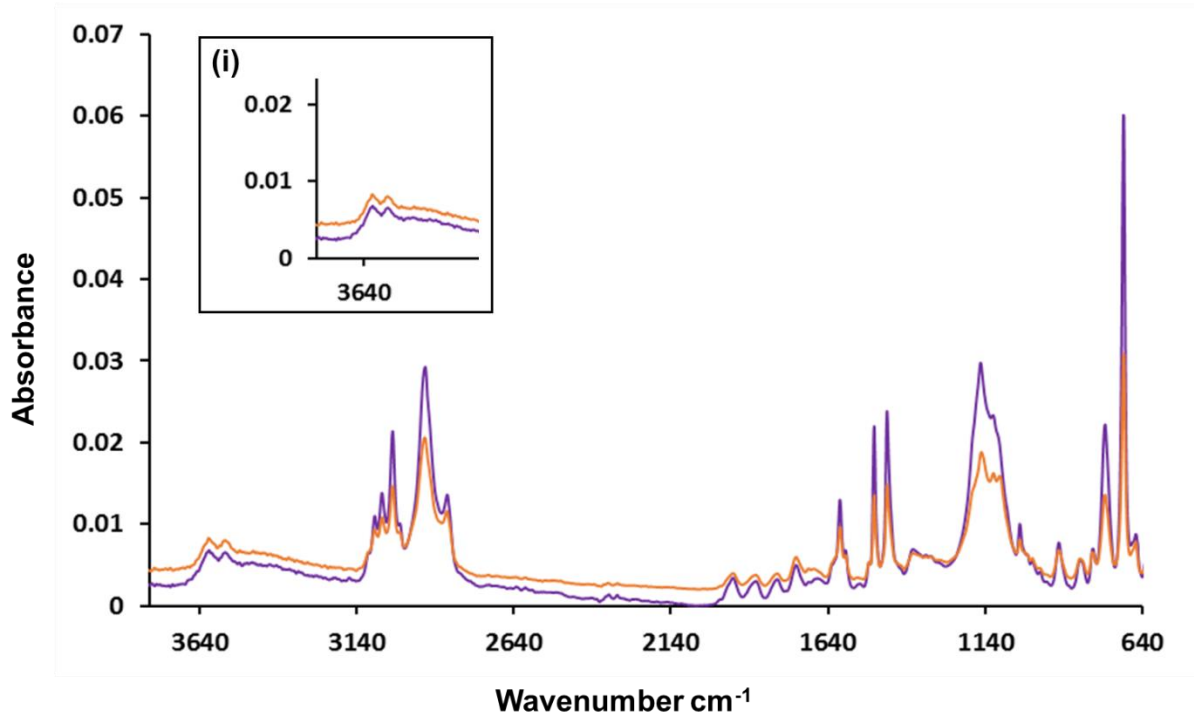

Figure 2.19: *FTIR absorption spectra of overlayed GOPSDVB20 (orange, batch 1) and GOPSDVB26 (purple, batch 2) where (i) is showing the expected OH absorption region.*

2.3.6.4 ZetaSIZER analysis of PS-co-DVB polyHIPEs modified with GONPs

In order to understand the effect of the GONPs within solution, particle size analysis using a ZetaNanoZS was utilised. In Figure 2.20, the particle size distributions were measured in order to establish the effect of 20 ppm of GONP in water. This analysis was important because fabrication of GOPSDVB66 resulted in stability issues and required the emulsion to be transferred to a mold immediately. Therefore, the effect of GONP in water, in the aqueous phase and with the surfactant were analysed. The hydrodynamic radius (d_{hyd}) was found to be 312.6 d nm where the polydispersity index (PDI) was 0.2. Due to the particles being close to the upper limit of 300 nm there was not a high degree of aggregation present. However, from the results obtained in Figure 2.20, it was clear that a more complex size distribution would be expected once the GONPs were incorporated into the emulsion. The particle size of 20 ppm GONPs within the aqueous phase of the emulsion was also investigated using the ZetaNanoZS and gave such a large average particle size of 3.14×10^4 nm a plot was not obtained. In addition, the PDI was 0.8 where the particle size was greater than 500 nm; resulting in a high degree of aggregation. This would explain why phase separation was observed when the GONPs and aqueous phase were incorporated and added dropwise to the organic phase. This would suggest that both the initiator and electrolyte used were sources of the phase inversion observed upon fabrication.

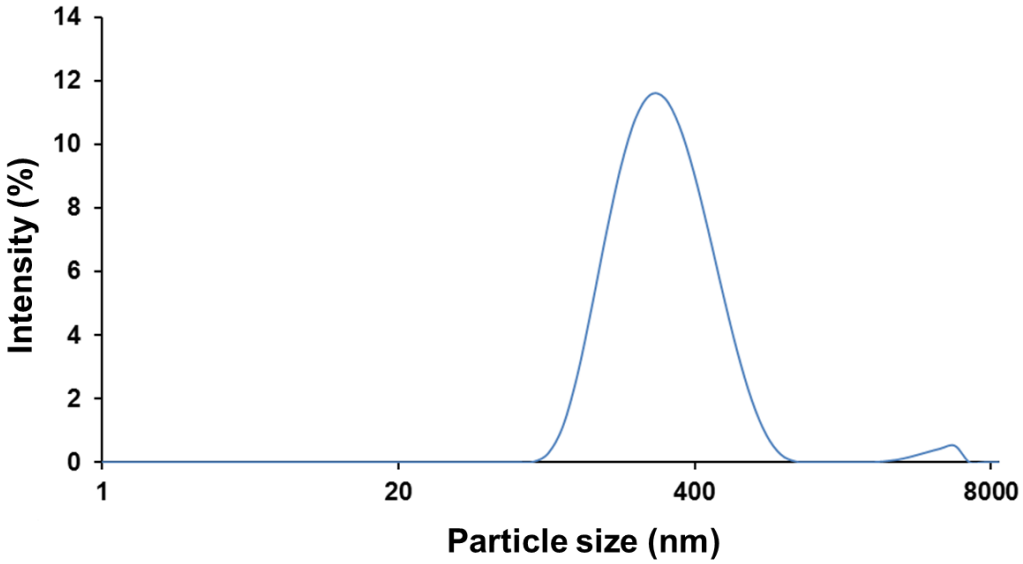

Figure 2.20: *Particle size distributions using ZetaNanoZS to establish the effect of 20 ppm of GONP in water.*

Finally, the particle size resulting from the incorporation of GONPs with Span 80 was investigated. This resulted in an average particle size of 320 nm, which is presented in Figure 2.21. The PDI value was found to be 0.6, therefore a high degree of aggregation was found for GONPs with surfactant. A polydisperse particle nature was expected as most of the polyHIPEs fabricated were shown to give decreasing void and window diameters upon addition of Span 80. This decrease was suspected to be caused by the interaction of GONPs with Span 80. The main particle sizes were reported at 130.9 and 7770.1 d nm^{-1} at 65.4% and 34.6% respectively. It was hypothesised that the smaller particles arose from the surfactant and the larger particles were a result of aggregates formed by the surfactant and GONPs. The particle size results report a large difference in particle size distributions with respect to the aqueous phase and GONPs as well as an adverse interaction with the surfactant.

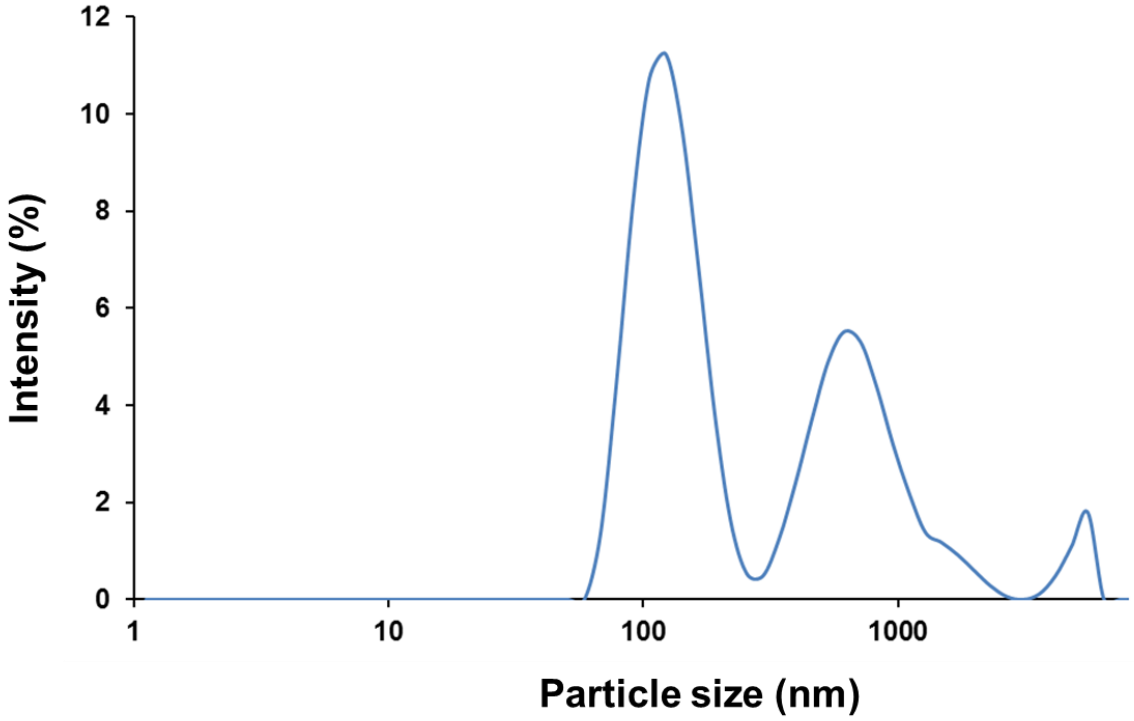

Figure 2.21: *Particle size distributions using ZetaNanoZS to establish the effect of 20 ppm of GONP with surfactant.*

2.3.6.5 TGA of PS-co-DVB polyHIPE modified with GONPs

Thermal stability profiles were analysed using TGA under N_2 to determine if the addition of GONPs influenced the material's thermal resistance limits. It was expected that increased incorporation of GONP would increase the thermal resistance of the final polymer. Figure 2.22 shows that the only the GOPSDVB20 had a substantial reduced mass. At the highest temperature investigated, 600°C, only a 10% loss was observed. The increasing concentrations of GONPs appeared to have no effect on the thermal stability of the polyHIPEs and had similar thermal degradation trends to that of the blank polyHIPE (GOPSDVB). The preliminary results here illustrated a considerable improvement in the thermal stability of addition of 20 ppm GONPs to the polyHIPE.

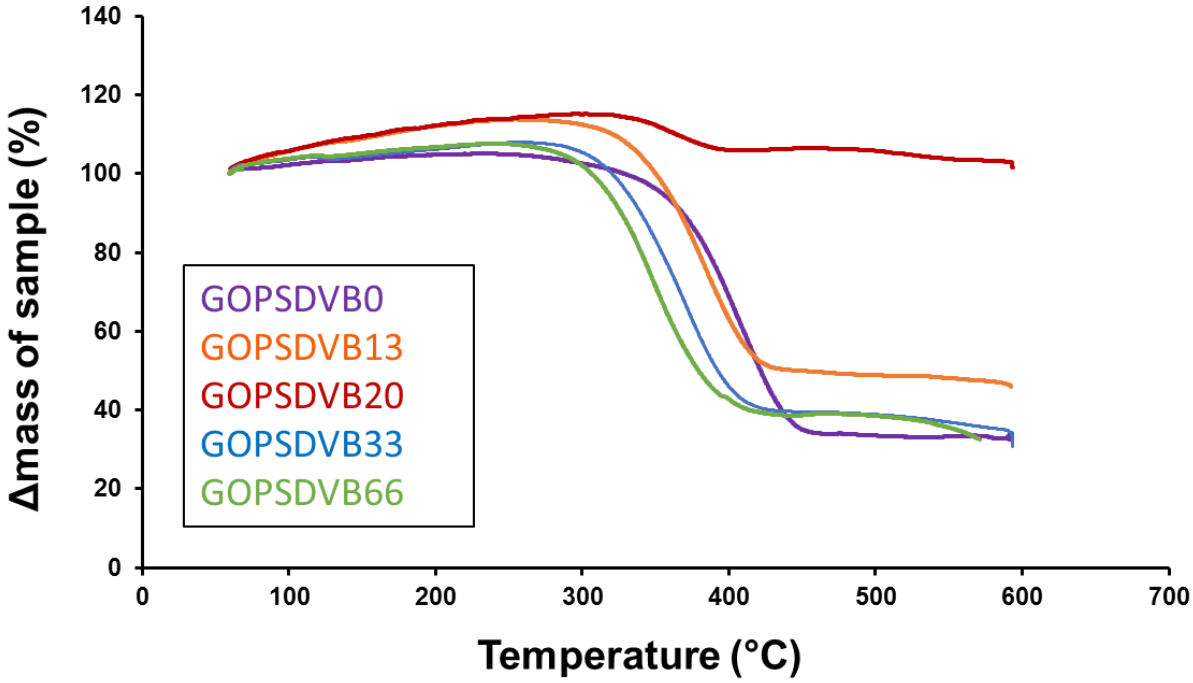

Figure 2.22: *TGA showing the decrease in percentage mass of polyHIPEs with increasing temperature. Here polyHIPEs with increasing concentrations of GONPs were analysed.*

However, upon repeating TGA on the GOPSDVB20 bulk sample as shown in Figure 2.23, it was observed that thermal degradation of the polyHIPE was similar to all of the other GONP modified polyHIPEs. Therefore, no significant improvement of GONP modified polyHIPEs was apparent and was no longer investigated for increased thermal stability.

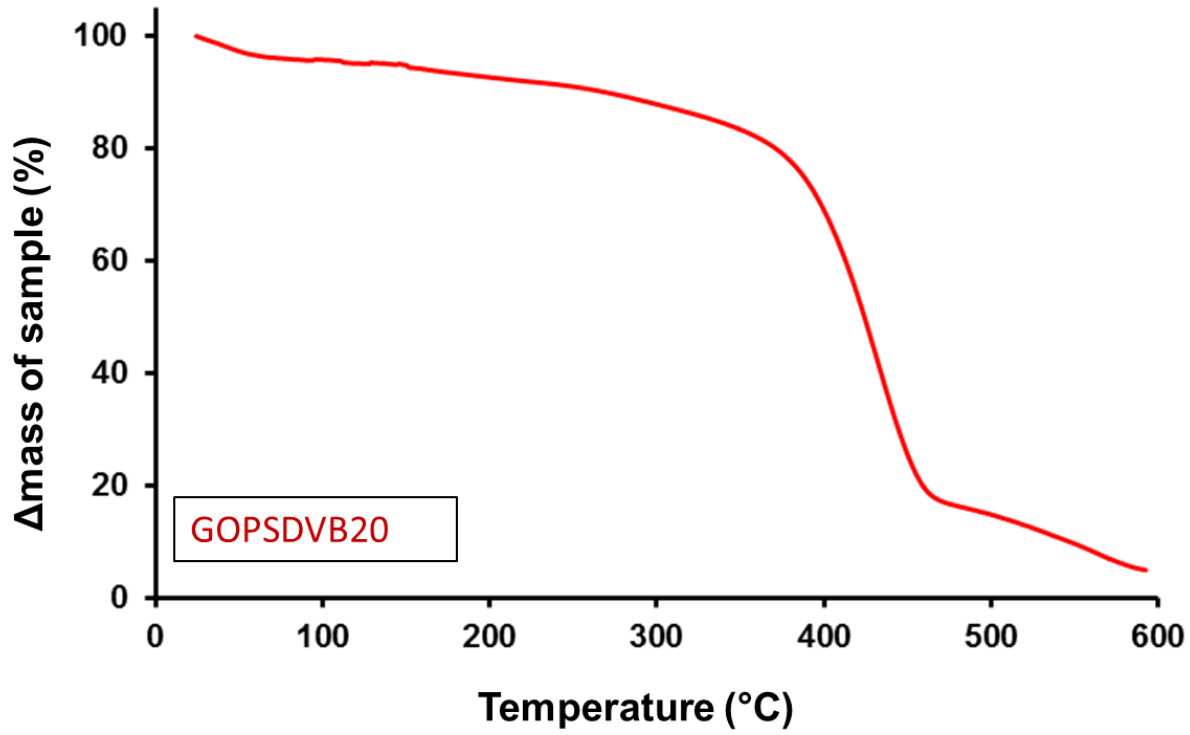

Figure 2.23: *Repeated TGA analysis of GOPSDVB20 to confirm thermal stability effects.*

2.4 Conclusion

The studies from this chapter have detailed the fabrication of three discrete polyHIPEs, based on their monomer type. GMA based polyHIPEs were investigated due to their potential for surface area modification. These polyHIPEs contained a unique pore structure with very few interconnecting windows present. When polymerised within the PEEK tubing the GMA polyHIPEs were seen to contract away from the tubing walls, making PEEK an unsuitable housing material. To increase the surface area of the polyHIPEs, the bulk material was aminated and then agglomerated with gold NPs. However, due to the poor network of interconnecting pores only the amination of the exterior region of the polyHIPE was successful. Thus, the GMA polyHIPE was deemed unsuitable as a stationary phase material.

The investigation of VBC polyHIPEs, which also contain a reactive group similar to GMA, which makes them amenable to surface modifications. The VBC monomer resulted in polyHIPEs, which contained large craters, were present throughout the material. Many of the craters present also had no interconnecting windows. To decrease the frequency of these craters the monomer Sty was included in an attempt to decrease crater formation. It was found that at 75% Sty the craters were no longer observed. Unfortunately, at this percentage of Sty, aggregates formed on the surface of the material. Such morphological features would have a negative effect of the separation efficiencies and retention mechanisms of a polyHIPE, therefore this material was not investigated any further.

PS-*co*-DVB polyHIPEs were illustrated to result in the best morphological structure for flow through applications. PS-*co*-DVB materials however, are known to have low surface areas. Further investigations into the use of polystyrene polyHIPEs

showed that decreasing the aqueous phase led to an increase in surface area. Toluene was also added to the emulsion as an additional porogen in an attempt to further increase surface area. Toluene appeared not to impact void and window sizes in a linear fashion. However, this was suspected to be a result of the temperature change of the emulsion during polymerisation which would decrease the density of the components in the emulsion. As the toluene incorporated polyHIPEs did not result in high surface area or demonstrate excellent mechanical rigidity they were no longer investigated as stationary phase materials. However, the interest in PS-*co*-DVB polyHIPEs, albeit with a lower surface area than hoped, were characterised as possessing a morphology amenable to separation applications, they were investigated as potential stationary phases for LC applications in Chapter 3.

The modification of PS-*co*-DVB polyHIPEs using GONPs was also investigated. FESEM results showed a change in surface roughness with the 20 ppm incorporated polyHIPE but no with the other GONP modified polyHIPEs. The presence of GONPs on the surface of the polyHIPEs were not confirmed, however preliminary results reported for FTIR analysis indicated the strong possibility of GONPs present on the surface of 20 ppm incorporated polyHIPEs due to the findings of distinct OH absorption peaks. To further establish the presence of GONPs on the surface of the polyHIPE, the GOPSDVB20 polyHIPEs were fabricated within a capillary for use in the separations of alkylbenzenes in Chapter 4.

2.5 References

[1] M.S. Silverstein, Polymer, 55 (2014) 304.

[2] S. Asliyuce, L. Uzun, A.Y. Rad, S. Unal, R. Say, A. Denizli, Journal of Chromatography B-Analytical Technologies in the Biomedical and Life Sciences, 889 (2012) 95.

[3] K. Yao, S. Shen, J. Yun, L. Wang, F. Chen, X. Yu, Biochemical Engineering Journal, 36 (2007) 139.

[4] M. Erzengin, N. Unlu, M. Odabasi, Journal of Chromatography A, 1218 (2011) 484.

[5] R.D. Arrua, P.R. Haddad, E.F. Hilder, Journal of Chromatography A, 1311 (2013) 121.

[6] R. Dario Arrua, A. Nordborg, P.R. Haddad, E.F. Hilder, Journal of Chromatography A, 1273 (2013) 26.

[7] F. Svec, Journal of Chromatography A, 1217 (2010) 902.

[8] R. Butler, C.M. Davies, A.I. Cooper, Advanced Materials, 13 (2001) 1459.

[9] R. Butler, I. Hopkinson, A.I. Cooper, Journal of the American Chemical Society, 125 (2003) 14473.

[10] H. Zhang, A.I. Cooper, Soft Matter, 1 (2005) 107.

[11] H. Zhang, G.C. Hardy, M.J. Rosseinsky, A.I. Cooper, Advanced Materials, 15 (2003) 78.

[12] H. Maekawa, J. Esquena, S. Bishop, C. Solans, B.F. Chmelka, Advanced Materials, 15 (2003) 591.

[13] H. Zhang, G.C. Hardy, Y.Z. Khimyak, M.J. Rosseinsky, A.I. Cooper, Chemistry of Materials, 16 (2004) 4245.

[14] A. Imhof, D.J. Pine, Nature, 389 (1997) 948.

[15] B.P. Binks, Advanced Materials, 14 (2002) 1824.

[16] I.J. Brown, D. Clift, S. Sotiropoulos, Materials Research Bulletin, 34 (1999) 1055.

[17] A.H. Lu, W. Schmidt, B. Spliethoff, F. Schüth, Advanced Materials, 15 (2003) 1602.

[18] A. Barbetta, N.R. Cameron, Macromolecules, 37 (2004) 3188.

[19] P. Hainey, I.M. Huxham, B. Rowatt, D.C. Sherrington, L. Tetley, Macromolecules, 24 (1991) 117.

[20] S. Yang, L. Zeng, Z. Li, X. Zhang, H. Liu, C. Nie, H. Liu, European Polymer Journal, 57 (2014) 127.

[21] V.O. Ikem, A. Menner, A. Bismarck, Angewandte Chemie-International Edition, 47 (2008) 8277.

[22] A. Menner, V. Ikem, M. Salgueiro, M.S.P. Shaffer, A. Bismarck, Chemical Communications (2007) 4274.

[23] X. Li, C. Zhu, Y. Wei, Z. Lu, Colloid and Polymer Science, 292 (2014) 115.

[24] S. Aland, A. Voigt, Colloids and Surfaces A: Physicochemical and Engineering Aspects, 413 (2012) 298.

[25] B.P. Binks, S.O. Lumsdon, Langmuir, 17 (2001) 4540.

[26] E. Vignati, R. Piazza, T.P. Lockhart, Langmuir, 19 (2003) 6650.

[27] P.J. Colver, S.A.F. Bon, Chemistry of Materials, 19 (2007) 1537.

[28] S. Kovacic, N.B. Matsko, G. Ferk, C. Slugovc, Journal of Materials Chemistry A, 1 (2013) 7971.

[29] S. Zhou, A. Bismarck, J.H.G. Steinke, Journal of Materials Chemistry, 22 (2012) 18824.

[30] Y.H. Chen, N. Ballard, S.A.F. Bon, Chemical Communications, 49 (2013) 1524.

[31] S. Wang, Z. Zhang, H. Liu, W. Zhang, Z. Qian, B. Wang, Colloid and Polymer Science, 288 (2010) 1031.

[32] S. Kovacic, A. Anzlovar, B. Erjavec, G. Kapun, N.B. Matsko, M. Zigon, E. Zagar, A. Pintar, C. Slugovc, Acs Applied Materials & Interfaces, 6 (2014) 19075.

[33] M.G. Schwab, I. Senkovska, M. Rose, N. Klein, M. Koch, J. Pahnke, G. Jonschker, B. Schmitz, M. Hirscher, S. Kaskel, Soft Matter, 5 (2009) 1055.

[34] J. Urban, F. Svec, J.M.J. Frechet, Analytical Chemistry, 82 (2010) 1621.

[35] J. Urban, F. Svec, J.M.J. Frechet, Journal of Chromatography A, 1217 (2010) 8212.

[36] I. Pulko, J. Wall, P. Krajnc, N.R. Cameron, Chemistry – A European Journal, 16 (2010) 2350.

[37] B.C. Benicewicz, G.D. Jarvinen, D.J. Kathios, B.S. Jorgensen, Journal of Radioanalytical and Nuclear Chemistry, 235 (1998) 31.

[38] E.H. Mert, M.A. Kaya, H. Yildirim, Designed Monomers and Polymers, 15 (2012) 113.

[39] I. Pulko, M. Kolar, P. Krajnc, Science of the Total Environment, 386 (2007) 114.

[40] R.J. Wakeman, Z.G. Bhumgara, G. Akay, Chemical Engineering Journal, 70 (1998) 133.

[41] S. Shu, H. Kobayashi, M. Okubo, A. Sabarudin, M. Butsugan, T. Umemura, Journal of Chromatography A, 1242 (2012) 59.

[42] P. Krajnc, N. Leber, D. Stefanec, S. Kontrec, A. Podgornik, Journal of Chromatography A, 1065 (2005) 69.

[43] Y. Tunc, C. Golgelioglu, A. Tuncel, K. Ulubayram, Separation Science and Technology, 47 (2012) 2444.

[44] R. Dario Arrua, M. Cristina Strumia, C.I. Alvarez Igarzabal, Materials, 2 (2009) 2429.

[45] U. Sevšek, J. Brus, K. Jeřabek, P. Krajnc, Polymer, 55 (2014) 410.

[46] P. Krajnc, N. Leber, J.F. Brown, N.R. Cameron, Reactive and Functional Polymers, 66 (2006) 81.

[47] J.M. Williams, D.A. Wrobleski, Langmuir, 4 (1988) 656.

[48] A. Menner, A. Bismarck, Macromolecular Symposia, 242 (2006) 19.

[49] N.R. Cameron, D.C. Sherrington, L. Albiston, D.P. Gregory, Colloid and Polymer Science, 274 (1996) 592.

[50] I. Pulko, P. Krajnc, Macromolecular Rapid Communications, 33 (2012) 1731.

[51] S.D. Kimmins, N.R. Cameron, Advanced Functional Materials, 21 (2011) 211.

[52] E.P. Nesterenko, P.N. Nesterenko, D. Connolly, F. Lacroix, B. Paull, Journal of Chromatography A, 1217 (2010) 2138.

[53] M.R. Buchmeiser, Polymeric materials in Organic Synthesis, John Wiley & Sons, Federal republic of Germany, 2006.

[54] N.R. Cameron, A. Barbetta, Journal of Materials Chemistry, 10 (2000) 2466.

[55] R.J. Carnachan, M. Bokhari, S.A. Przyborski, N.R. Cameron, Soft Matter, 2 (2006) 608.

[56] R.F. Ding, Y. Hu, Z. Gui, R.W. Zong, Z.Y. Chen, W.C. Fan, Polymer Degradation and Stability, 81 (2003) 473.

[57] S. Essiz, B. Sari, Advances in Polymer Technology, 33 (2014).

[58] G.H. Teo, Y.H. Ng, P.B. Zetterlund, S.C. Thickett, Polymer, 63 (2015) 1.

[59] P. Innocenzi, Journal of Non-Crystalline Solids, 316 (2003) 309.

Chapter Three

Characterisation of chromatographic performance using the separation of small molecules with PS-co-DVB polyHIPEs in HPLC

“Opportunity is missed by most people because it is dressed in overalls and looks like work”- **Thomas Edison.**

3. Aim

The main objective of this chapter was to investigate the reverse phase high performance liquid chromatography (RP-HPLC) separation of small molecules using PS-*co*-DVB polyHIPE stationary phases housed within silcosteel. The materials generated here are the first instance of small molecule separation using polyHIPEs in HPLC. The chromatographic performance of these materials was characterised using van Deemter curves, backpressure profiles, swelling and permeability studies. The materials fabricated were shown to withstand a range of solvents and resulted in low backpressures at relatively high flow rates. The materials from batch to batch were found to be highly reproducible. The separation characteristics observed here showed high separation capacity where five analytes were base line separated from each other. The chromatographic performance also indicated strategies required to increase the separation efficiency of the materials as well as the suitability of silcosteel as a column housing.

3.1 Introduction

The highly interconnected macroporous network of polyHIPEs are an attractive stationary phase material for chromatographic separations [1, 2]. PolyHIPEs have been predominantly used in the separation of large biomolecules [3]. Separations of biomolecules are challenging, however a low surface area material such as a polyHIPE can be applied at high flow rates under gradient conditions leading to a fast separation of the analytes, demonstrating the speed of the separation of these materials. In many cases, the retention factors and peak shape of these analytes were poor, particularly where these materials were utilised in liquid chromatographic separations [3-5]. In addition, separations under gradient conditions limit the extrapolation about characteristic information about the polyHIPE as a separation material. This is because under such conditions, chromatographic characterisation tools such as van Deemter plots, pressure testing and swelling and permeability studies that are crucial in the development of these materials as usable stationary phases are inaccurate [6, 7]. Therefore, as well as addressing the application of the polyHIPE materials it is essential to characterise the materials to understand how they can be further developed as a stationary phase material.

While polyHIPEs have been used as stationary phases for fast separations of a variety of biomolecule mixtures, the use of polyHIPEs in HPLC for small molecule separations has not been observed in the literature. The first instances of small molecule separation involving chromatography was demonstrated using CEC of PS-*co*-DVB and IDA-*co*-DVB polyHIPEs as CEC stationary phases to separate alkylbenzenes. CEC is often used as a method to overcome issues relating to diffusion, commonly observed in HPLC to avail of the EOF for flow generation where

backpressures generated using mechanical may be problematic [8, 9]. CEC also has the advantage of generating higher plate counts and subsequently narrow peaks even with materials of low surface area [10].

Unfortunately, CEC has not realised its potential due to significant technical hurdles, with the result that HPLC remains the technology of choice for industrial analysis. Recently, a study used small molecules, nanoparticles of difference sizes, and polyHIPE materials in HPLC. However, the separation of the nanoparticles was not carried out in a mixed injection on the polyHIPEs but rather by injecting each sample individually. To date, application of polyHIPE materials as RP stationary phases for the separation of small analytes has not been explored, and their potential in this domain has not been evaluated [11].

3.1.1 Characterisation of chromatographic performance

Chromatographic characterisation of stationary phase material has been well developed in published literature [12-14]. Backpressure measurements, swelling and permeability studies and kinetic performance evaluation are the most common parameters evaluated.

3.1.1.1 Backpressure measurements

Backpressure measurements are used to characterise the pore volume of a column under constant temperature. The tolerance of a material to both applied pressure and different solvents can be established by performing pressure tests using the most commonly used HPLC solvents (MeOH, ACN and water) at varying flow rates. Backpressure measurements must be carried out under constant temperature because the viscosity of the solvent changes as the temperature increases. As well as understanding the pressure and solvent tolerance of one material, the backpressures

of different columns can also be compared to one another [15]. This is particularly useful where monoliths are concerned, as each monolith will polymerise with its own unique channels. Thus, any differences between the columns from batch to batch or within batch to batch can be distinguished. Connolly *et al.* used backpressure measurements to establish the difference between grafted and ungrafted GMA monoliths [16]. The swelling of the pores from the grafted chains resulted in higher backpressures, thus a difference between two monoliths was demonstrated.

3.1.1.2 Swelling and permeability studies

In addition to backpressure measurements, swelling and permeability studies can determine the influence of solvents on the pore structure of materials for chromatography. Here at a constant flow rate, pressure and temperature with the viscosity of the solvents can be used to calculate the permeability of the material. Where permeability decreases, it is most likely due to shrinkage of the pores resulting from swelling due to the solvent used. Most commonly, Darcy's Law is used to calculate this flow of solvent through a porous bed (Equation 1) [5, 17].

$$k = \frac{Q.\eta L}{\Delta P.A} \qquad \text{Equation 1}$$

Here, k is the permeability coefficient (m^2), Q is the flow rate (m^3/s), η is the viscosity of a given solvent (Pa/s), ΔP is the change in pressure (Pa), L is the column of flow length (m) and A is the internal area of the column (m^2). Previous studies have obtained information about the permeabilities of emulsion templated materials to investigate the application of gradient profiles and high flow rates suitable for the materials [4, 5]. In this chapter, we have applied polyHIPEs in order to calculate the permeability of PS-*co*-DVB polyHIPE columns produced in comparison to traditional organic monoliths produced in the literature.

3.1.1.3 Van Deemter plots

As studies of backpressures, swelling and permeability alone will not give an accurate flow profile of a polymer monolith, van Deemter plots have been used by chromatographers to determine the kinetic performance of a column and establish the optimum flow rate. Here, the plate height is plotted against varied linear velocities. The van Deemter plot has three significant terms, the A term the B term and the C term, which are shown in Figure 3.1. The A term refers to Eddy diffusion which arises from multiple paths that an analyte can take through a material. The B term, longitudinal diffusion, results from the gradient of concentration of the analyte band forming a hydrodynamic flow profile. Finally, the C term accounts for diffusion that exists when the analyte partitions between the mobile and stationary phase. The lowest point of this plot which equates to the narrowest plate height, determines the optimum linear velocity to be used in a separation [6]. Generally, silica monoliths produce a low C term allowing for the use of higher flow rates and resulting in less diffusion due to the convective nature of the flow. However, it is noted that organic monoliths give a higher C term, and thus a higher C term is expected for PS-*co*-DVB columns [1, 2, 18]. More importantly, as well as establishing the column kinetic performance, the van Deemter plots can give an indication of the presence of voids within the column. A van Deemter plot produced by a column with voids should therefore, produce plots which deviate from the typical trend, indicating a problem with the material fabricated.

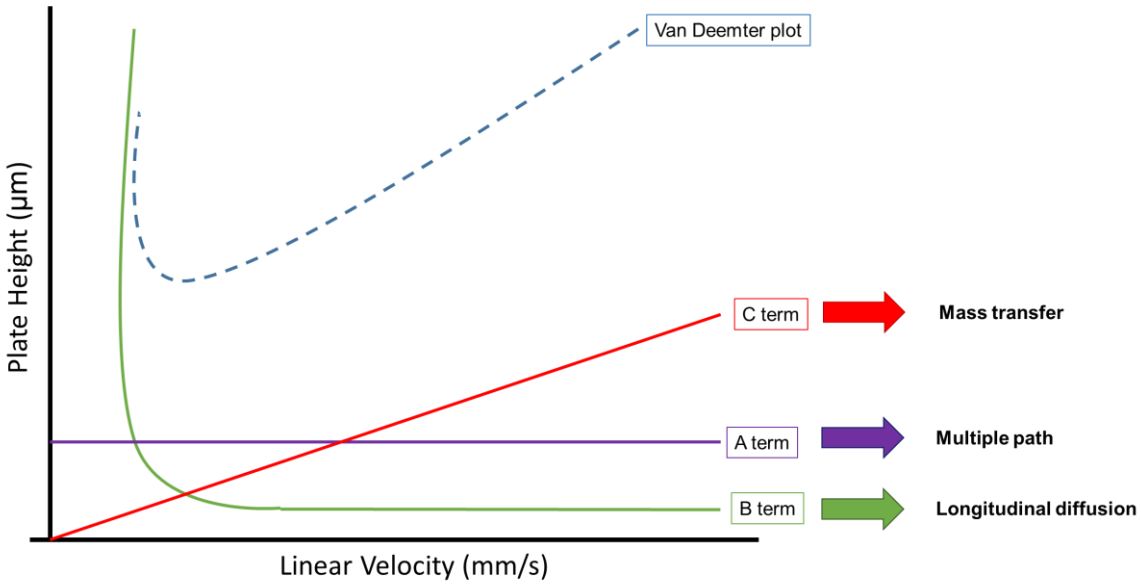

Figure 3.1: *Van Deemter plot and the terms which contribute to diffusion in liquid chromatography.*

In this chapter, the isocratic RP-HPLC separation of small molecules has been achieved using polyHIPEs as stationary phases. A series of alkylbenzenes were separated in 30 minutes. In addition to demonstrating their separation capacity, this separation was used characterise their separation performance. This represents the first time that traditional polyHIPE morphology has been characterised chromatographically. The PS-*co*-DVB polyHIPE fabricated in this study, unlike many of the more hydrophilic polyHIPEs fabricated for RP-HPLC of large biomolecules in earlier studies, has a distinct void and window morphology which should result in decreased dispersion effects [4, 5, 19]. This work uses a polyHIPE microbore column of 100 mm long silicosteel tubing which is compatible with pressures generated in capillary LC, a housing that has not been employed with polyHIPE materials previously. The chromatographic efficiency of these columns were evaluated using pressure, swelling and permeability studies as well as van Deemter profiles and chromatographic separation of alkylbenzenes in isocratic and gradient modes.

3.2 Materials and methods

Millipore ultrapure water purified to a resistance of > 18 MΩcm was used in all instances. Ethylbenzene >99.8%, propylbenzene >99%, butylbenzene >99%, pentylbenzene 99%, Calcium dihydrochloride > 99%, Span ®80, 3-glycidoxypropyl-trimethoxysilane ≥ 98%, potassium persulphate (PPS), styrene (Sty) ≥ 99%, divinylbenzene (DVB) 80% isomeric mix were purchased from Fluka (Sigma Aldrich, Tallaght Ireland). All solvents were used as received and were of analytical HPLC grade. All silcosteel tubing (1.02 mm in I.D.) was supplied by RESTEK (Belfast, Northern Ireland).

3.2.1 Instrumentation

Backpressure, swelling and permeability studies were performed using an Ultimate 3000 LC, where an ultrasonicator (Branson 5510) was used to degas mobile phases. Van Deemter curves were established using an Agilent 1200 and columns were imaged using an optical microscope (Meijic Techno EMZ-STR).

3.2.2 Methods

3.2.2.1 Backpressure, permeability and swelling tests

Backpressure and permeability and swelling tests were carried out using a capillary LC where each column was successfully flushed through with solvents water, ACN and MeOH at flow rates of 0-1.2 mL min^{-1} in 0.2 mL min^{-1} increments. The backpressure produced at each flow rate for each solvent was recorded in triplicate. The permeability of each column at 0.6 mL min^{-1} was calculated using Darcy's Law using Equation 1 [5, 17].

3.2.2.2 PolyHIPE column selectivity and efficiency

The expected reverse phase interactions of the PS-*co*-DVB columns produced were confirmed using the methylene selectivity. Here the ln(k'), where k' is the separation capacity (or retention factor), plotted against the corresponding number of carbons on the increasing alkylbenzene chain to give a linear graph if the retention method is a reverse phase interaction [20-22].

Column efficiency was calculated by injecting a propylbenzene standard onto the column at increasing flow rates to calculate the number of theoretical plates (N) using Equation 2.

$$N = 16 \left(\frac{t_r}{w}\right)^2 \qquad \text{Equation 2}$$

Where N is the number of theoretical plates, t_r is retention time and w is the of the base of the peak. The height equivalent theoretical plate was subsequently calculated according to Equation 3.

$$H = \frac{L}{N} \qquad \text{Equation 3}$$

Where H is the height equivalent theoretical plate, L is the length of the column in mm and N is the number of theoretical plates. H in µm was plotted against linear velocity in mm second^{-1} to result in the van Deemter plot.

3.2.2.3 Chromatographic conditions

Alkylbenzene separation was carried out by using mixed standard solution (0.1 ppm) of toluene, ethylbenzene, propylbenzene, butylbenzene and pentylbenzene prepared in ACN using an Agilent 1200. The HPLC system consisted of a quaternary pump including an online vacuum degasser, an autosampler and a UV detector at 214 nm. Chromatographic separation was achieved on a polyHIPE columns of 100 mm x

1.02 mm i.d.). Mobile phase conditions of the isocratic system was 50:50 ACN:Water. The mobile phases were filtered and then degassed using an ultrasonicator.

3.3 Results and discussion

3.3.1 Backpressure studies of 90% PS-*co*-DVB polyHIPEs in silcosteel columns

Backpressure measurements were used to establish the pressures resulting from solvent flow through the 90% PS-*co*-DVB silcosteel columns. Here increasing flow rates (0 to 1.2 mL min^{-1}) were applied to duplicate columns 1 and 2 and their corresponding backpressures were recorded when the pressure had stabilised. In Figure 3.2, the backpressure curves of the three columns prepared using separate emulsions were linear and give similar backpressures. This indicated a linear dependence of column pressure on flow rate, demonstrating a good mechanical stability of the columns. This shows that the polyHIPE material is suitable for use within a high-pressure system. The highest backpressures were observed using column 1. Backpressure measurements carried out repeatedly on a single column resulted in %RSD up to 20%, while %RSD values from batch to batch were up to 24% both being relatively high %RSD values. Both single column and batch to batch reproducibility showed large %RSD figure as flow paths formed within each column was not uniform.

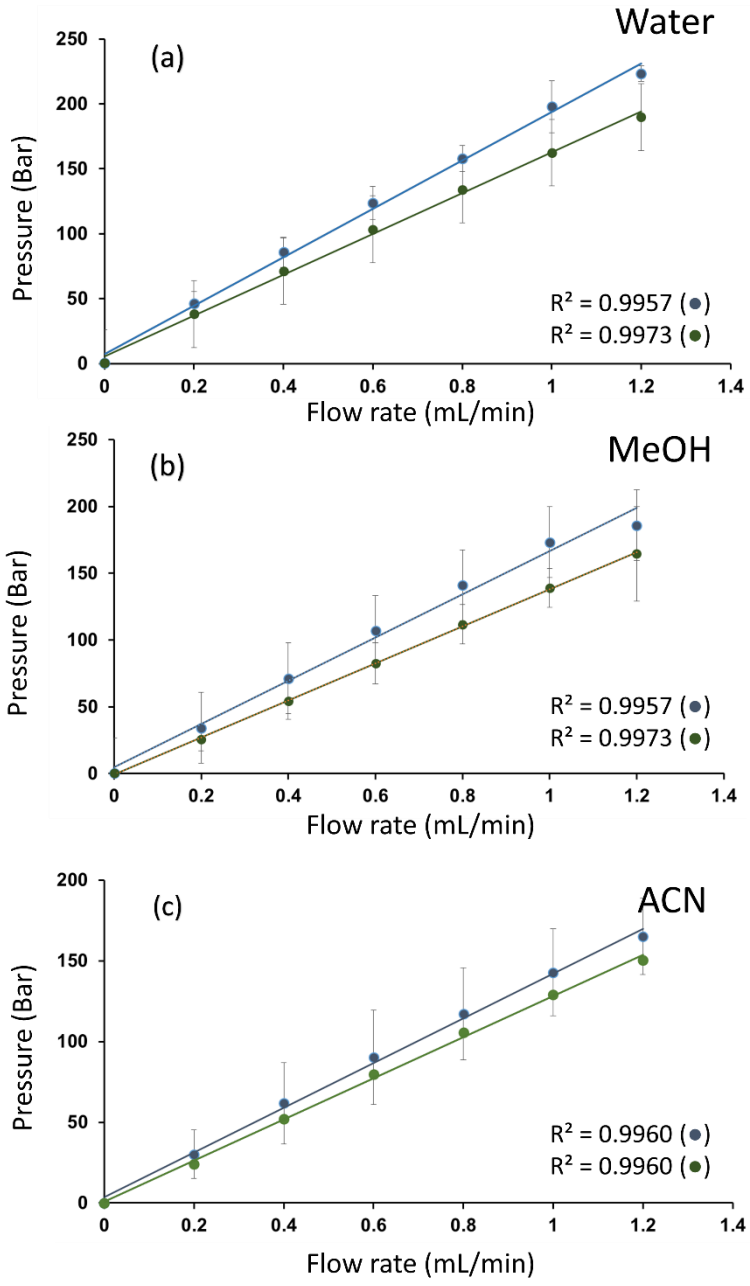

Figure 3.2: *Backpressure profiles of PS-co-DVB produced in silcosteel where blue was column 1 and green was column 2. Backpressure measurements were taken in triplicate using solvents (a) water, (b) MeOH and (c) ACN over a flow rate of 0 to 1.2 mL min^{-1} at room temperature.*

Table 3.1 below shows the increase of the slope of the profile for each solvent. ACN resulted in a lower slope, which indicates that it generated a lower backpressure than that of MeOH or water. The general trend observed for the columns was that

backpressure was the lowest for ACN and highest for water. The trend observed was expected, as the viscosity of water is the highest at 0.8937 mPa second^{-1} (25°C) [23]. Therefore the higher the viscosity of the solvent the higher the backpressure generated by the column.

Table 3.1: *Slope of backpressure profiles using common HPLC solvents*

Solvent	Column 1 Bar/ ml mL^{-1}	Column 2 Bar/ ml mL^{-1}
ACN	138.61	122.00
MeOH	161.64	138.80
Water	186.43	157.09

3.3.2 Swelling and permeability studies of PS-*co*-DVB polyHIPEs in silcosteel columns

The permeabilities of the 90% PS-*co*-DVB columns were calculated (Equation 1) to establish the swelling and shrinkage effects of the solvents [24]. The surface area of these materials as discussed in Chapter 2 were reported at 20 $m^2 g^{-1}$ in addition to its relative porosity of 90% the polyHIPEs. Thus, it was expected that the materials would be significantly permeable. Table 3.2 lists the calculated permeabilities of the columns for each solvent using Darcy's Law. Typical organic polymer monoliths should have permeabilities within the range of 10^{-14} to 10^{-15} [25-27]. The permeabilities presented in Table 3.2 lie within a range of 10^{-16} to 10^{-17} and were therefore, lower than literature values [24, 26, 27], however they were still considered acceptable as the deviation was most likely resulted from using a column of larger diameter than previously reported for capillary columns [25]. It was expected that ACN would give the highest permeability due to its low viscosity and low backpressure from the

previous section. Despite having a lower backpressure, a decreased permeability was observed when using ACN. Conversely, water, which previously generated the highest backpressures, resulted in higher permeability coefficients for all columns when compared to ACN and MeOH. This result was unexpected as the viscosity of water at room temperature is higher than that of ACN and MeOH, thus a lower permeability value was expected. It is hypothesised that ACN had a shrinking effect on the pores of the polyHIPE materials as the permeability of these materials decreased by an order of magnitude [28, 29]. The precision of the resulting permeability coefficients was poor as the %RSD was calculated to be up to 20%, resulting from the variability on backpressure observed in the previous section. MeOH at higher flow rates for column 1 started to deviate from the linear trend expected, however such high flow rates with such low surface area materials would not be utilised in separations. More interestingly MeOH also appeared to give the lower permeabilities than that of water. The lower permeabilities that resulted could be a due to pore size change similar to that observed when using ACN, however the change with MeOH was not as substantial. Despite the effect of pore shrinkage observed by ACN, the general linear trend of the backpressure plots presented in the previous section suggests that the swelling and shrinking effects of the columns did not permanently alter the column.

Table 3.2: *Permeability (k) of 90% polystyrene-co-divinylbenzene polyHIPEs in silcosteel using varying solvents at 0.6 mL min^{-1}*

Column	**MeOH**	**ACN**	**Water**
	±2.57 x_{10}^{-17}	**±1.80 x_{10}^{-17}**	**±2.57 x_{10}^{-17}**
1	1.00x_{10}^{-16}	8.28 x_{10}^{-17}	1.67x_{10}^{-16}
2	1.17 x_{10}^{-16}	8.98x_{10}^{-17}	1.98x_{10}^{-16}

3.3.3 Determination of column efficiency

As the polyHIPEs were demonstrated to be mechanically stable and consistent with permeabilities appropriate for HPLC, they were characterised chromatographically in terms of their kinetic performance. by determining the van Deemter plots of each column (Figure 3.3). Propylbenzene was injected at varying flow rates and N and HETP were calculated using Equation 2 and Equation 3, respectively. From Figure 3.3, both column 1 and 2 were found to have similar van Deemter plots. An optimum flow rate of 0.04 mL min^{-1} was determined with N values of 474.679 and 454.93 and HETP values of 210.67 and 219.81 µm for columns 1 and 2 respectively. The van Deemter plots for column 1 and 2 showed little evidence of eddy diffusion or longitudinal diffusion. A higher instance of the latter results of diffusion would result in a flatter van Deemter profile upon increase of the A term and a sharper increase of the plot at lower flow rates for the B term [30]. However, the diffusion attributed to these columns was mostly due to a large amount of resistance to mass transfer between the stationary phase and the mobile phase. The time taken for an analyte band to flow through and partition between the stationary phase and the mobile phase was expected to increase in this study due to the presence of voids and interconnecting windows, as this morphology within a larger diameter polyHIPE the skeleton windows could be acting as mixing vessels. However, it is not unusual to have little improvement of the resistance to mass transfer using monolithic stationary phases [1, 2, 18, 30]. In addition, previous studies have shown that the morphology of polyHIPEs can result in large dispersion effects and a corresponding decrease in separation efficiency [3].

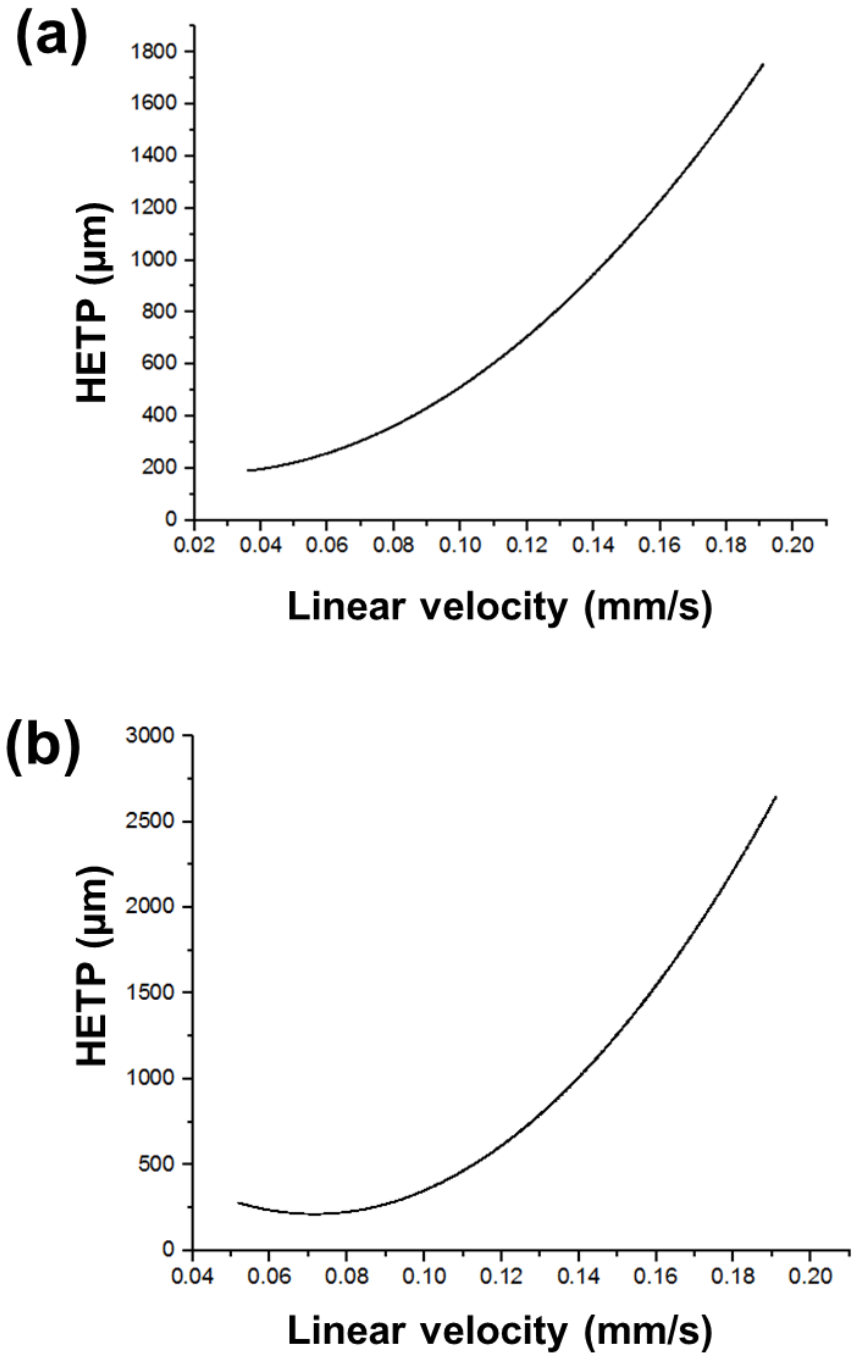

Figure 3.3: *Van Deemter plots for PS-co-DVB polyHIPE columns (a) column 1 and (b) column 2 fabricated.*

The van Deemter profiles of polyHIPE materials in the literature have been demonstrated using capillary electrochromatography (CEC), which, show a greater effect of the B term (longitudinal diffusion) due to a EOF coupled with a pressure driven

flow. Similar to our study, previous results reported the C term (mass transfer) to have a large effect on diffusion most likely a direct result of the polyHIPE morphology [1, 2]. CEC separations will still produce sharper peaks and less diffusion due to the plug flow profile of the EOF leading to a more efficient separation [31]. However, it is expected that if a capillary of a similar dimension to that used in CE studies were applied to an LC system, the peak shape would significantly be affected by the C term and more band broadening would be present in the resulting chromatograms. In addition, the low surface area of these unmodified polyHIPE materials will ultimately result in lower efficiencies and a higher plate height [32, 33]. For both these reasons, the relatively poor separations observed here are typical for these materials.

3.3.3.1 Determination of column efficiency in void containing column

In contrast to column 1 and 2, a third column (column 3) was found to have slightly higher permeabilities of 1.22×10^{-16}, 9.40×10^{-17} and 2.15×10^{-16} for MeOH, ACN and water respectively. Furthermore, the lowest backpressure was observed with column 3 as shown in Figure 3.4. However from the latter information and the Figure 3.4 below it is difficult to say whether the differences are due to unique flow paths or possible column voids.

Upon investigating the optimum flow rate a poor van Deemter profile was obtained when compared to columns 1 and 2 as shown in Figure 3.5. This was hypothesised to be due to possible voids present within the column. Interestingly, as the backpressure for this column in particular was found to be the lowest it supports the suggestion of the presence of voids within the column. As well as establishing the optimum flow rate of 0.04 mL min^{-1}, it was illustrated that the van Deemter plot could successfully be utilised to determine the presence of voids. As column 3 was shown to contain voids and was therefore defective, it was not characterised any further.

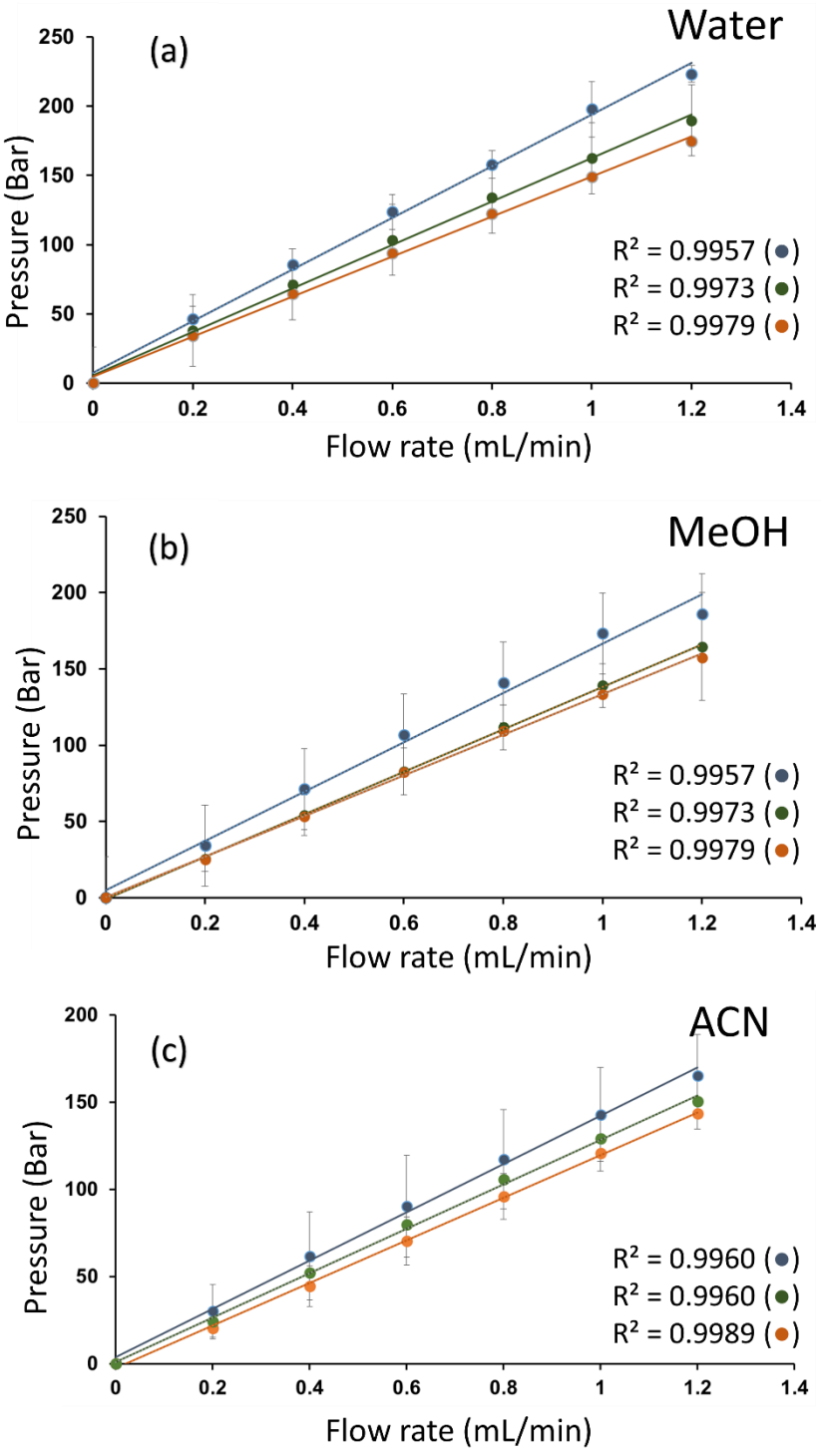

Figure 3.4: *Backpressure profiles of PS-co-DVB produced in silcosteel where blue was column 1, green was column 2 and orange was column 3. Backpressure measurements were taken in triplicate using solvents (a) water, (b) MeOH and (c) ACN over a flow rate of 0 to 1.2 mL min-1 at room temperature.*

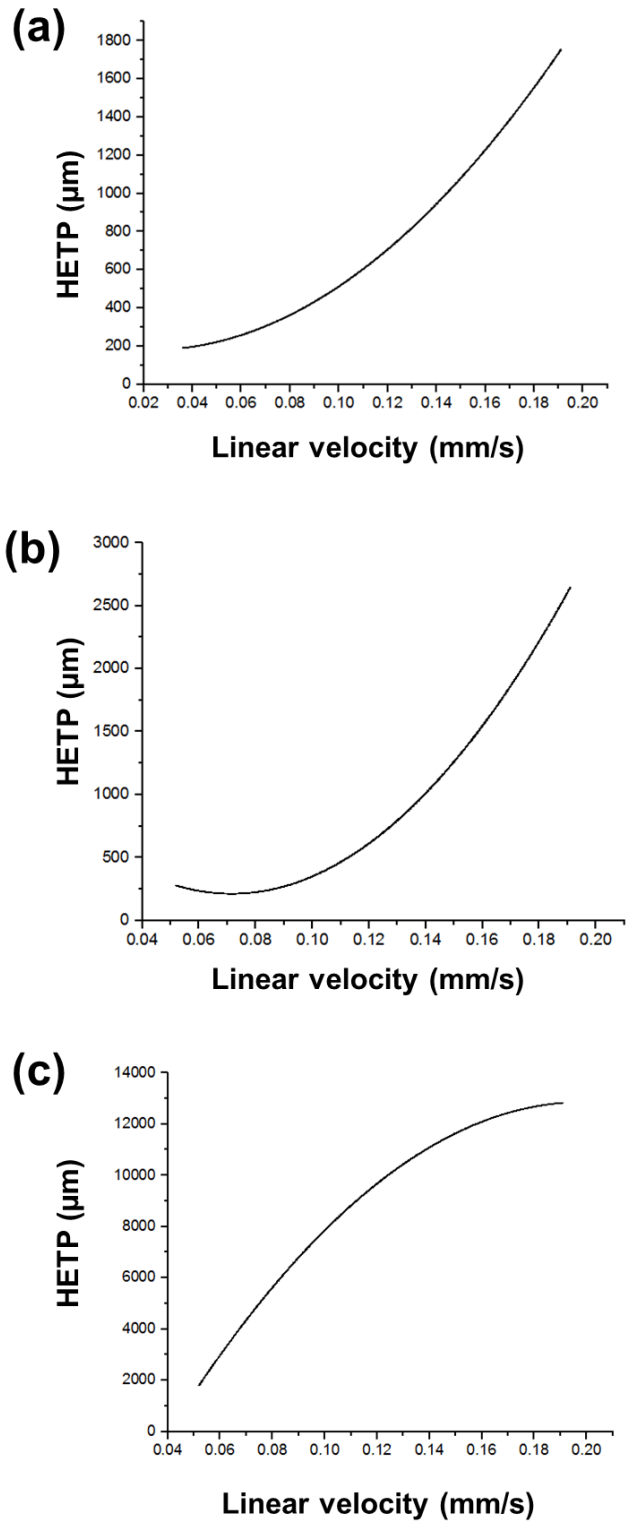

Figure 3.5: *Comparison of Van Deemter plots for PS-co-DVB polyHIPE with no voids (a) column 1 and (b) column 2 as well as (c) void containing column 3.*

3.3.4 Chromatographic separations of 90% PS-*co*-DVB polyHIPEs in silcosteel columns

3.3.4.1 Isocratic separation of alkylbenzenes

The chromatographic performance of these PS-*co*-DVB polyHIPE columns was evaluated by the separation of selected alkylbenzenes. To date, polyHIPE materials have only been applied in biological separations in LC although reports of separation of small molecules such as alkylbenzenes have been reported in CEC [1, 2, 4, 11]. In this study, the elution order of the alkylbenzenes was in accordance to the analyte's increasing hydrophobicity. It is well established that the mechanism of RP separations is due to the repulsion of the analytes from the mobile phase into the stationary phase [13, 20-22]. This increase of retention is due to the increasing number of carbons is known as the methylene group selectivity and was expected to be the mechanism for the separation of alkylbenzenes in this study. Figure 3.6 below demonstrates the methylene selectivity between column 1 and 2. Here the ln (k') was plotted against the increasing number of carbons in the alkylbenzenes (n_c). The resulting graph of column 1 and 2 demonstrated high linearity with R^2 values of 0.9995 and 0.9997 respectively, confirming the retention increase to be attributed to the increase in alkyl chain length for each analyte.

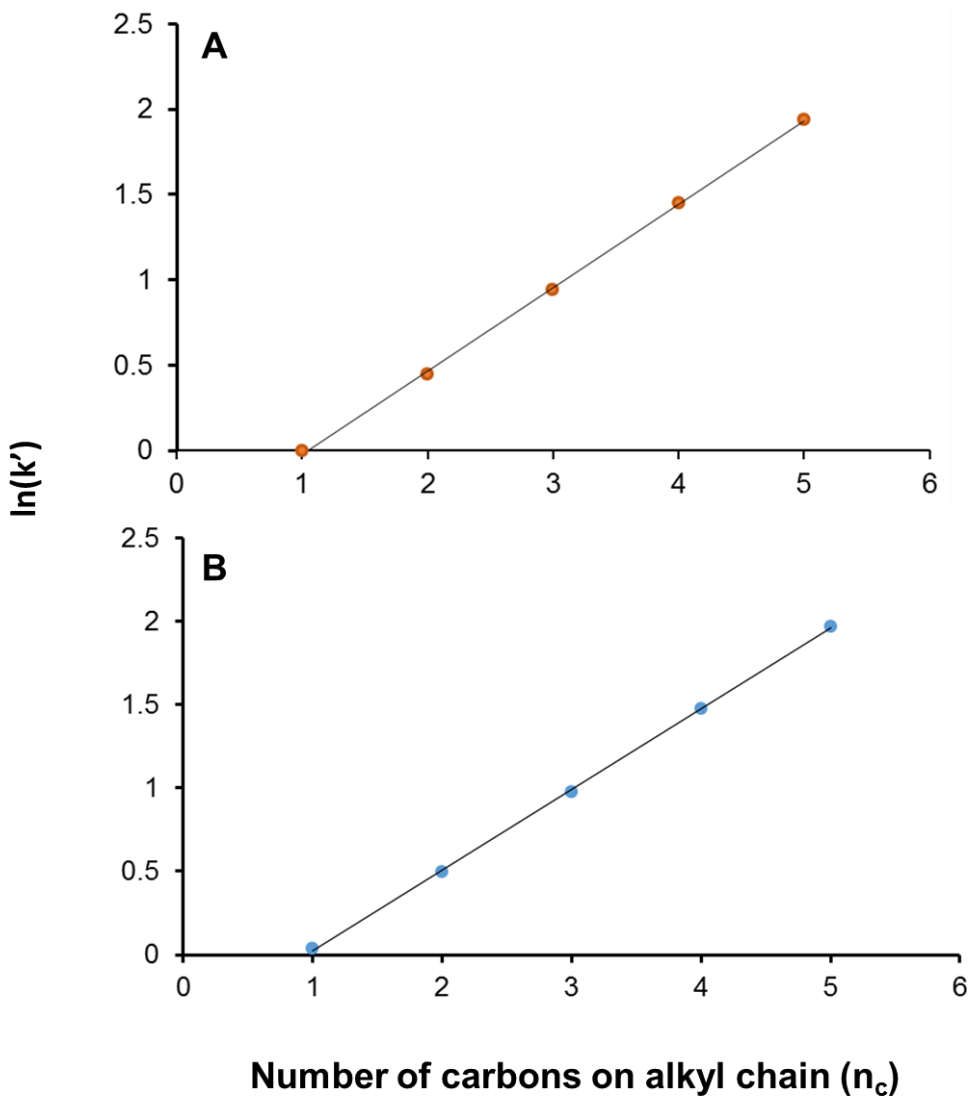

Figure 3.6: *Methylene selectivity for column 1 (A) and column 2 (B) for the increasing alkylbenzene chain (toluene to pentylbenzene).*

In Table 3.3, the separation performance characteristics t_r (retention time), k (retention factor), α (selectivity), R_s (resolution), N (efficiency) and A_s (peak asymmetry) highlight the similarities and differences between the two columns. The results generated are very promising indicators of separation capacity of the polyHIPE columns.

Table 3.3: *Separation characteristics of column 1 and column 2 for alkylbenzenes*

Alkylbenzene separation	t_r	k'	α	R_s	N	A_s
Column 1						
Toluene	6.09±0.026	1.00	1.61	1.66	628.12	1.33
Ethylbenzene	7.92±0.006	1.56	1.64	0.73	513.86	1.00
Propylbenzene	11.00±0.004	2.56	1.66	0.81	449.74	1.33
Butylbenzene	16.26±0.050	4.26	1.63	0.92	429.85	1.08
Pentylbenzene	24.59±0.070	6.95	1.63	0.91	410.52	1.23
Column 2						
Toluene	5.97±0.016	1.04	1.58	2.52	755.13	1.43
Ethylbenzene	7.73±0.030	1.64	1.62	0.85	571.00	1.60
Propylbenzene	10.72±0.021	2.66	1.65	1.05	490.53	1.25
Butylbenzene	15.79±0.065	4.38	1.63	1.28	441.31	1.64
Pentylbenzene	23.83±0.106	7.13	1.63	1.31	431.21	1.32

The alkylbenzene separation in Figure 3.7 (i) of the polyHIPE column 1 resulted in a poorer resolution relative to column 2. While each batch of emulsion was prepared in an identical process, the resulting heterogeneities in the distribution of the macropores throughout the polyHIPE are expected due to its manner of fabrication.

The limitations of monolithic columns, particularly in terms of their variability in geometry and spatial distribution of flow through pores is well documented [34, 35]. These limitations also applied to the polyHIPE columns fabricated within this study; however as discussed below, the column to column reproducibility was less than 3%. The band broadening effects observed were expected due to the low surface area and the diffusion effects established in the previous section. In addition, low N values of 474.679 and 454.93 and HETP values of 210.67and 219.81 µm for columns 1 and 2 respectively also contributed to the band broadening effects. The previous van Deemter study suggests that the majority of the diffusion stems from the C term. It could also be argued that, the high degree of diffusion may also be due to a competing separation mechanism. In this case a potential alternative separation mechanism could be as a result of size exclusion, as the void and window structures within the skeleton of the polyHIPE acts as a type of molecular sieve for the alkylbenzene analytes. However, generally with additional competing modes of separation there can be significant tailing effects. In such instances the asymmetry factor is greater than 2, which was not observed here and so would make a competing mode of separation an unlikely cause for the band broadening effects observed in this work [36]. In this study the peak symmetry had an acceptable degree of tailing where all analytes gave a value below the acceptable tailing factor limit of 2 [37]. In addition, the linearity of the methylene selectivity confirms the increased retention upon increase of alkyl chain length of the analytes, despite the band broadening effects observed in this separation. In addition, although increased efficiencies were obtained in the CEC separation of alkylbenzenes as shown in Figure 3.7 (ii), the peak shape upon increased alkyl chain length followed a similar trend of increasing peak broadness, which has been reported in similar separations [38-40].

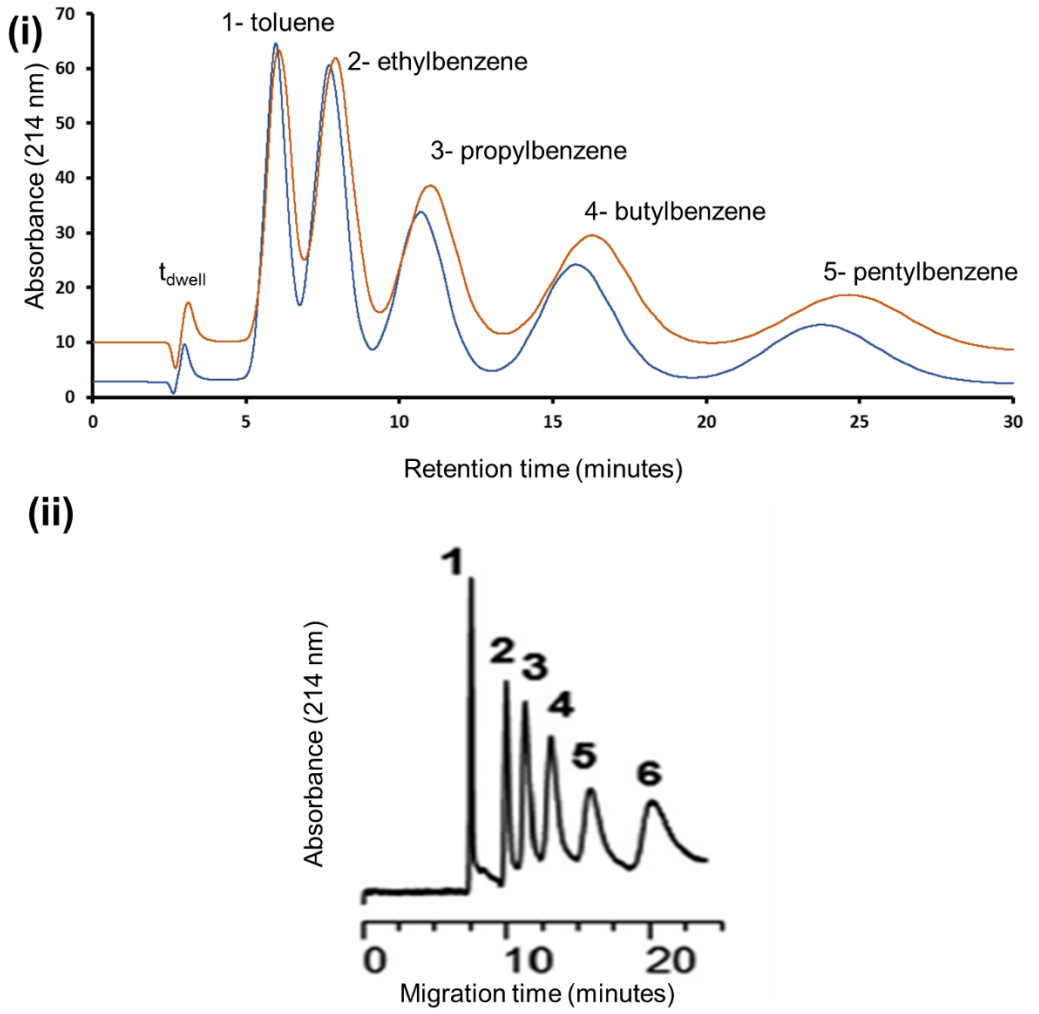

Figure 3.7: *(i) Alkylbenzene separation (0.1 ppm) at flow rate 0.04 mL min^{-1} at wavelength of 214 nm and injection volume of 1 µL (MP- 50:50 ACN:H_2O and SP- 90% PS-co-DVB polyHIPE column of 100 mm x 1.02 mm i.d. dimension where (orange) Column 1 and (blue) Column 2. (ii) CEC separation of alkylbenzenes (1-6) thiourea, benzene, toluene, ethylbenzene, propylbenzene, and butylbenzene respectively, at ACN ratio (v/v) of: 60/40 [2].*

While column 1 did not achieve complete baseline separation, the mixed standard components were distinguishable from each other. When compared to other PS-*co*-DVB monoliths of similar surface area (23 m^2 g^{-1}) which did not attain baseline separation of alkylbenzenes, the polyHIPE monolith presented here achieved a

successful isocratic separation of alkylbenzenes [41]. This is exceptional using a material, which was found in Chapter 2 to exhibit a low surface area (20 m^2 g^{-1}).

As noted in Table 3.3 the number of theoretical plates is lower than previously observed in similar materials with smaller dimensions in the literature [1, 2]. Conversely, retention capacity was greater than 1 in all cases indicating that the analytes had an affinity for the stationary phase and did not elute at the dwell volume. Selectivity was greater than 1.5 for all analytes indicating the ability of the material to differentiate between the different analytes within the sample.

Table 3.4: *Average retention time of alkylbenzenes of column 1 and 2 to observe degree of deviation (n=3)*

Analyte	%RSD Column 1	%RSD Column 2
Toluene	0.43	0.26
Ethylbenzene	0.08	0.39
Propylbenzene	0.04	0.19
Butylbenzene	0.30	0.41
Pentylbenzene	0.28	0.44

Table 3.4 shows the %RSD of three injections of the mixed standard on each column. An low %RSD of less than 0.44% was observed and thus the columns were of acceptable reproducibility [36, 37]. Variance in retention time was hypothesised to be due to the unique pore formation associated with material fabrication and is expected with monolithic stationary phases [34, 35]. However, despite the variance due to fabrication being observed, the batch to batch reproducibility of the injections on the two separate columns at less than 0.44% RSD was statistically indistinguishable at 95% confidence and comparable to LC separations on polyHIPE

columns in the literature [42]. Therefore, it can be concluded that the separations obtained using PS-*co*-DVB polyHIPE stationary phases are consistent and reproducible in terms of retention times, enhancing their potential application in chromatographic separations.

3.4 Conclusions

The PS-*co*-DVB polyHIPE columns within microbore silcosteel housing were characterised for chromatographic performance by pressure testing, swelling and permeability tests and application in chromatographic separation. Backpressure and swelling studies of these materials illustrated their stability when subjected to different common HPLC solvents. The backpressure measurements showed that the solvent with the highest backpressure was water which was expected as it had the highest viscosity, whereas the lowest backpressure was generated using ACN. However, when swelling and permeability tests were carried out on the columns, ACN flow through the columns resulted in the lowest permeability. Therefore, it was hypothesised that ACN resulted in a shrinking effect on the macropores of the PS-*co*-DVB polyHIPEs. Overall, the permeability was found to be two orders of magnitude lower than that of other traditional polymer monoliths. Nonetheless, the permeabilities were acceptable for use in chromatography.

As well as establishing the permeability and backpressure of the materials, van Deemter profiles were used to determine the kinetic performance in addition to indicating the presence of voids for the three columns produced. From this study column 3 was found to contain voids. The voids were not distinguishable using backpressure measurements alone highlighting the importance of van Deemter plots. In addition, the optimum flow rate of the two functioning columns was found to be 0.04 mL min^{-1}. A successful isocratic separation of alkylbenzenes using silcosteel columns was achieved. Despite the low efficiencies observed with these materials, the columns obtained separation with retention factors greater than 1, selectivity greater that 1.5, peak asymmetry less than 2 and reproducibility between batches of less than 3%.

The PS-*co*-DVB polyHIPEs in this study were unmodified and were of a low surface area. Despite this the polyHIPE materials were found to have a remarkable separation capacity. The polyHIPE columns were also able to successfully separate a mixture of alkylbenzenes with high consistency, stability and reproducibility. Although low column efficiencies were observed, a high degree of selectivity was shown in the chromatograms of the analytes and demonstrates the separation potential which can be achieved by this study. This study has highlighted the potential of these unmodified polyHIPE materials. The resulting separations indicate the future promise of these materials once they are strategically modified to have both high surface area and adequate mechanical rigidity for pressure driven flow. The following chapter, therefore, will investigate graphene oxide modified polyHIPE materials in fused silica capillary columns to include surface area and enhance reproducibility for the separation of alkylbenzenes.

3.5 References

[1] Y. Tunc, C. Golgelioglu, N. Hasirci, K. Ulubayram, A. Tuncel, Journal of Chromatography A, 1217 (2010) 1654.

[2] Y. Tunc, C. Golgelioglu, A. Tuncel, K. Ulubayram, Separation Science and Technology, 47 (2012) 2444.

[3] P. Krajnc, N. Leber, D. Stefanec, S. Kontrec, A. Podgornik, Journal of Chromatography A, 1065 (2005) 69.

[4] J. Yang, G.L. Yang, H.Y. Liu, L.G. Bai, Q.X. Zhang, Chinese Journal of Chemistry, 28 (2010) 229.

[5] C.H. Yao, L. Qi, H.Y. Jia, P.Y. Xin, G.L. Yang, Y. Chen, Journal of Materials Chemistry, 19 (2009) 767.

[6] S.C. Moldoveanu, V. David, Essentials in Modern Hplc Separations (2013) 1.

[7] T. Teutenberg, High-Temperature Liquid Chromatography: a User's Guide for Method Development (2010) 1.

[8] D. Hindocha, N.W. Smith, P.J. Borman, Chromatographia, 53 (2001) S276.

[9] J.H. Knox, I.H. Grant, Chromatographia, 24 (1987) 135.

[10] J. Lin, J. Lin, X. Lin, X. Wu, Z. Xie, Electrophoresis, 31 (2010) 1674.

[11] C.H. Yao, L. Qi, G.L. Yang, F.Y. Wang, Journal of Separation Science, 33 (2010) 475.

[12] D.N. Bassanese, A. Soliven, P.G. Stevenson, G.R. Dennis, N.W. Barnett, R.A. Shalliker, X.A. Conlan, Journal of Separation Science, 37 (2014) 1937.

[13] J. Zhong, M. Hao, R. Li, L. Bai, G. Yang, Journal of Chromatography A, 1333 (2014) 79.

[14] M.-L. Chen, L.-M. Li, B.-F. Yuan, Q. Ma, Y.-Q. Feng, Journal of Chromatography A, 1230 (2012) 54.

[15] T. Rohr, E.F. Hilder, J.J. Donovan, F. Svec, J.M.J. Frechet, Macromolecules, 36 (2003) 1677.

[16] D. Connolly, B. Paull, Journal of Separation Science, 32 (2009) 2653.

[17] L. Pal, M.K. Joyce, P.D. Fleming, Tappi Journal, 5 (2006) 10.

[18] A.M. Siouffi, Journal of Chromatography A, 1126 (2006) 86.

[19] P. Krajnc, N. Leber, D. Štefanec, S. Kontrec, A. Podgornik, Journal of Chromatography A, 1065 (2005) 69.

[20] A. Tchapla, H. Colin, G. Guiochon, Analytical Chemistry, 56 (1984) 621.

[21] B.L. Karger, J.R. Gant, A. Hartkopf, P.H. Weiner, Journal of Chromatography, 128 (1976) 65.

[22] N. Tanaka, E.R. Thornton, Journal of the American Chemical Society, 99 (1977) 7300.

[23] L. Korson, Drosthan.W, F.J. Millero, Journal of Physical Chemistry, 73 (1969) 34.

[24] C. Martin, J. Coyne, G. Carta, Journal of Chromatography A, 1069 (2005) 43.

[25] R.D. Arrua, P.R. Haddad, E.F. Hilder, Journal of Chromatography A, 1311 (2013) 121.

[26] K.-F. Du, D. Yang, Y. Sun, Journal of Chromatography A, 1163 (2007) 212.

[27] Q. Zhang, J. Guo, F. Wang, J. Crommen, Z. Jiang, Journal of Chromatography A, 1325 (2014) 147.

[28] K.N. Smirnov, I.A. Dyatchkov, M.V. Telnov, A.V. Pirogov, O.A. Shpigun, Journal of Chromatography A, 1218 (2011) 5010.

[29] R.J. Vonk, A. Vaast, S. Eeltink, P.J. Schoenmakers, Journal of Chromatography A, 1359 (2014) 162.

[30] H. Oberacher, A. Premstaller, C.G. Huber, Journal of Chromatography A, 1030 (2004) 201.

[31] S. Ghosal, Annual Review of Fluid Mechanics, 38 (2006) 309.

[32] M.S. Silverstein, Polymer, 55 (2014) 304.

[33] F. Svec, Journal of Chromatography A, 1217 (2010) 902.

[34] M. Díaz-Bao, R. Barreiro, J. Miranda, A. Cepeda, P. Regal, Chromatography, 2 (2015) 79.

[35] F. Svec, C.G. Huber, Analytical Chemistry, 78 (2006) 2100.

[36] R.L. Snyder, J.J. Kirkland, V.J. Dolan, Introduction to Modern Liquid Chromatography, John Wiley & Sons, Hoboken, New Jersey, 2011.

[37] J.J. Gilroy, J.W. Dolan, LC•GC Europe, 7 (2004).

[38] J. Urban, F. Svec, J.M.J. Frechet, Analytical Chemistry, 82 (2010) 1621.

[39] J. Urban, F. Svec, J.M.J. Frechet, Journal of Chromatography A, 1217 (2010) 8212.

[40] A. Svobodová, T. Křížek, J. Širc, P. Šálek, E. Tesařová, P. Coufal, K. Štulík, Journal of Chromatography A, 1218 (2011) 1544.

[41] Q.C. Wang, F. Švec, J.M.J. Fréchet, Journal of Chromatography A, 669 (1994) 230.

[42] J. Yang, G. Yang, H. Liu, L. Bai, Q. Zhang, Journal of Applied Polymer Science, 119 (2011) 412.

Chapter Four

Application of Graphene oxide modified polyHIPEs for increased reproducibility in HPLC separations

“One sometimes finds what one is not looking for.”- **Sir Alexander Fleming.**

4. Aim

The aim of this chapter was apply GONP modified PS-*co*-DVB polyHIPE materials within capillary columns for separation of small molecules using RP-HPLC. The columns were characterised in their oxidised and reduced forms in terms of their chromatographic performance. The reduction of the GONPs was found to alter the column's surface chemistry and reduce the retention interactions with the analytes.

4.1 Introduction

An underlying issue that exists when using monolithic stationary phases, is the ability to produce monoliths that are reproducible between batches. During the polymerisation process it is known that the pores channels which form are unique to each individual monolith. Therefore, as a result the flow path through each material is different. Previously, monolithic columns produced have required to be scaled down to shorter column formats known as membranes and short monolithic columns (SMC). However, due to batch to batch reproducibility issues SMC monolithic columns in particular were not successful when produced for commercial use [1]. More complex methods of improving batch to batch reproducibility includes the use of more sophisticated housings such as tube in tube fabrication [2]. While modification of the monolith structure itself can be challenging to optimise, surface modification can be used to increase reproducibility of the HPLC separation [3-5]. Surface modifications using GONPs will be explored in detail in this chapter.

4.1.1 Graphene oxide materials

Increasing interest in graphene and its derivatives has recently been dominating research in areas such as electrochemistry, physics and materials chemistry to name a few [6-10]. Graphene oxide (GO) is derived from the oxidation of graphite (natural mineral from metamorphic rock) with potassium permanganate and sulfuric acid [6, 11]. While graphite is comprised of multiple layers of graphene (single layer of carbon in hexagonal honeycomb confirmation), GO is formed from the oxidation of graphite forming one or multiple layers of GO. The oxidation process also increases the instance of hydrophilic groups on the surface. This increased interest in

graphene related technology is a direct result of the interesting physical properties associated with GO such as high thermal stability, enhanced conductive properties when reduced and high surface area [6]. This has led to the development of graphene-incorporated materials in areas such as electrochemical sensing, conducting fabrics for wearable sensors and chromatography [7-10, 12-23]. Of particular interest here is the application of GO in the area of material fabrication and its significance to the particular area of separation science.

4.1.2 Graphene oxide modified polymers

One of the most prominent applications of GO has been in the development of polymeric materials. Particularly interesting uses of GO-polymer composites include electrochemistry [7, 9, 23] and photovoltaic cells [8]. Use of GO in electrochemical sensors in particular have been shown to reinforce polymeric materials used as electrodes in addition to increasing sensitivity due to its large surface area and has low noise effects electronically [23, 24]. In addition, GO has been added as a doping agent with conjugated organic polymers and had been found to increase conductivity facilitated by proton sources in the GO material [7]. More interestingly, GO has been utilised in the fabrication of some interesting polymer materials such as flame retardant materials for fire safety of polymers, showing the increased importance of the incorporation of GO in materials applications [10, 12, 13, 15, 25]. GONPs also have the appeal of being amphiphilic, and are thus suitable for use as a Pickering agent to form an emulsion. Pickering studies using GO have resulted in the formation of polystyrene particles coated in GO and even hollow hybrid polymer GO particles [26-32]. The growth of the use of GONPs particularly with emulsion polymerisation is

exciting for developing GONP modified polyHIPE materials and enhancing the materials in terms of stability and surface area.

4.1.3 Significance of graphene oxide nanoparticles as stationary phase materials

The pinnacle applications of GONPs in separation science stemmed from the interest of the materials in polymer and electrochemical technologies. The GONP materials were applied initially as solid phase extraction materials, a welcome change from the insoluble graphene solid phase techniques that were being developed at the time. Due to the presence of oxygen, GONPs had greater solubility in various solvents making it an ideal SPE material for extractions of small molecules, bulky and aromatic compounds and large biomolecules [17, 19, 21, 22]. A GONP/silica hybrid stationary phase aminated and functionalised with C18 ligands was one of the first instances in which GO was used in liquid chromatography; here the separations were dominated by π-π interactions [33]. The GONP modified stationary phases facilitated the change of elution orders of analytes including PAHs, anilines and phenols when compared to commercial C18 stationary phases [18]. Another GONP/silica hybrid stationary phase bonded with C18 ligands was modified with gold NPs and used in RP-HPLC and HILIC (hydrophilic interaction liquid chromatography) for separation of isomeric dihydroxylbenzenes, alkylbenzenes, nucleosides and amino acids [14]. Additionally the use of GONP functionalised monoliths have also been demonstrated in the literature where GONPs were silanised and was used as a crosslinker for the polymerisation of GMA and EDGMA [16]. The resulting monoliths were shown to separate mixtures of steroids as well as more polar analytes such as aromatic amines. The use of GO in stationary phases as a method to form graphene coated stationary

phases is of increasing interest. This is generally achieved by the reduction of the GONPs with hydrazine hydrate, however the reduction is also possible using ascorbic acid. The incorporation of reduced GONPs allows the stationary phase to have enhanced conductive properties, which could allow for interesting electrochemically functionalised separations. Such modifications have already been demonstrated in the separation of acid nitrophenol isomers, basic nitroaniline isomers, and neutral PAHs using open tubular capillary electrochromatography (OTCEC) [34].

In this study, GONPs were incorporated into PS-*co*-DVB polyHIPEs, fabricating novel chromatographic stationary phases. They were successfully applied for the RP-HPLC separation of alkylbenzenes. The GONPs were reduced in situ by flushing with ascorbic acid and, subsequently, characterisation illustrated that the GONP reduction altered the surface chemistry and associated retention mechanisms, demonstrating their enhanced functionality.

4.2 Materials

Millipore ultrapure water purified to a resistance of > 18 MΩcm was used in all instances. Ethylbenzene >99.8%, propylbenzene >99%, butylbenzene >99%, pentylbenzene 99% and ascorbic acid >99%. All solvents were used as received and were of analytical HPLC grade. The polyHIPEs used were fabricated in Chapter 2 Section ***2.2.3.7*** and the aqueous solution of GONPs was donated by the University of Wollongong.

4.2.1 Instrumentation

Separation of alkylbenzenes were used using an Ultimate 3000 LC and a ultrasonicator (Branson 5510) was used to degas mobile phases. In addition, a Harvard 33 syringe pump was used for any flow through modification required. It should be noted that the Ultimate 3000 LC which was used in this work had a faulty injector, this however would only affect retention times if the column was overloaded.

4.2.2 Methods

4.2.2.1 Reduction of GONP modified columns

A number of 20 ppm GONP modified PS-*co*-DVB polyHIPE columns were fabricated within fused silica capillary as described in Chapter 2, Section ***2.2.3.7***. These columns were reduced using an adapted procedure [35]. Briefly, a syringe pump flowing a solution of 2 m*M* ascorbic acid at 0.3 µl min^{-1} for 1 h. The column was washed with water for 30 min and then with MeOH for 1 h before using for LC separation. This procedure was also repeated with a non-modified PS-*co*-DVB polyHIPE column to use as a control. The reduced GONP column was named as

rGONP PS-*co*-DVB polyHIPE and the ascorbic acid treated PS-*co*-DVB polyHIPE was named as ascorbic acid treated PS-*co*-DVB polyHIPE.

4.2.2.2 Chromatographic conditions

Alkylbenzene separation was carried out by using mixed standard solution of toluene, ethylbenzene, propylbenzene, butylbenzene and pentylbenzene prepared in ACN using an Agilent 1200. The HPLC system consisted of a quaternary pump including an online vacuum degasser, an autosampler and a UV detector. Chromatographic separation was achieved on the polyHIPE columns (229 mm x 250 µm i.d.). Mobile phase conditions of the isocratic system was 50:50 (ACN:Water) and was filtered and then degassed using an ultrasonicator. The isocratic separation was carried out using an Ultimate 3000 LC with an operating flow rate of 5 µL min^{-1} and a UV detection at 214 nm.

4.3 Results and discussion

4.3.1 Isocratic separation of alkylbenzenes using GONP modified PS-*co*-DVB polyHIPE within fused silica capillary housing

The separation of alkylbenzenes on both unmodified PS-*co*-DVB and GONP modified PS-*co*-DVB capillary columns of 229 mm x 250 µm were achieved. Similar to the retention mechanism observed in Chapter 3, a linear relationship was determined with the retention of the analytes increasing with increasing number of alkyl groups on the analyte molecules (Figure 4.1) [33, 36, 37].

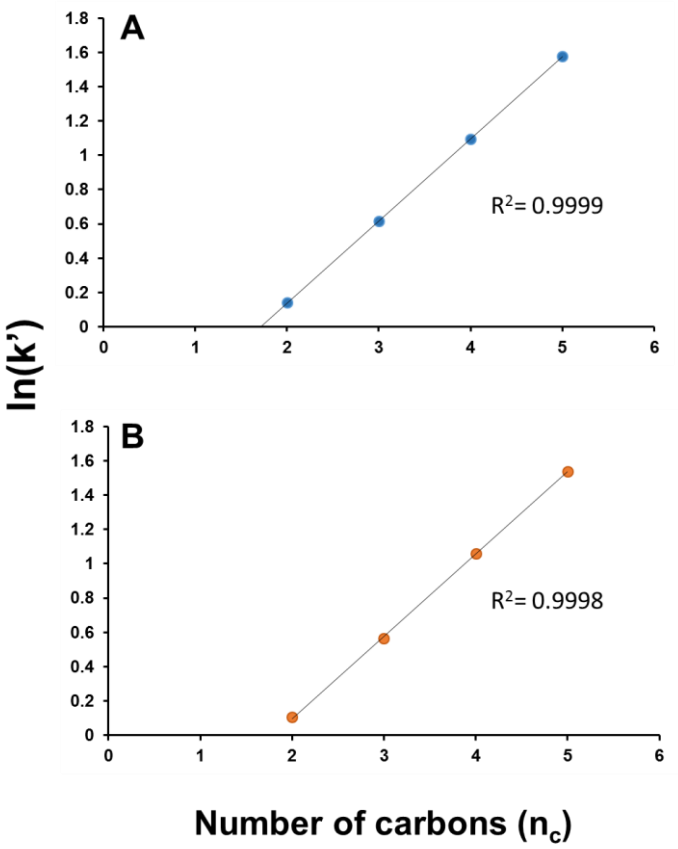

Figure 4.1: *Methylene selectivity for PS-co-DVB column (A) and 20 ppm GONP PS-co-DVB column (B) for the increasing alkylbenzene chain (ethylbenzene to pentylbenzene).*

This supports RP adsorption as the primary chromatographic interaction mechanism. Both columns achieved high linearity with corresponding correlation coefficients of values of 0.9998 and 0.9999 respectively. The methylene selectivity graphs illustrated in Figure 4.1 show the trend was similar for both the modified and unmodified columns as the alkyl chain increases. This trend has been reported previously in the literature using similar materials [33, 36, 37].

Despite the little change observed in retention times, Figure 4.2 shows a remarkable separation was achieved by the GONP modified column, which was found in Chapter 2 to have a surface area of only 16 m^2 g^{-1}.

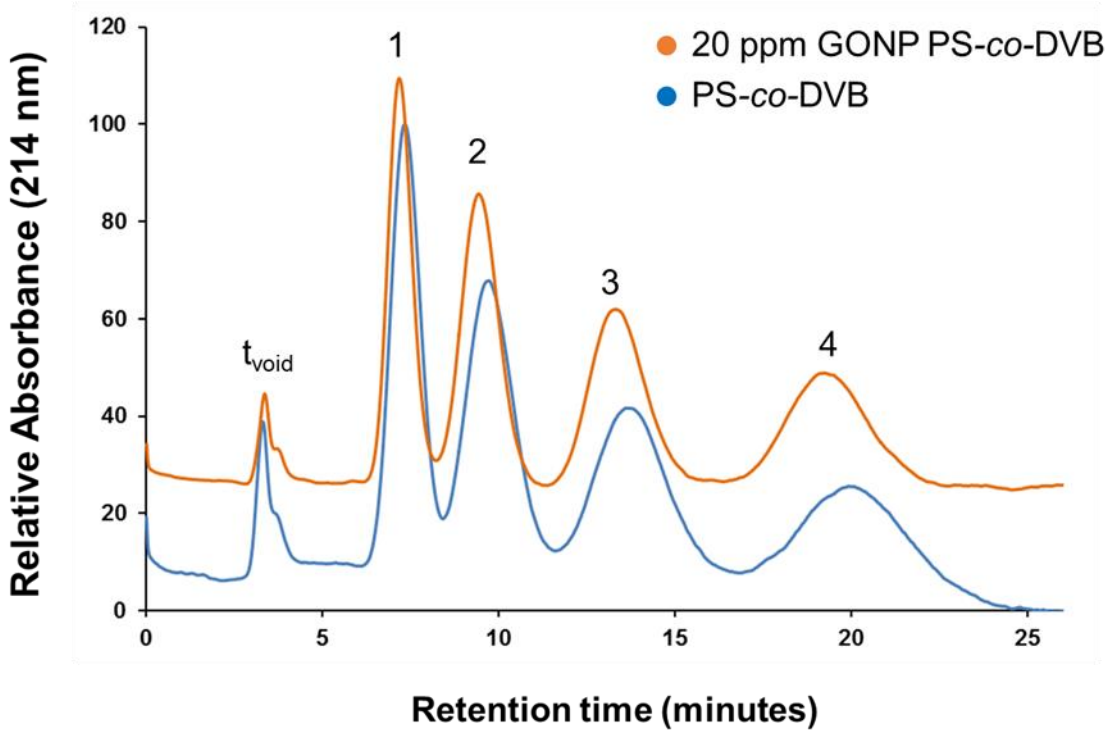

Figure 4.2: *Isocratic alkylbenzene separation on 22.9 cm x 250 µm i.d. capillary columns of 20 ppm GONP PS-co-DVB column* ***(orange)*** *and PS-co-DVB polyHIPE* ***(blue)****. Mobile phase 50:50 ACN:Water, sample concentration 0.5 ppm, injection*

volume 0.1 µL flow rate 5 µL/min, detection wavelength 214 nm. Analytes noted as ethylbenzene (1), propylbenzene (2), butylbenzene (3) and pentylbenzene (4).

The unmodified polyHIPE fabricated was found to have a surface area of 25 m^2 g^{-1}, thus a significant 40% decrease in surface area nonetheless achieved similar separation capacities which are shown in Table 4.1. The BET surface area analysis was repeated on a different batch of GONP modified PS-*co*-DVB polyHIPE to ensure that there was a decreased surface area resulting from the inclusion of GONPs. The repeated analysis gave a surface area of 12 m^2 g^{-1}.

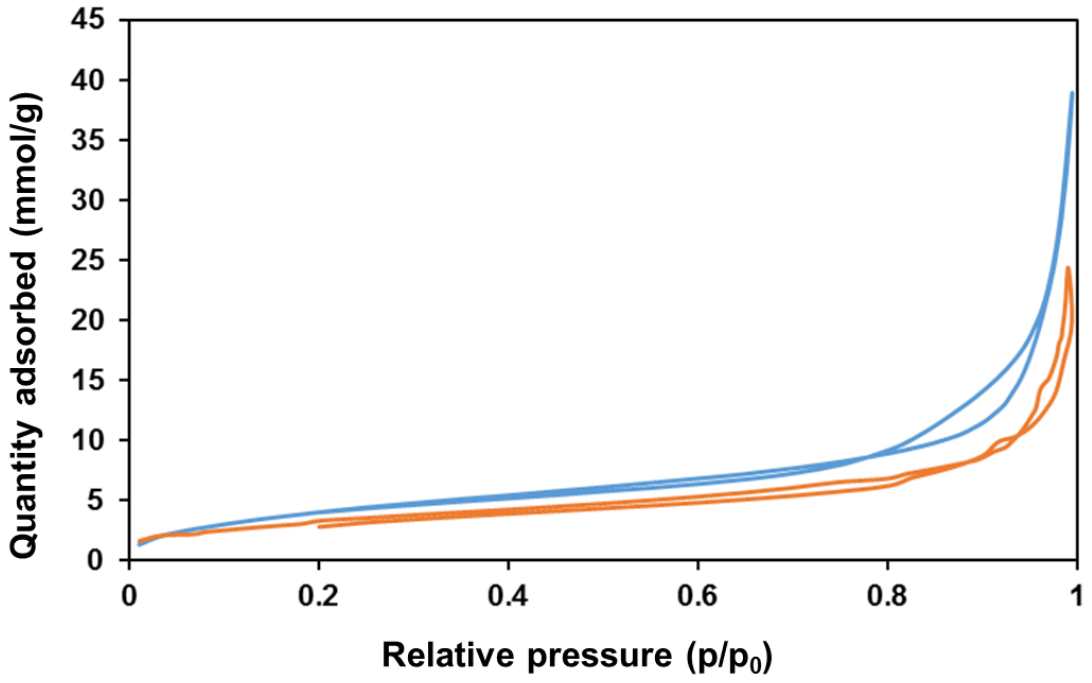

Figure 4.3: *BET isotherms of GONP modified PS-co-DVB polyHIPEs at where the blue plot represents batch 1 and the orange plot represents batch 2.*

From the BET plot presented above in Figure 4.3 it can be observed that the second batch of the material fabricated was of lower surface area due to a lower quantity of N_2 gas adsorbed and some hysteresis was observed. Thus the addition of GONPs does appear to reduce the surface area of the polyHIPE materials. Due to the apparent enhanced separation by the lower surface area GONP material, it was hypothesised that the presence of GONPs and the "popcorn effect" demonstrated in the morphology of these materials could have resulted in possible superior adsorption of the analytes.

Table 4.1: *Separation performance characteristics of PS-co-DVB and 20 ppm GONP PS-co-DVB columns (n=3)*

Column	t_r (min)	%RSD (%)	R_s	k'
PS-co-DVB				
Ethylbenzene	7.27±0.06	0.9	1.14	1.15±0.02
Propylbenzene	9.62±0.10	0.1	1.26	1.85±0.02
Butylbenzene	13.48±0.16	1.2	1.36	2.99±0.05
Pentylbenzene	19.73±0.21	1.2	2.09	4.85±0.06
20 ppm GONP PS-co-DVB				
Ethylbenzene	6.94±0.02	0.3	1.25	1.11±0.01
Propylbenzene	9.11±0.02	0.3	1.34	1.76±0.01
Butylbenzene	12.80±0.05	0.5	1.51	2.89±0.02
Pentylbenzene	18.60±0.10	0.6	1.91	4.65±0.03

When compared to similar separations in the literature, utilising hybrid GONP/silica stationary phases, an isocratic separation resulted in a co-elution of alkylbenzenes [14]. When the hybrid material was functionalised with gold NPs the alkylbenzenes were baseline separated. However, the later eluting peaks showed a high degree of peak tailing in comparison to the separations presented here despite the material having surface areas of up to 391 $m^2 g^{-1}$. Since retention time and elution order is of main interest here, the results should not be affected negatively other than discrepancy in peak height and area.

As well as the GONP columns showing superior adsorption effects, the retention time reproducibility of both columns was excellent with maximum %RSD of up to 1.2% as presented in Table 4.1. These %RSD values were comparable to a similar separation observed in the literature using CEC [38, 39]. In addition, the resolution (R_s) of the analytes for both columns were greater than 1 meaning that all peaks could be differentiated easily. The polyHIPEs within capillary housing therefore, have shown greater resolution and lower retention time as well as higher reproducibility in their separations of alkylbenzenes compared to previous monolithic chromatographic separations.

4.3.2 Isocratic separation of alkylbenzenes using reduced GONP modified PS-*co*-DVB polyHIPE within fused silica capillary housing

The GONP incorporated polyHIPEs were reduced as described in Section ***4.2.2.1*** of this chapter. Methylene selectivity plots illustrated that there was no change in retention mechanism once the GONP column was reduced. In Figure 4.4 the linear plot shows that upon increasing alkyl chain the retention of the analytes increased based on the ln(k'). Therefore, it was expected that no change in the elution order of

the analytes would be observed, thus the selectivity of the material was to remain the same.

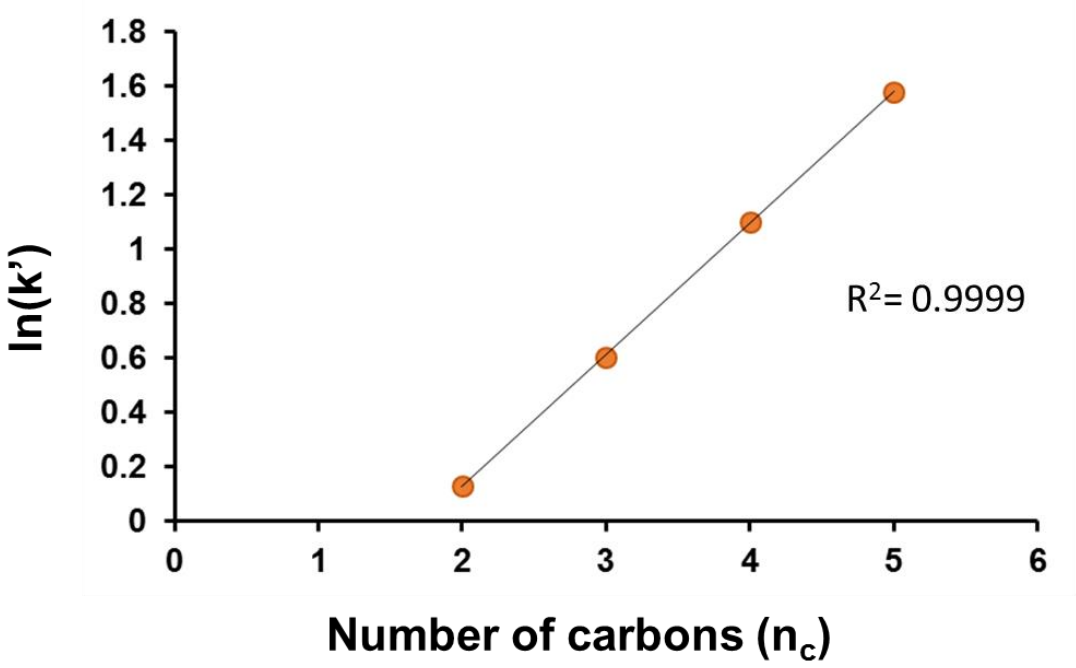

Figure 4.4: *Methylene selectivity for rGONP PS-co-DVB column for the increasing alkylbenzene chain (ethylbenzene to pentylbenzene).*

When the alkylbenzenes were separated isocratically it was expected that upon reduction of the GONP modified column, the retention time should have increased. It was hypothesised that the reduction of GONPs would eliminate hydrophilic groups on the surface of the polyHIPE resulting in the formation of graphene. Graphene being more hydrophobic than GONPs was expected to increase the retention time of the analytes.

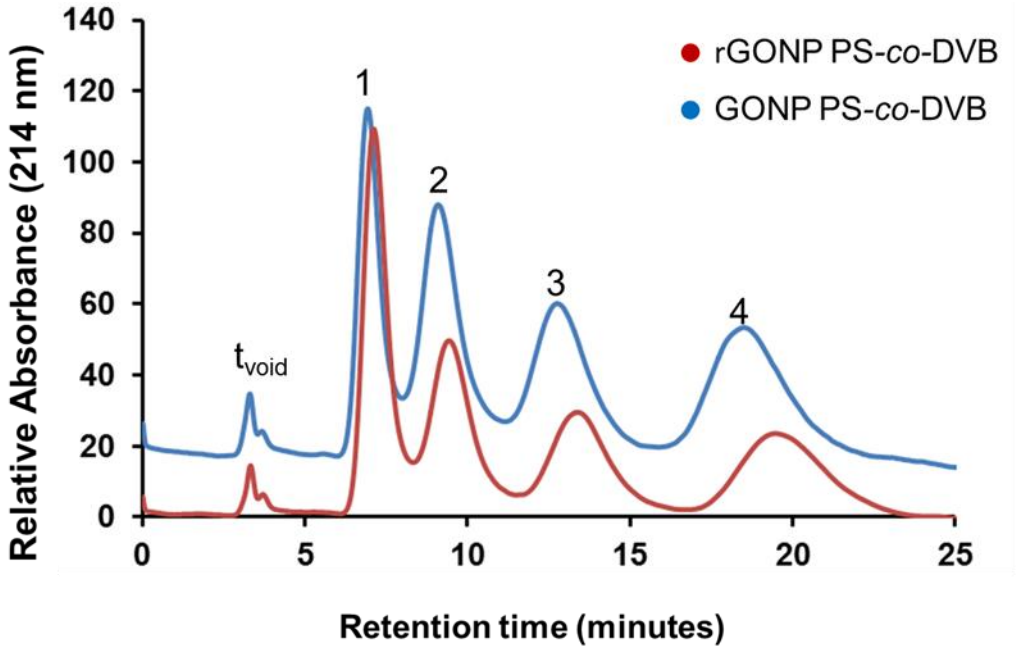

Figure 4.5: *Isocratic alkylbenzene separation on 22.9 cm x 250 µm i.d. capillary columns of rGONP PS-co-DVB column (red) and GONP PS-co-DVB polyHIPE (blue). Mobile phase 50:50 ACN:Water, sample concentration 0.5 ppm, injection volume 0.1 µL flow rate 5 µL/min, detection wavelength 214 nm. Analytes noted as ethylbenzene (1), propylbenzene (2), butylbenzene (3) and pentylbenzene (4).*

As shown in Figure 4.5, however, the peak shape and elution order of the separation remained similar to the previous separation and similar to alkylbenzene separations in the literature [40-42]. The only variation was a slight increase in retention time observed. This retention time change being so small it would not be certain to say that the retention time increase was attributed to the reduction of the stationary phase material. The rGONP columns showed the expected enhanced retention capacities for the later eluting analytes as shown in Table 4.2. The change in retention factor was quite small for the early eluting peaks however the retention factor increases with later eluting peaks. It is thought that the loading of GONP would

have a significant effect on the available rGONPs to interact with the analytes. This would facilitate a greater surface area of GONPs accessible to be reduced and a more prominent change in retention time would be observed. Additionally, the R_s of the isocratic separation was shown to decrease, however the R_s values which were calculated were all greater than 1, illustrating that the peaks were distinguishable from each other [43-45].

Table 4.2: *Separation performance characteristics of rGONP PS-co-DVB and 20 ppm GONP PS-co-DVB columns (n=3)*

Column	t_r (min)	%RSD (%)	R_s	k'
20 ppm GONP PS-co-DVB				
Ethylbenzene	6.94±0.02	0.3	1.25	1.11±0.01
Propylbenzene	9.11±0.02	0.3	1.34	1.76±0.01
Butylbenzene	12.80±0.05	0.5	1.51	2.89±0.02
Pentylbenzene	18.60±0.10	0.6	1.91	4.65±0.03
rGONP PS-co-DVB				
Ethylbenzene	7.11±0.003	0.05	1.24	1.14±0.00
Propylbenzene	9.11±0.016	0.17	1.41	1.83±0.00
Butylbenzene	13.35±0.033	0.25	1.56	3.01±0.01
Pentylbenzene	19.46±0.10	0.12	2.24	4.85±0.01

A noticeable increase in the reproducibility from injection to injection was observed resulting in %RSD values of less than 0.25% once the columns were reduced. These %RSD values were comparable to those observed in similar separations in the literature [38, 39, 46]. Despite no major difference in retention times and slightly lower R_s values, the reproducibility in the injections shows the potential of polyHIPEs where monoliths are typically known to have poor reproducibility [47]. In addition, the polyHIPE still maintained its outstanding separation performance for such a low surface area material, highlighting the potential that these GONP modified materials could have once a higher surface area was attainable.

4.3.3 Isocratic separation of alkylbenzenes using ascorbic acid treated PS-*co*-DVB polyHIPE within fused silica capillary housing

It was necessary to perform treatment with ascorbic acid on the control column with no GONPs to ascertain if there was any difference in separation performance and retention. The retention mechanism was found to be a reverse phase separation where the retention increased upon increase of alkyl chains on the analytes. Since the methylene selectivity plot (Figure 4.6) resulted in a highly linearity and R^2 values of 0.9999, the elution order observed in the previous separations was also expected for this column.

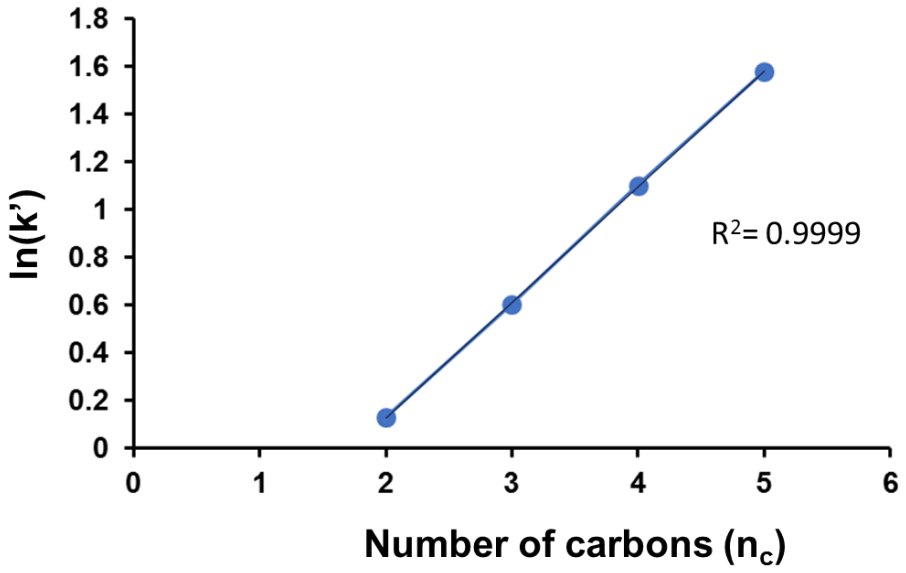

Figure 4.6: *Methylene selectivity for ascorbic acid treated PS-co-DVB column for the increasing alkylbenzene chain (ethylbenzene to pentylbenzene).*

The isocratic separation of the ascorbic acid treated PS-*co*-DVB column gave similar separation performance to the rGONP column in terms of resolution. Both the isocratic separation in Figure 4.7 and the R_s values in Table 4.3 showed a decreased R_s once the column was treated with ascorbic acid. There was a significant degree of co-elution between ethylbenzene and propylbenzene giving lower R_s value of 0.98. However, the remaining R_s values were all greater than 1 and all the analyte peaks were distinguishable from each other.

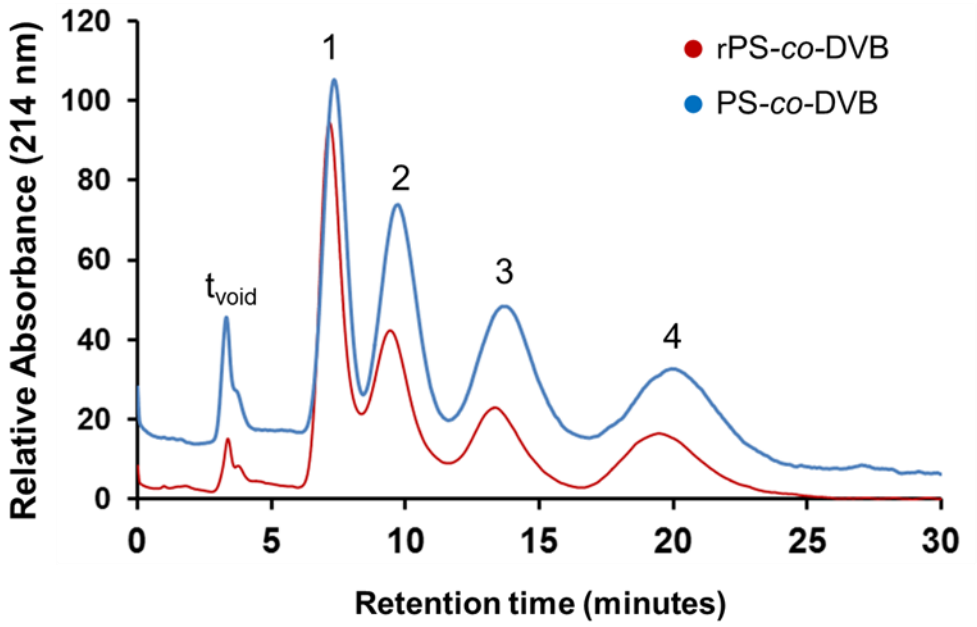

Figure 4.7: *Isocratic alkylbenzene separation on 22.9 cm x 250 µm i.d. capillary columns of ascorbic acid treated PS-co-DVB column **(red)** and PS-co-DVB polyHIPE **(blue)**. Mobile phase 50:50 ACN:Water, sample concentration 0.5 ppm, injection volume 0.1 µL flow rate 5 µL/min, detection wavelength 214 nm.*

It was hypothesised that reduction of the columns with ascorbic acid affected on the resolution of the analytes, which was possibly due to an alteration to the surface of the polyHIPE material. In addition, a slight increase in retention time was observed in ascorbic acid treated PS-*co*-DVB columns and could be due to the effect of ascorbic acid. However, upon statistical analysis it was found at 95% confidence there was no significant difference between the retention time of the reduced and non-reduced column. The retention capacity of the ascorbic acid treated PS-*co*-DVB columns was decreased slightly upon reduction with ascorbic acid. In contrast to the latter, the rGONP columns increased in retention capacity especially for the later eluting

analytes. This increase in retention capacity observed for the rGONPs could suggest that the columns may have been successfully reduced.

Table 4.3: *Separation performance characteristics of PS-co-DVB and ascorbic acid treated PS-co-DVB columns*

Column	t_r (min)	R_s	%RSD (%)	k’
PS-co-DVB				
Ethylbenzene	6.94±0.02	1.25	0.3	1.15±0.02
Propylbenzene	9.11±0.02	1.34	0.3	1.85±0.02
Butylbenzene	12.80±0.05	1.51	0.5	2.99±0.05
Pentylbenzene	18.60±0.10	1.91	0.6	4.85±0.06
Ascorbic acid treated PS-co-DVB				
Ethylbenzene	7.13±0.04	0.98	0.5	1.13±0.03
Propylbenzene	9.38±0.05	1.27	0.5	1.78±0.01
Butylbenzene	13.26±0.09	1.42	0.6	2.93±0.03
Pentylbenzene	19.41±0.06	1.66	0.3	4.73±0.05

Despite the continuing trend of decrease in R_s upon ascorbic acid reduction for both the blank and GONP modified column, another apparent trend was the high reproducibility of the injection to injection retention times. Here %RSD values lower than 0.6% resulted, highlighting the column’s superior reproducibility, capacity as well as stability despite reduction with ascorbic acid. Given the documented differences in pore structures of monolithic stationary phases [47, 48], which result in low

reproducibility, the columns fabricated with GONPs and without have shown exceptional chromatographic performance in this regard.

4.4 Conclusions

The PS-*co*-DVB polyHIPE columns and the GONP modified columns within fused silica capillary tubing were evaluated for their retention mechanism, retention times as well as retention factors prior to and post reduction with ascorbic acid. It was found using methylene selectivity plots that the columns both prior to and after reduction had the same reverse phase separation mechanism as observed in Chapter 3. Upon isocratic separation of the alkylbenzenes it was confirmed that there was no change in elution order.

Although change in elution order was not expected, due to the reduction of the GONP columns, an increased retention time was expected. It was found that both the rGONP and ascorbic acid treated PS-*co*-DVB demonstrated decreased resolution upon reduction using ascorbic acid. In addition, there was a slight increase in retention times for the GONP modified columns however, this increase was slight and could not solely be attributed to the reduction of the GONPs. Nonetheless, the later eluting analytes butylbenzene and propylbenzene had a greater increase in both retention time and retention capacity. This signified that following extensive characterisation by x-ray photoelectron spectroscopy the promising modification using GONPs and polyHIPEs can be achieved in the future. Additionally a potential area to explore would be GONP loading which could potentially be increased by using smaller NP sizes.

While retention times did not significantly differ and decreased resolution and surface area resulted in the GONP column and the rGONP column, the separation

efficiency for such a low surface area material was remarkable. While one hypothesis of the lower surface area was due to blockage of pores by the GONPs, it was also hypothesised that the addition of GONPs gave the polyHIPE material an enhanced adsorption capacity. Thus the resulting separations to the of the GONP polyHIPE column were similar to the blank material, which had a greater surface area by 40%. In addition, the injection to injection replication of both columns prior to and post reduction were considerably low with respect to the variability which is expected with monolithic columns. This study has highlighted the potential of these GONP modified polyHIPE materials once reduced. The resulting separations indicate the future promise of these materials once they modification procedure is revised to include smaller GONPs to hopefully increase surface area for more efficient separations.

4.5 References

[1] D. Josic, J. Reusch, K. Loster, O. Baum, W. Reutter, Journal of Chromatography, 590 (1992) 59.

[2] A. Podgornik, M. Barut, A. Strancar, D. Josic, T. Koloini, Analytical Chemistry, 72 (2000) 5693.

[3] S. Currivan, P. Jandera, Chromatography, 1 (2014) 24.

[4] P. Floris, B. Twamley, P.N. Nesterenko, B. Paull, D. Connolly, Microchimica Acta, 181 (2014) 249.

[5] P. Floris, B. Twamley, P. Nesterenko, B. Paull, D. Connolly, Microchimica Acta, 179 (2012) 149.

[6] Y. Zhu, S. Murali, W. Cai, X. Li, J.W. Suk, J.R. Potts, R.S. Ruoff, Advanced Materials, 22 (2010) 3906.

[7] Y. Gao, H.-L. Yip, K.-S. Chen, K.M. O'Malley, O. Acton, Y. Sun, G. Ting, H. Chen, A.K.Y. Jen, Advanced Materials, 23 (2011) 1903.

[8] S.-S. Li, K.-H. Tu, C.-C. Lin, C.-W. Chen, M. Chhowalla, Acs Nano, 4 (2010) 3169.

[9] L.L. Zhang, S. Zhao, X.N. Tian, X.S. Zhao, Langmuir, 26 (2010) 17624.

[10] W. Hu, B. Yu, S.-D. Jiang, L. Song, Y. Hu, B. Wang, Journal of Hazardous Materials.

[11] C.N.R. Rao, A.K. Sood, K.S. Subrahmanyam, A. Govindaraj, Angewandte Chemie-International Edition, 48 (2009) 7752.

[12] H. Gui, P. Xu, Y. Hu, J. Wang, X. Yang, A. Bahader, Y. Ding, RSC Advances, 5 (2015) 27814.

[13] B. Yu, Y. Shi, B. Yuan, S. Qiu, W. Xing, W. Hu, L. Song, S. Lo, Y. Hu, Journal of Materials Chemistry A, 3 (2015) 8034.

[14] X. Liang, X. Wang, H. Ren, S. Jiang, L. Wang, S. Liu, Journal of Separation Science, 37 (2014) 1371.

[15] B. Yu, X. Wang, X. Qian, W. Xing, H. Yang, L. Ma, Y. Lin, S. Jiang, L. Song, Y. Hu, S. Lo, RSC Advances, 4 (2014) 31782.

[16] Y. Li, L. Qi, H. Ma, Analyst, 138 (2013) 5470.

[17] R. Sitko, B. Zawisza, E. Malicka, Trac-Trends in Analytical Chemistry, 51 (2013) 33.

[18] X. Liang, S. Liu, X. Song, Y. Zhu, S. Jiang, Analyst, 137 (2012) 5237.

[19] Q. Liu, J. Shi, G. Jiang, Trac-Trends in Analytical Chemistry, 37 (2012) 1.

[20] M.-M. Wang, X.-P. Yan, Analytical Chemistry, 84 (2012) 39.

[21] Q. Liu, J. Shi, J. Sun, W. Thanh, L. Zeng, G. Jiang, Angewandte Chemie-International Edition, 50 (2011) 5913.

[22] S. Zhang, Z. Du, G. Li, Analytical Chemistry, 83 (2011) 7531.

[23] Y. Li, X. Li, C. Dong, J. Qi, X. Han, Carbon, 48 (2010) 3427.

[24] Y. Mao, Y. Bao, S. Gan, F. Li, L. Niu, Biosensors and Bioelectronics, 28 (2011) 291.

[25] K. Zhou, W. Yang, G. Tang, B. Wang, S. Jiang, Y. Hu, Z. Gui, RSC Advances, 3 (2013) 25030.

[26] G.H. Teo, Y.H. Ng, P.B. Zetterlund, S.C. Thickett, Polymer, 63 (2015) 1.

[27] S.C. Thickett, P.B. Zetterlund, Journal of Colloid and Interface Science, 442 (2015) 67.

[28] S.H.C. Man, D. Ly, M.R. Whittaker, S.C. Thickett, P.B. Zetterlund, Polymer, 55 (2014) 3490.

[29] S.H.C. Man, S.C. Thickett, M.R. Whittaker, P.B. Zetterlund, Journal of Polymer Science Part a-Polymer Chemistry, 51 (2013) 47.

[30] S.H.C. Man, N.Y.M. Yusof, M.R. Whittaker, S.C. Thickett, P.B. Zetterlund, Journal of Polymer Science Part a-Polymer Chemistry, 51 (2013) 5153.

[31] S.C. Thickett, P.B. Zetterlund, Current Organic Chemistry, 17 (2013) 956.

[32] S.C. Thickett, P.B. Zetterlund, Acs Macro Letters, 2 (2013) 630.

[33] A. Tchapla, H. Colin, G. Guiochon, Analytical Chemistry, 56 (1984) 621.

[34] X.L. Liu, X. Liu, L.P. Guo, L. Yang, S.T. Wang, Electrophoresis, 34 (2013) 1869.

[35] M.J. Fernandez-Merino, L. Guardia, J.I. Paredes, S. Villar-Rodil, P. Solis-Fernandez, A. Martinez-Alonso, J.M.D. Tascon, Journal of Physical Chemistry C, 114 (2010) 6426.

[36] N. Tanaka, E.R. Thornton, Journal of the American Chemical Society, 99 (1977) 7300.

[37] C. Horváth, W. Melander, I. Molnár, Journal of Chromatography A, 125 (1976) 129.

[38] Y. Tunc, C. Golgelioglu, A. Tuncel, K. Ulubayram, Separation Science and Technology, 47 (2012) 2444.

[39] Y. Tunc, C. Golgelioglu, N. Hasirci, K. Ulubayram, A. Tuncel, Journal of Chromatography A, 1217 (2010) 1654.

[40] J. Urban, F. Svec, J.M.J. Frechet, Analytical Chemistry, 82 (2010) 1621.

[41] J. Urban, F. Svec, J.M.J. Frechet, Journal of Chromatography A, 1217 (2010) 8212.

[42] Q.C. Wang, F. Švec, J.M.J. Fréchet, Journal of Chromatography A, 669 (1994) 230.

[43] S.C. Moldoveanu, V. David, Essentials in Modern Hplc Separations (2013) 1.

[44] R.L. Snyder, J.J. Kirkland, V.J. Dolan, Introduction to Modern Liquid Chromatography, John Wiley & Sons, Hoboken, New Jersey, 2011.

[45] J.J. Gilroy, J.W. Dolan, LC•GC Europe, 7 (2004).

[46] J. Yang, G. Yang, H. Liu, L. Bai, Q. Zhang, (2011).

[47] F. Svec, C.G. Huber, Analytical Chemistry, 78 (2006) 2100.

[48] M. Díaz-Bao, R. Barreiro, J. Miranda, A. Cepeda, P. Regal, Chromatography, 2 (2015) 79.

Chapter Five

PolyHIPE coated columns as single injection stationary phases in capillary electrochromatography

"Have no fear of perfection; you'll never reach it." - **Marie Curie.**

5. Aim

The aim of this chapter was to develop polyHIPE capillary columns using PS-*co*-DVB polyHIPEs as coatings for OTCEC. The coating method was utilized so that columns could be fabricated to analyse complex samples. To facilitate this evaluation, an alkylbenzene mixture was utilised for analysis. The OTCEC columns were evaluated for their separation capacity and their separation capacity was compared to RP-HPLC stationary phases characterised in Chapter 3.

5.1 Introduction

Capillary electrochromatography is an orthogonal separation technique where CE has been used in conjunction with chromatographic stationary phases to achieve complete separation. Traditionally these stationary phases have utilised packed beds ranging in diameters from 50-200 µm in size [1]. However, issues with the use of such packed beds in CEC include the use of end frits that result in deterioration of the column bed over time. In addition, voids typically appear with prolonged use of such packed bed columns [2, 3]. To overcome such issues, monolithic columns have been introduced into CEC analysis which negated the requirement of frits, resulted in lower backpressures and decreased wall effects [1]. While monolithic columns proved to be advantageous for the latter within the area of CEC, limitations with the use of these monolithic columns still persist. Such limitations include repeatability concerns post in situ monolith fabrication and pore morphology variation. These batch to batch variations of monolithic stationary phases are well documented [4-6]. Variations in pore size diameter are particularly significant in CEC application. In the event that reduction in pore size is sufficient to cause overlap of the electrical double layer formed on the surface of the polymer within the void, the EOF will collapse. This will negatively effect the eletrolyte flow through the capillary with a corresponding impact on separation [7]. A potential strategy to overcome this severe limitation is to utilise capillaries which are coated, but not filled, with stationary phase.

Employing CEC columns with stationary phase coating is frequently referred to as OTCEC. OTCEC coatings include dynamic, static or hybrid coatings. Dynamic coatings are not attached to the fused silica capillary wall, with surfactants frequently employed in this application. Static coatings that are attached to the capillary walls

such as nanoparticles have been previously used as a pseudo-stationary phase in CEC [8-15]. A combination of both static and dynamic coatings form the hybrid coatings can be used in CEC [16]. Advantages of these coated columns in CEC include: flexibility in the stationary phase type, control and stabilisation of EOF, no pressure limitations and reduced column bleeding (which is observed mainly with packed columns). These advantages have led coated columns to becoming more appealing within the area of CEC.

Previous reports have shown successful separations using static columns using nanomaterials. Multiple groups have proficiently demonstrated decreased wall effects using modified polymeric nanoparticles such as VBC NPs for protein separations [8, 9]. Other studies also demonstrated the separation of anions using aminated latex nanoparticles using an isotachophoretic gradient separation [10-12]. This gradient boundary was formed using a competing anion with a higher mobility migrated ahead of the analyte anions [12]. Furthermore, the use of nanoparticles was not only restricted to organic nanoparticles, with inorganic nanoparticles also used in OTCEC. AuNPs have been used in OTCEC with particular success in the separation of drug substances and even neutral analytes such as PAHs [13, 14]. Furthermore, metal oxide nanoparticles such as TiO_2 have been successful in the separation of protein isoforms such as conalbumin and ovalbumin [15]. Nanomaterial coated columns in CEC have shown impressive separation capabilities and highlight the potential for novel OTCEC columns.

As well as nanomaterial modified OTCEC columns, the use of polymer coated columns present a potential alternative method to reduce wall effects and decrease blockages within CEC. Within the OTCEC column, a layer of polymer can be polymerised on the internal surface of the capillary, increasing the interaction of the

analyte with the stationary phase. CE is a commonly used method for chiral separations [17-21]. Therefore, it is not surprising that use of OTCEC coated polymers has been explored to further enhance this area of separations without the use of expensive buffer additives such as cyclodextrins. The use of MIPs within polymer coated columns have been shown to improve the column selectivity. The separation of ketoprofen enantiomers has been demonstrated using MIP coated polymer columns in OTCEC [22]. Similarly polymer coated MIP columns were used for the separation of ketoprofen and naproxen [23]. The ability to incorporate molecular imprinted polymers (MIPs) into the polymer coating highlights the additional modifications that can be made to these types of OTCEC columns. Use of these polymer coated columns in CEC have resulted in promising separations due to increased selectivity imparted by the polymers used.

Although coated polymer columns are proving to be interesting alternative stationary phases in the development of CEC methods, polymer coated OTCEC columns in particular, still present technical hurdles during fabrication. A major weakness in polymer coated OTCEC columns is finding a reactive monomer for the desired functionalisation [24]. The improvement in fabrication and application of polymer coated technologies in OTCEC is therefore quite topical and an area which is still being researched. PS-*co*-DVB polyHIPEs in Chapter 3 were demonstrated to exhibit a remarkable separation capacity, given its low surface area and relatively high plate height. If these factors could be overcome, the polyHIPEs separation capacity could be significantly enhanced. Multiple strategies exist which could overcome these limitations. In Chapter 4, GONPs were incorporated in an attempt to increase surface area. An alternative strategy to improve separation capacity is to reduce plate height and increase separation efficiency. As determined by van Deemter, plate height is

proportional to Eddy diffusion, longitudinal diffusion and resistance to mass transfer. This is typically characterised in chromatographic separations by a parabolic flow profile for analyte bands. In contrast, in CE, the analyte bands have a planar profile, as the flow is generated from a plug flow as opposed to a pressure differential. Utilising a plug flow and therefore generating a planar analyte band profile should result in a significantly enhanced separation efficiency, which when combined with the high intrinsic separation capacity of polyHIPEs, has potential to result in a stationary phase with considerable separation capacity. In this chapter, the separation efficiency was combined with separation capacity of the polyHIPEs to determine the extent to which the combination could improve separation.

5.2 Materials

Millipore ultrapure water purified to a resistance of > 18 MΩcm was used in all instances. PolyHIPE emulsion was as prepared in Chapter 2, toluene, ethylbenzene, propylbenzene, pentylbenzene, acetonitrile, sodium phosphate monobasic, sodium tetraborate decahydrate and sodium dodecyl sulfate (SDS), was used as received (Sigma Aldrich, Tallaght). All fused silica tubing (100 and 250 µm in I.D.) was supplied by CM Scientific (West Yorkshire UK) and silanised as per Chapter 2.

5.2.1 Instrumentation

All morphological characterisation was carried out using a Hitachi S-3400N scanning electron microscope, and all samples were gold sputtered using a 750T sputter coater, Quorum Technologies (UK). All electrophoretic experiments were carried out using an Agilent 7100 Capillary Electrophoresis system while rinsing columns were carried out a Dionex Ultimate 3000 LC Ultimate capillary LC instrument.

5.2.2 Methods

5.2.2.1 Fabrication of PS-co-DVB polyHIPE emulsion coated capillaries for CEC

A 90% PS-*co*-DVB polyHIPE emulsion was prepared as detailed in Chapter Two Section ***2.2.3.5***. The lengths of the columns were varied depending on the final application, which is detailed in Table 5.1 below. For the CE separations carried out longer columns of 48.5 cm were utilised to establish separations on the uncoated columns. To establish the length of polymerisation time that was required to form coated columns, shorter columns (10 cm) were produced. These columns underwent one emulsion filling step (10 cm columns filled entirely) and were left to polymerise for 1 h, 2 h and 4 h. To establish parameters for separation, shorter columns of 41 cm were produced and followed multiple coating and polymerisation steps. For multiple coating and polymerisation steps, the 41 cm capillary was filled up to 20 cm only and left to polymerise for 1 h at 60°C in a water bath. The column was then removed from the water bath, attached to a capillary LC instrument, and washed with MeOH until the excess emulsion was washed out. For multiple coatings, the entire process of filling the capillary to polymerisation was repeated e.g. for a 2 h coating, polymerisation and wash steps were carried out twice.

Table 5.1: *Lengths of columns fabricated*

Column type	Total length (cm)	Effective length (cm)
Test polymerisation time	10	n/a
CE separations	48.5	40.5
CEC column separations	41	32.5

5.2.2.2 Electrochromatographic conditions

The buffers used in the analysis were pH adjusted as required with dilute NaOH. All buffers used were prepared daily. Two main buffers were used in this body of work. Buffer 1 consisted of 5 m*M* sodium tetraborate decahydrate and sodium phosphate monobasic, 2.5 m*M* in 40% ACN at pH. Buffer 2 consisted of 5 m*M* Sodium phosphate monobasic, 2.5 m*M* and 40 m*M* SDS at pH 9. All samples were made to 1% v/v in ACN. Both buffer and samples were degassed and filtered into sample vial prior to analysis. The analysis was carried out using an Agilent 7100 CE at 214 nm for the detection of alkylbenzenes.

5.3 Results and discussion

5.3.1 Establishing separation of alkylbenzenes using standard CE methods

The OTCEC polyHIPE columns fabricated in this chapter have been fabricated within the confines of silanised fused silica capillary; it was first imperative to establish that any pendent vinyl groups did not give false results for the alkylbenzene separations. Therefore, a separation of ethylbenzene and pentylbenzene was carried out using only silanised fused silica capillary tubing as shown in Figure 5.1.

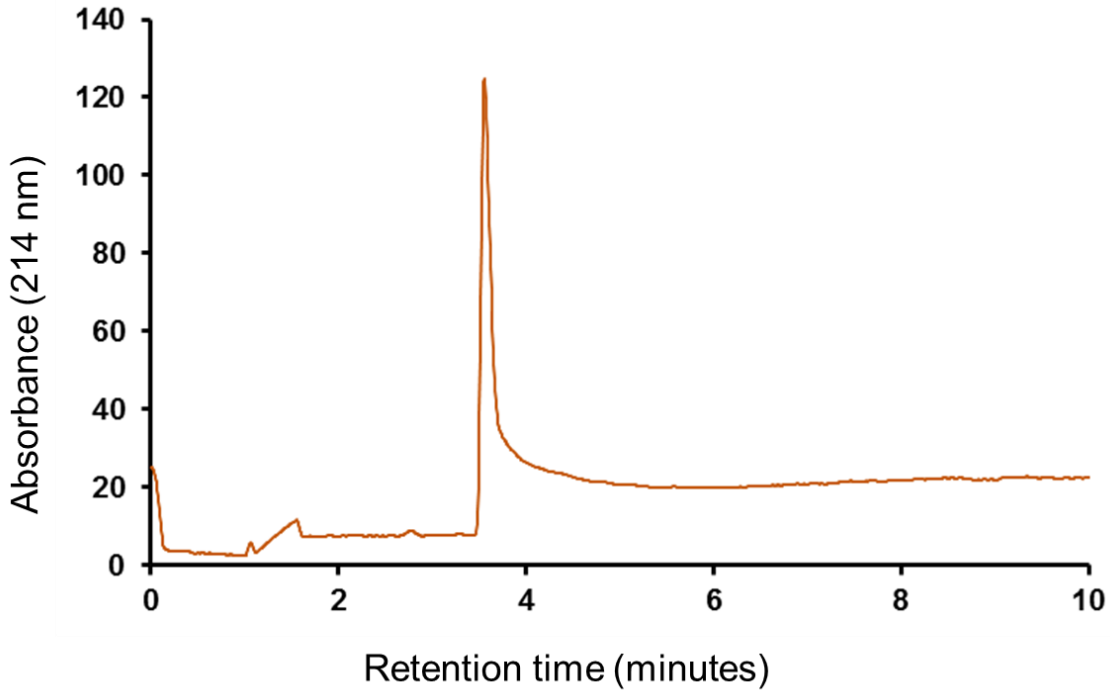

Figure 5.1: *Mixed standard 1 % v/v of ethylbenzene and pentylbenzene. Buffer conditions: 5 mM sodium tetraborate decahydrate and sodium phosphate monobasic, 2.5 mM at pH 9. Injection conditions: Electrokinetic injection at 5 kV for 3 s. The length of the capillary used was 48.5 cm of 100 µm I.D. The capillary used for this separation was silanised.*

When compared to the alkylbenzene separation on bare fused silica that was not silanised in Figure 5.2, the analytes using the silanised capillary had a lower electrophoretic mobility in comparison to bare fused silica capillary and eluted roughly 1 min later. However, the co-elution of the analytes indicated that the silanising agent used in the wall modification did not affect the separation. More importantly, Figure 5.2 demonstrates the separation of alkylbenzenes using a 40:60 ACN: phosphate buffer on bare fused silica capillary.

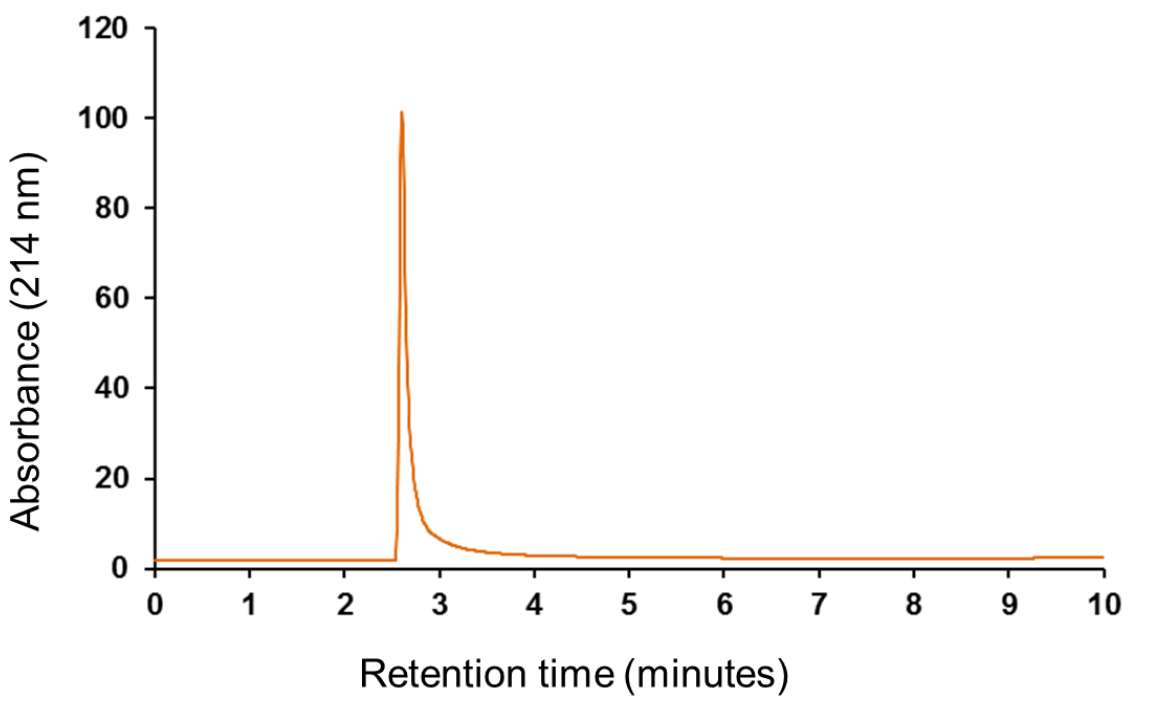

Figure 5.2: *Mixed standard 1 % v/v of alkylbenzene mixture of toluene, ethylbenzene and propylbenzene. Buffer condition: 5 mM sodium tetraborate decahydrate and sodium phosphate monobasic, 2.5 mM at pH 9 (60:40 buffer:ACN ratio). Injection conditions: Electrokinetic injection 5kV for 3s. The length of the capillary used was 48.5 cm of 100 µm I.D..*

As all analytes present were neutral, this capillary zone electrophoresis separation was not suitable for neutral analytes, therefore as expected, all of the

analytes co-eluted at 2.6 min. It was hypothesised that incorporation of a micellar agent should separate the alkylbenzenes due to the difference in interaction the analytes with the micelles present in the buffer. SDS (Critical micelle concentration of 8.2 m*M*) of a concentration of 40 m*M* was added to the buffer mixture of sodium and tetraborate buffer to establish a separation of the alkylbenzenes using bare fused silica capillary. The selectivity of the analytes was enhanced by using the micelles present to act as a dynamic pseudo-stationary phase where each analyte interacted with the micelles within the buffer solution. In this way, a hybrid coating was obtained. This addition of SDS resulted in the separation of toluene ethylbenzene and propylbenzene, as demonstrated in Figure 5.3 below.

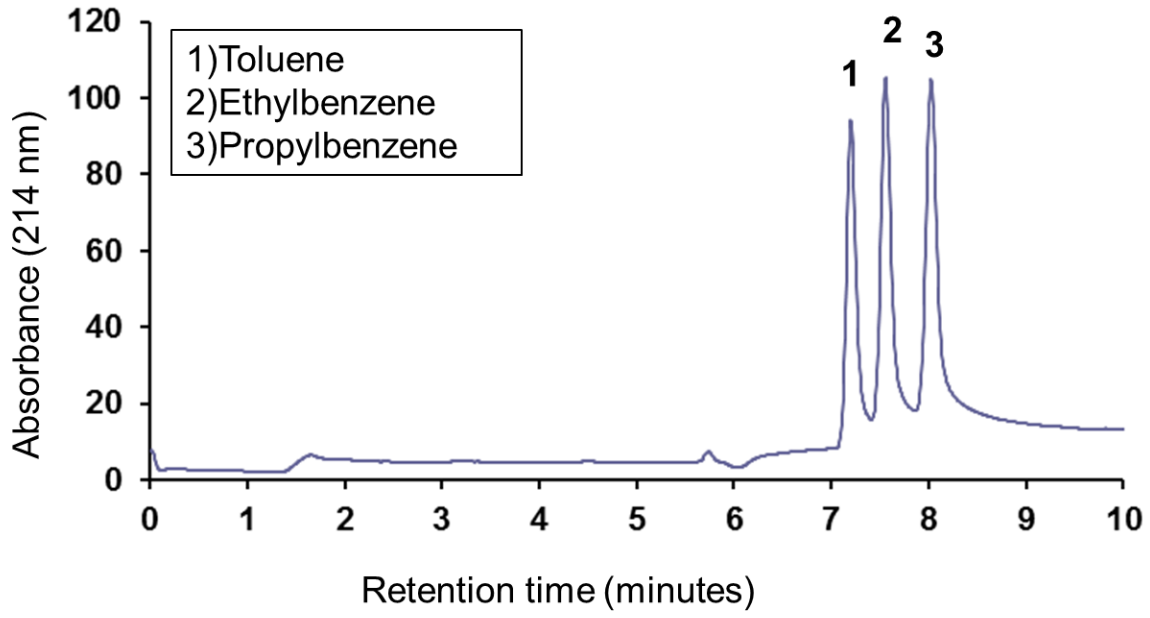

Figure 5.3: *Mixed standard 1 % v/v of alkylbenzene mixture of toluene, ethylbenzene and propylbenzene. Buffer conditions: 5 mM Sodium phosphate monobasic, 2.5 mM and 40 mM SDS at pH 9. Injection conditions: Electrokinetic injection at 5 kV for 3 s. The length of capillary used was 48.5 cm of 100 µm I.D.*

PolyHIPE emulsions were used to coat the walls of the fused silica capillary columns as a different strategy to improve the selectivity of the nuetral analytes in place of using buffer additives such as SDS. The fabrication strategies of these columns were explored in the section below.

5.3.2 Strategy 1: One shot fabrication of static PS-*co*-DVB polyHIPE OTCEC columns

The optimisation of polymerisation time to fabricate a single layer of polyHIPE on the surface of the capillary housing was determined by polymerising short columns (10 cm) at different times. SEM results in Figure 5.4 below show that as expected; when the time for the polymerisation was increased, a thicker layer of polyHIPE material was present on the surface of the capillary. A uniform polyHIPE layer was difficult to fabricate as demonstrated in the figure below, nonetheless the 2h coating was found to be the optimum polymerisation time, resulting in a more uniform coating. However, when this fabrication time was utilised for longer columns, high backpressure measurements up to 60 bar resulted. It was hypothesised that this high backpressure could be due to a blockage at some points within the capillary in areas that had polymerised fully. Additionally, as evidenced in Figure 5.4 (b) the coating did not appear to be uniform. Due to problems resulting from blockages and non-uniformity along the column, the single polymerisation strategy was deemed insufficient, and it was not pursued any further to form OTCEC polyHIPE columns.

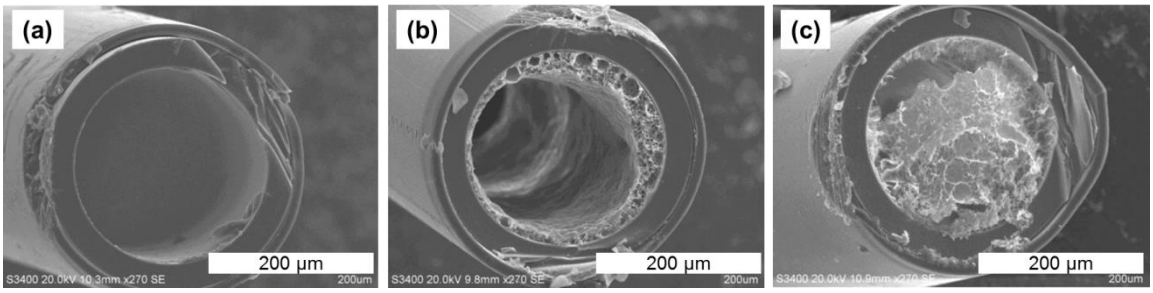

Figure 5.4: *Polymerisation of emulsion coated capillary where columns were polymerised for (a) 1 h (b) 2 h and (c) 4 h. Scale bars at 200 µm and magnification of 270x for all images.*

5.3.3 Multiple layer fabrication of static PS-*co*-DVB polyHIPE OTCEC columns

In effort to fabricate amore even OTCEC coating, multiple sequential thin films of polyHIPE were coated on the inner capillary walls. The greater the number of coatings, the higher the likelihood that a blockage would occur, rendering the OTCEC unusable. However, the greater the number of coatings the greater the separation capacity of the OTCEC. The optimal number of coating was therefore chosen as the minimum number required to obtain baseline resolution of the alkylbenzene analytes.

5.3.4 Chromatographic separation of alkylbenzenes on single layer fabricated static PS-*co*-DVB polyHIPE OTCEC columns

Upon application of one layer of coated PS-*co*-DVB column to the separation of ethylbenzene and pentylbenzene, the analytes were observed to co-elute as shown in Figure 5.5 below. This result was most likely because the polyHIPE layer on the capillary walls was not thick enough to provide a selective enough separation.

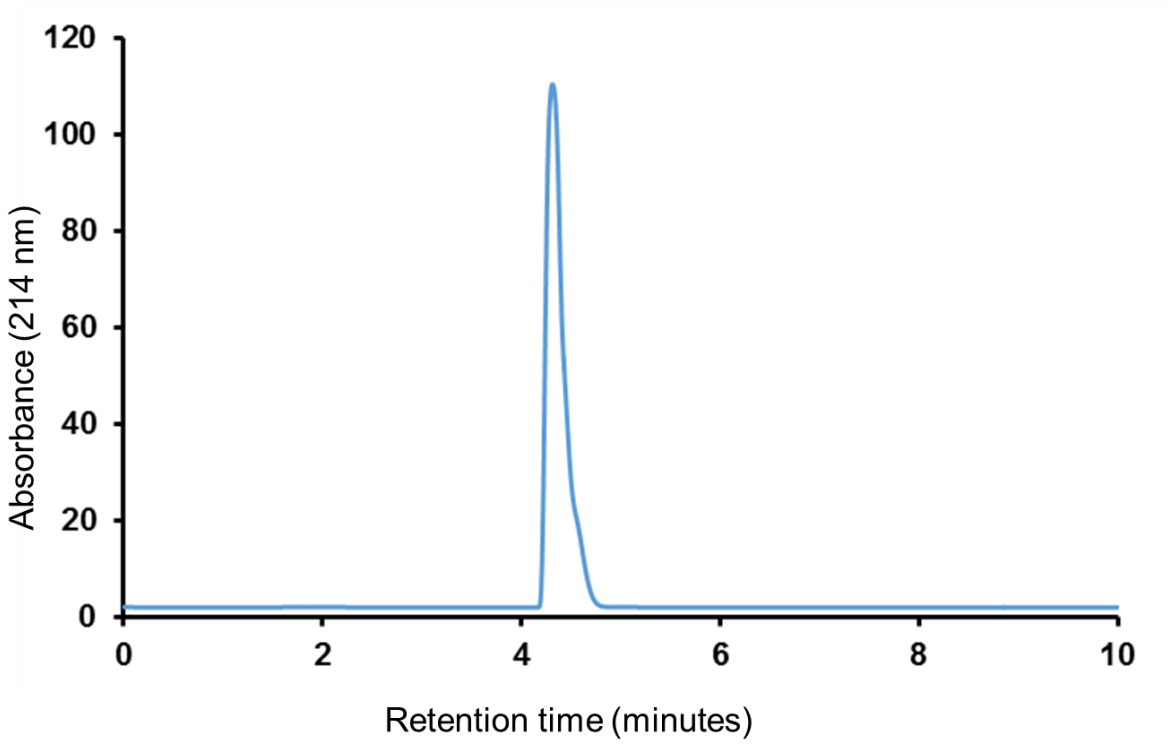

Figure 5.5: *Mixed standard 1 % v/v of ethylbenzene and pentylbenzene. Buffer conditions: 5 mM sodium tetraborate decahydrate and sodium phosphate monobasic, 2.5 mM at pH 9 (60:40 buffer:ACN ratio).. Injection conditions: Electrokinetic injection at 5 kV for 3 s. The length of the capillary 41 cm of 100 µm I.D.. The column was coated with one layer of polyHIPE emulsion.*

5.3.4.1 Chromatographic separation of alkylbenzenes on double layer fabricated static PS-co-DVB polyHIPE OTCEC columns

A second PS-*co*-DVB layer was fabricated by coating a single coated capillary for 2 h before removing the excess emulsion with MeOH. The resulting separation here illustrated the increased polyHIPE coating shown in Figure 5.6 below. The second layer had an increased interaction with the analytes in as the two analytes were starting to co-elute to a lesser extent, thus increasing the selectivity of the resulting separation. This layering method was hypothesised to help develop an evenly distributed coating on the wall of the capillary, therefore eliminating gaps that

may have been present with only single coating of the capillary walls. However, since the two analytes still co-eluted, it was neccessary to carry out this separation using an additional coated layer of polyHIPE emulsion.

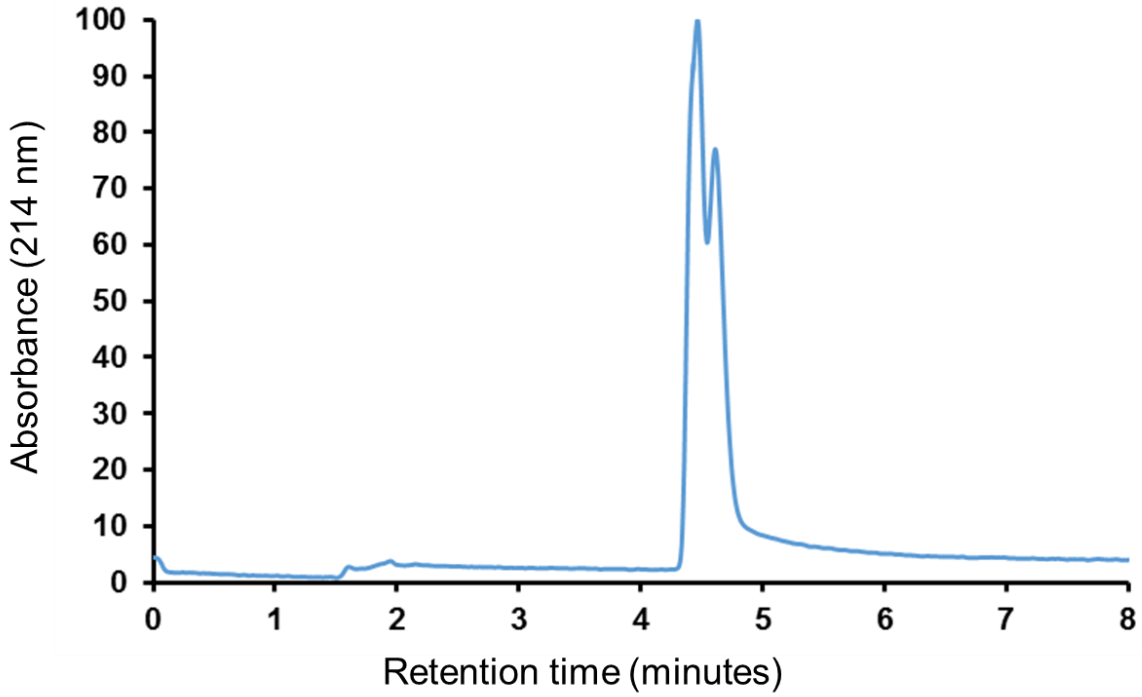

Figure 5.6: *Mixed standard 1 % v/v of ethylbenzene and pentylbenzene. Buffer conditions: 5 mM sodium tetraborate decahydrate and sodium phosphate monobasic, 2.5 mM at pH 9 (60:40 buffer:ACN ratio). Injection conditions: Electrokinetic injection at 5 kV for 3 s. The length of the capillary 41 cm of 100 µm I.D.. The column was coated with two layers of polyHIPE emulsion.*

5.3.4.2 Chromatographic separation of alkylbenzenes on triple layer fabricated static PS-co-DVB polyHIPE OTCEC columns

When the third coat of the polyHIPE emulsion was applied, the successful separation of the alkylbenzenes ethylbenzene and pentylbenzene was achieved and is shown in Figure 5.7. It was therefore determined that three coats of the emulsion

was the minimum required to give a baseline separation of the two alkylbenzene analytes.

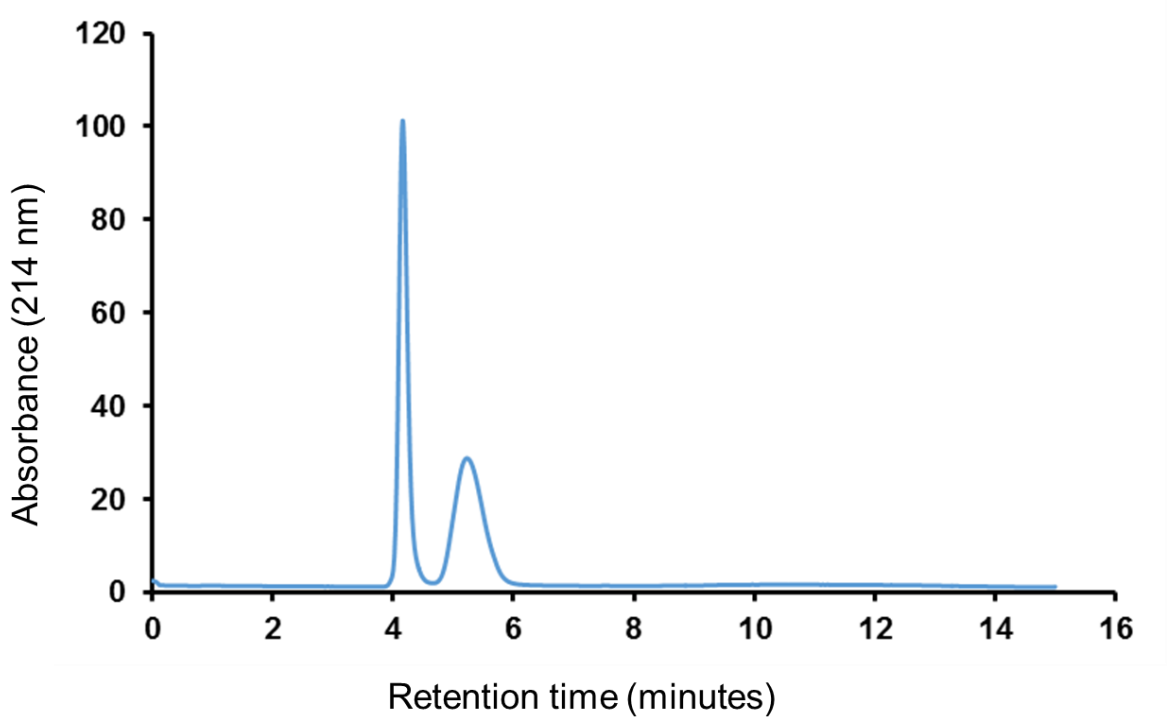

Figure 5.7: *Mixed standard 1 % v/v of ethylbenzene and pentylbenzene. Buffer conditions: 5 mM sodium tetraborate decahydrate and sodium phosphate monobasic, 2.5 mM at pH 9 (60:40 buffer:ACN ratio). Injection conditions: Electrokinetic injection at 5 kV for 3 s. The length of the capillary used was 41 cm of 100 µm I.D.. The column was coated with three layers of polyHIPE emulsion.*

As discussed by Aydogan, incomplete coating on OTCEC inner walls were identifiable by poor separation performance, as characterised by co-eluting alkylbenzenes. On separation of an alkylbenzene mix, OTCEC coatings were deemed as reliable and promising in terms of column preparation [24]. In the work here the first instance of a polyHIPE OTCEC column was developed as shown in Figure 5.8 below.

Nonetheless, an interesting observation was that by using the coating procedure it was possible that there was a formation of fractals which migrate to the edge of the

capillary housing. This was suspected to be the reason why the coating stayed at the edge of the coating upon repeated coatings.

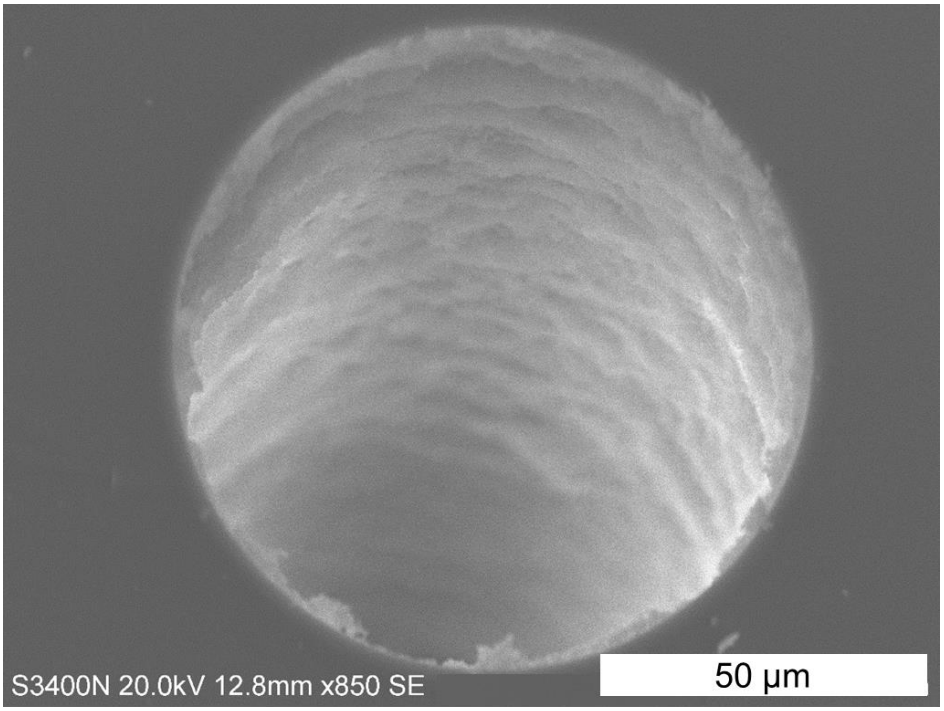

Figure 5.8: *SEM image of an OTCEC PS-co-DVB column after 3 multiple coats of emulsion.*

However, in contrast to the work by Ayodagan, reproducibility was assessed in terms of repeated use of a single column, as opposed to multiple newly fabricated columns. This was because this more closely represents real life applications of such columns. Unfortunately, the trend repeatedly observed was that the separation capacity of the columns rapidly deteriorated as shown in Figure 5.9 below. Within a short number of injections, resolution between the alkylbenzene analytes was lost completely. The rapid loss in resolution was accompanied by a significant increase in analyte diffusion and peak broadening, possibly indicating leeching of the polyHIPE coating out of the capillary.

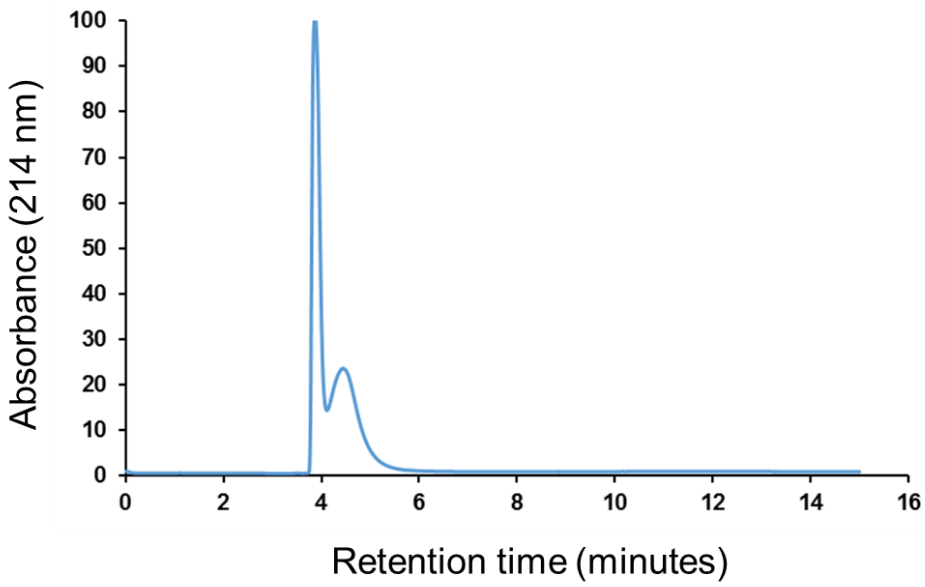

Figure 5.9: *Repeat injection of mixed standard 1 % v/v of ethylbenzene and pentylbenzene showing the deterioration of column efficiency. Buffer conditions: 5 mM sodium tetraborate decahydrate and sodium phosphate monobasic, 2.5 mM at pH 9 (60:40 buffer:ACN ratio). Injection conditions: Electrokinetic injection at 5 kV for 3 s. The length of the capillary used was 41 cm of 100 µm I.D.. The column was coated with three layers of polyHIPE emulsion.*

In this work chapter, static coatings using polyHIPE emulsions have been used in the separation of alkylbenzenes. However, a highly hydrophobic stationary phase for a reverse phase separation mechanism in CEC requires the use of organic modifiers. Organic modifiers such as acetonitrile and methanol are commonly used in RP-HPLC within capillary columns with little issues to degradation to the column packing or capillary. However, within CEC formats this has not been reported to be the case. Use of organic modifiers over longer periods of analysis times have been shown to have dramatic effects on the polyimide coatings on capillaries as shown in Figure 5.10 below [25-27].

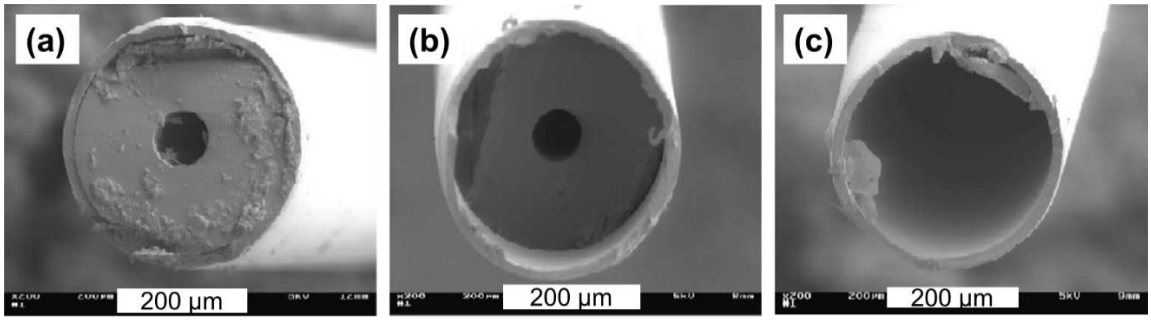

Figure 5.10: *SEM images illustrating the effect of organic modifiers on the ends of raw FS capillaries kept in (a) acetone, (b) methanol and (c) acetonitrile for 4 weeks [25].*

It was hoped that by using bulk fabricated polyHIPE emulsions, this issue would have been overcome. This deterioration of capillary is an increasing and ongoing issue within CEC. This influence of the organic phase modifier has been a critical issue impeding the application of CEC which polyHIPE coatings cannot overcome.

5.3.5 Comparative study on the chromatographic parameters of alkylbenzene separations observed using different polyHIPE formats

In spite of significant technical hurdles, CEC continues to be explored worldwide. While the polyHIPE OTCEC capillary columns developed here do not overcome these hurdles, they do allow the chromatographic potential of polyHIPE stationary phases in multiple formats to be evaluated to determine whether the traditional advantages of CEC columns are also applicable to polyHIPE morphologies. To evaluate the impact that the polyHIPE coated columns in OTCEC formats with respect to the previous chapters of this study, their chromatographic parameters were calculated. The chromatographic parameters were compared to detail which areas the materials have shown to excel as well as areas in which there needs to be significant improvements in the future. These parameters have been calculated with respect to

the separation of ethylbenzene and pentylbenzene and are presented in Table 5.2 below.

Table 5.2: *Comparison of separation parameters investigated using polyHIPEs from Chapter 3, 4 and 5 for the separation of ethylbenzene (EB) and pentylbenzene (PenB)*

Parameter	Unmodified column Chapter 3	GONP surface modified column Chapter 4	Increased separation efficiency using polyHIPE coated columns Chapter 5
t_r ***(minutes)***	7.82 (EB) 24.21 (PenB)	6.94 (EB) 18.60 (PenB)	4.16 (EB) 5.23 (PenB)
R_s ***(PenB/EB)***	2.73	4.13	2.80
α	3.09	2.68	1.25
N	132 (EB) 70 (PenB)	465 (EB) 303 (PenB)	1966 (EB) 3460 (PenB)
Run time (minutes)	30	25	10

PolyHIPEs utilised as OTCEC coatings resulted in the lowest alkylbenzene retention formats. Here, the separation was completed in under 6 minutes while the total run time was allowed to be 10 minutes. In contrast to the latter, the RP-HPLC separations on both the unmodified and the GONP modified column the runtime was significantly longer (up to 30 minutes) with subsequently longer retention times (up to 24 minutes). Both the unmodified and coated RP columns attained similar R_s values

with a difference of 0.07 in R_s. The GONP modified polyHIPE was to have the greatest R_s of 4.13.

Nonetheless, column formats had a R_s greater than 1, which meant that the peaks were distinguishable from each other. In terms of selectivity (α), the greatest selectivity was demonstrated by the unmodified column. This is possibly because this material was extremely hydrophobic. The GONP modified column showed an intermediate selectivity while the OTCEC polyHIPE column had the lowest selectivity, most likely due to the low coating of the material on the surface of the capillary. An improved efficiency was shown using the unmodified polyHIPE column upon addition of GONP. The OTCEC, despite resulting in a lower selectivity, had the greatest efficiency, presumably as a direct result of the plug profile associated with CE techniques. While the N values were significantly lower than reported by other groups using OTCEC columns [10-12, 22], the increase in N compared to the RP-HPLC columns fabricated demonstrates that technical hurdles in relation to high organic modifier content in mobile phase can be overcome. This could be achieved by developing separations not requiring these high organic phase contents, or increase robustness of capillaries on exposure to these organic modifiers. Even for polyHIPE morphologies, the OTCEC format retains the traditional advantages in terms of increased separation efficiency. The potential of OTCEC polyHIPE coated columns is realised as an improvement to polyHIPE technology. From this chapter it is evident that OTCEC polyHIPE coated columns could have large potential if the blockage issues can be overcome and a homogenous coating of the polyHIPE layer is attained.

5.4 Conclusion

The PS-*co*-DVB polyHIPE emulsion coatings were initially investigated at various polymerisation times. However, it was later established that shorter polymerisation times and multiple coats were required to increase the coverage of the polyHIPE layer on the walls of the capillary. The hourly increase in polyHIPE polymerisation depth was investigated utilising the separation of alkylbenzenes ethylbenzene and pentylbenzene. It was shown that upon increase of the polyHIPE emulsion layer, baseline separation of the two analytes was achieved. Despite the separation of only two analytes when compared to the separation, the polyHIPE coated columns showed potential in forming an interaction site along the walls of the capillary resulting in the modest separation observed within this chapter. Nonetheless, problems of decreasing separation capacity and possible blockages arose when repeated injections were attempted to reproduce this separation.

The columns ultimately were unable to be applied in fast single injection separations due to the inability to consistently separate the analytes ethylbenzene and pentylbenzene. The polyHIPE coated columns for OTCEC were ultimately not deemed suitable for the intended purpose and aims of this chapter. However, upon the comparison of the OTCEC columns chromatographic parameters from previous chapters, the coated columns presented similar R_s to an unmodified column with a low overall runtime of only 10 minutes. However, the most significant improvement demonstrated by these materials was their increase in N. Although N was lower than most OTCEC columns, the coated columns here excelled in N when compared to the polyHIPEs in Chapter 3 and 4.

Given the results obtained in this chapter, it was shown that OTCEC polyHIPE columns did have potential in increasing the efficiency of CEC separation. However, an important limitation lies in the applicability of the columns to the separation of more analytes, and the reproducibility of injections per column. It was shown that the window of separation between the analytes ethylbenzene and pentylbenzene were still very close to achieve baseline resolved separations of alkylbenzenes using the coated columns. Furthermore, the major limitation in such separations attributed also to the deterioration of the capillaries upon prolonged contact with organic modifiers, particularly ACN. Thus despite developing the OTCEC polyHIPE coated columns, the issue of the effect of the organic modifier on the column would be a limiting factor that polyHIPEs alone cannot overcome.

5.5 References

[1] F. Svec, T.B. Tennikova, Z. Deyl, Monolithic Materials: Preparation, properties and application, Elsevier, Netherlands, 2003.

[2] J.R. Mazzeo, I.S. Krull, Biotechniques, 10 (1991) 638.

[3] C.A. Lucy, N.E. Baryla, K.K.C. Yeung, Methods in molecular biology (Clifton, N.J.), 276 (2004) 1.

[4] F. Svec, C.G. Huber, Analytical Chemistry, 78 (2006) 2100.

[5] N. Tanaka, H. Kobayashi, N. Ishizuka, H. Minakuchi, K. Nakanishi, K. Hosoya, T. Ikegami, Journal of Chromatography A, 965 (2002) 35.

[6] M. Motokawa, H. Kobayashi, N. Ishizuka, H. Minakuchi, K. Nakanishi, H. Jinnai, K. Hosoya, T. Ikegami, N. Tanaka, Journal of Chromatography A, 961 (2002) 53.

[7] J.F. Borowsky, B.C. Giordano, Q. Lu, A. Terray, G.E. Collins, Analytical Chemistry, 80 (2008) 8287.

[8] C.G. Huber, A. Premstaller, Journal of Chromatography A, 849 (1999) 161.

[9] G. Kleindienst, C.G. Huber, D.T. Gjerde, L. Yengoyan, G.K. Bonn, Electrophoresis, 19 (1998) 262.

[10] M.C. Breadmore, A.S. Palmer, M. Curran, M. Macka, N. Avdalovic, P.R. Haddad, Analytical Chemistry, 74 (2002) 2112.

[11] M.C. Breadmore, M. Macka, N. Avdalovic, P.R. Haddad, Analytical Chemistry, 73 (2001) 820.

[12] M.C. Breadmore, M. Macka, N. Avdalovic, P.R. Haddad, Analyst, 125 (2000) 1235.

[13] L. Yang, E. Guihen, J.D. Holmes, M. Loughran, G.P. O'Sullivan, J.D. Glennon, Analytical Chemistry, 77 (2005) 1840.

[14] L. Yang, E. Guihen, J.D. Glennon, Journal of Separation Science, 28 (2005) 757.

[15] T. Li, Y. Xu, Y.-Q. Feng, Journal of Liquid Chromatography & Related Technologies, 32 (2009) 2484.

[16] J. Horvath, V. Dolnik, Electrophoresis, 22 (2001) 644.

[17] S. Conradi, C. Vogt, E. Rohde, Journal of Chemical Education, 74 (1997) 1122.

[18] E.D. Vega, K. Lomsadze, L. Chankvetadze, A. Salgado, G.K.E. Scriba, E. Calvo, J.A. Lopez, A.L. Crego, M.L. Marina, B. Chankvetadze, Electrophoresis, 32 (2011) 2640.

[19] H. Soini, M.L. Riekkola, M.V. Novotny, Journal of Chromatography, 608 (1992) 265.

[20] B. Koppenhoefer, U. Epperlein, B. Christian, Y.B. Ji, Y.Y. Chen, B.C. Lin, Journal of Chromatography A, 717 (1995) 181.

[21] A. Dhulst, N. Verbeke, Chirality, 6 (1994) 225.

[22] S.A. Zaidi, W.J. Cheong, Journal of Chromatography A, 1216 (2009) 2947.

[23] Z.-H. Wei, X. Wu, B. Zhang, R. Li, Y.-P. Huang, Z.-S. Liu, Journal of Chromatography A, 1218 (2011) 6498.

[24] C. Aydogan, Journal of Chromatography B-Analytical Technologies in the Biomedical and Life Sciences, 976 (2015) 27.

[25] F. Baeuml, T. Welsch, Journal of Chromatography A, 961 (2002) 35.

[26] K. Walhagen, K.K. Unger, A.M. Olsson, M.T.W. Hearn, Journal of Chromatography A, 853 (1999) 263.

[27] K. Walhagen, K.K. Unger, M.T.W. Hearn, Journal of Chromatography A, 894 (2000) 35.

Chapter Six

6. Future work and conclusions

6.1 The future of polyHIPEs in chromatography

In this thesis, the applicability of polyHIPE materials as versatile stationary phases in liquid chromatography for the separation of small molecules was investigated using various formulations of polyHIPE emulsions, in search of an ideal morphology, with strategies to increase both surface area and column efficiency was explored. Additional porogens, agglomeration of nanoparticles and incorporation of nanoparticles into the emulsion were studied in an effort to increase the surface area and to tailor selectivity of the polyHIPEs produced. From this study, it was concluded that polyHIPEs, although having a strong influence and initial potential in separation science, have major flaws in their morphology. The advantages of these materials, as highlighted in Chapter 1, are their large pore structures and high flow rates allowing the analysis of larger analytes such as biomolecules. Although the large pores appear to be advantageous, unfortunately, the void shape enhances diffusion effects. Previous studies have observed this band broadening effect to be emphasised, especially at high flow rates. It was also observed that when the morphological features of the polyHIPEs were removed, these dispersive effects were no longer present. In this chapter, the novel HPLC separation of alkylbenzenes for insight to their chromatographic performance characteristics as well as methods investigated to increase surface area and column efficiency will be concluded and future work in the area of supermacroporous materials in separation science will be explored.

Previous separations using polyHIPEs have predominantly been applied for separations of large biomolecules. Small molecule separations have only been

demonstrated in polyHIPEs fabricated for CEC [1, 2], where hydrodynamic flow properties arising from pressure driven flow are not an issue. In this thesis, a PS-*co*-DVB polyHIPE was successfully prepared, characterised and utilised under isocratic RP-HPLC conditions. While PS-*co*-DVB PolyHIPEs have not been utilised, traditional PS-*co*-DVB monoliths have been utilised in the past for RP-HPLC, predominantly with modification to increase surface area. Here the separation of alkylbenzenes has been demonstrated with a material surface area of only 20 m^2 g^{-1}, emphasising the enhanced surface interactions hypothesised to result from the polyHIPE morphology of voids and windows. The separation enabled the chromatographic performance of the materials to be characterised with respect to retention factor, efficiency, resolution and asymmetry, which has not yet been carried out for polyHIPEs under appropriate chromatographic conditions. This work has significantly contributed to knowledge with the field of polyHIPEs in separation science, as it fundamentally establishes the performance capabilities of polyHIPE materials as stationary phases in LC.

Once the chromatographic performance was established, it was necessary to explore potential avenues to increase surface area with respect to polyHIPEs as stationary phase materials. An increase in surface area was required to analyse samples that are more complex or have a higher number of analytes. To increase column efficiency, polyHIPE housing, addition of GONPs, and as an application within a different mode of chromatography, OTCEC, were explored. By fabricating polyHIPEs in different housing, an expected increase in column efficiency was observed when moving from silcosteel tubing to fused silica capillary tubing as housing. More importantly, upon modification using GONPs an added increase of column efficiency as well as adsorption characteristics demonstrated by the GONPs. Another strategy used to increase the column efficiency was to fabricate OTCEC columns using

polyHIPE emulsions. Here we show the first instance of an OTCEC polyHIPE column where by a multiply coated column observed the greatest column efficiency from the materials fabricated in this study. However, despite the superior efficiency, the column separated only two analytes with less than 1 minute migration time between them. Overall, the major limitation of these columns was injection-to-injection reproducibility. In the majority of cases, a rapid deterioration in separation was observed, which was hypothesised to result from a physical deterioration of the columns on exposure to organic solvents. This effect of organic modifier on polyimide coatings on capillary columns is ever increasing and unfortunately an issue which cannot be overcome with polyHIPE materials alone.

In contrast to increasing separation efficiency using OTCEC, strategies to increase the surface area presented significantly more promising results. While it was noted that the use of additional porogens produced slightly higher surface, the small increase in surface area is lower than that observed in organic polymer monoliths, and thus was not pursued to any great lengths. A more successful modification strategy explored to increase the surface area was the use of nanoparticles. This particular body of work highlighted the potential benefit of incorporating nanoparticles into the polyHIPE emulsion as opposed to merely using it as a stabiliser, as it demonstrated the potential of NPs to influence superior adsorption mechanisms. The use of GONPs incorporated within the emulsion, although resulting in a reduced surface area, showed the potential to alter the physical properties of the polyHIPE materials. The alkylbenzene separation resulted in similar retention times and higher efficiencies than that of the unmodified material, despite the GONP materials being lower in surface area. This was suspected to be due to an enhanced adsorption mechanism, resulting from the addition of GONPs.

In contrast to using nanoparticles within a polyHIPE emulsion to increase surface area, agglomeration of nanoparticles on an aminated GMA polyHIPE was attempted. However, the poor morphology of the GMA polyHIPEs were seen to decrease the permeability of the polyHIPEs, which would ultimately result in poor chromatography. In recent studies, a newly developed GMA polyHIPE has been noted to have a similar morphology to that of PS-*co*-DVB polyHIPEs which could be an ideal alternative to aminate and agglomerate with gold nanoparticles. Therefore, from this thesis it can be concluded that one of the most promising polyHIPE modifications to enable analytical separations is agglomeration with nanoparticles. This is because surface area can be increased without compromising structural rigidity and as modification occurs after polyHIPE fabrication, less emulsion related complexities can occur. A detailed strategy for the development of gold nanoparticle agglomerated polyHIPE is discussed below.

While PS-*co*-DVB polyHIPEs have demonstrated an ideal morphology in this thesis for further modifications, bulk PS-*co*-DVB is known to be difficult to modify without using very harsh conditions such as sulfonation and amination under reflux. In contrast to PS-*co*-DVB polyHIPEs, GMA polyHIPEs are modified easily due to the reactive epoxy ring on the surface of the materials. Until recently, GMA-*co*-EDGMA polyHIPEs were the only polyHIPEs using GMA which were fabricated. These polyHIPEs, unfortunately, had poor morphology with numerous craters evident and a low instance of interconnecting pores. In recent studies, Yang *et al.* fabricated GMA-*co*-DVB polyHIPEs using tripolyglycerol monostearate as a surfactant with a resulting morphology as shown below in Figure 6.1.

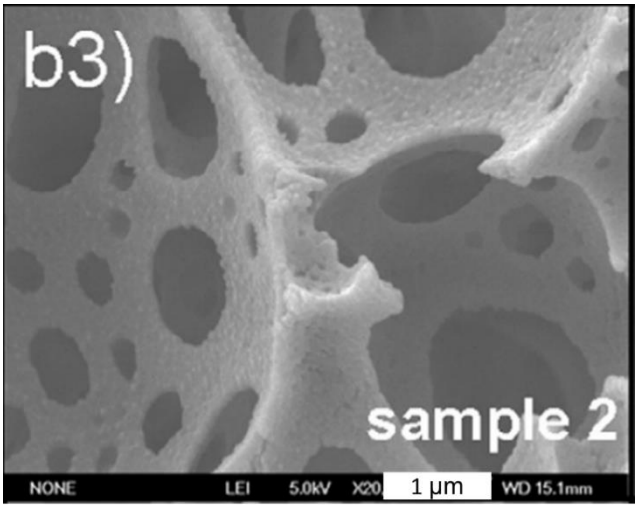

Figure 6.1: *SEM image of GMA-co-DVB polyHIPE. Magnification of 20,000x.*

These promising polyHIPEs could form the basis for their modification. The proposed strategy here would be to aminate the above polyHIPE with 1 *M* DEA solution and then agglomerate with gold nanoparticles in a similar manner to previous reports [3-6]. Once the polyHIPE is agglomerated with gold nanoparticles visual confirmation using FESEM would be required. The gold nanoparticles, as well as increasing surface area, can also be further modified in order to impart an alternative selectivity for separations. The modification of gold nanoparticles with lectins have enabled the separation of glycoproteins due to the lectin-glycoprotein interactions that exist. The analysis of glycoproteins would be an ideal application for these polyHIPEs as glycoproteins are important biomarkers for diseases such as cancer and rheumatoid arthritis [5, 7, 8]. Thus, separations of these analytes are important in monitoring biological pathways. Use of polyHIPEs in carbohydrate analysis would also further advance the field of polyHIPEs in separation science.

From the studies presented in this thesis, although polyHIPEs have not shown the most versatility as stationary phase materials they continue to exhibit extensive potential. This is especially observed in one pot synthesis methods. Their modification

using gold nanoparticles post polymerisation has proven to be the most promising. The suggested future work above tailors the selectivity and the surface area of the polyHIPEs by using modifications carried out in the past but not using polyHIPE materials. However, although the issue of surface area and selectivity are addressed, the general morphology of the polyHIPEs remains the same. This would ultimately result in increased diffusion effects when used in chromatography, which is poor in performance when compared to traditional organic monoliths. Therefore, once the issue of surface area and selectivity are overcome, the material's morphology will most likely remain as its major limitation in terms of enhanced diffusion effects.

6.2 Cryogels as supermacroporous materials in chromatography

6.2.1 Introduction to cryogels

In addition to polyHIPEs, cryogels are another class of supermacroporous polymer monoliths with the potential to be employed as stationary phases. Cryogels have large pore architecture similar in size to polyHIPEs. Most importantly, cryogels lack the concave void structures, which can lead to increased diffusion effects by polyHIPEs. Cryogels are a form of polymerised gels, where a gel is a substance which contains a polymer immobilised within a solvent. The polymers are generally connected by rigid bonds resulting in a 3D-structure. Gel preparation and the nature of the bonds result in homophase or heterophase morphology [9]. The term cryogel is used as cryogels are a supermacroporous gels formed by the process of freezing and defrosting. Thus the name cryogel, originates from the Greek term *kryos*, meaning ice or frost [10].

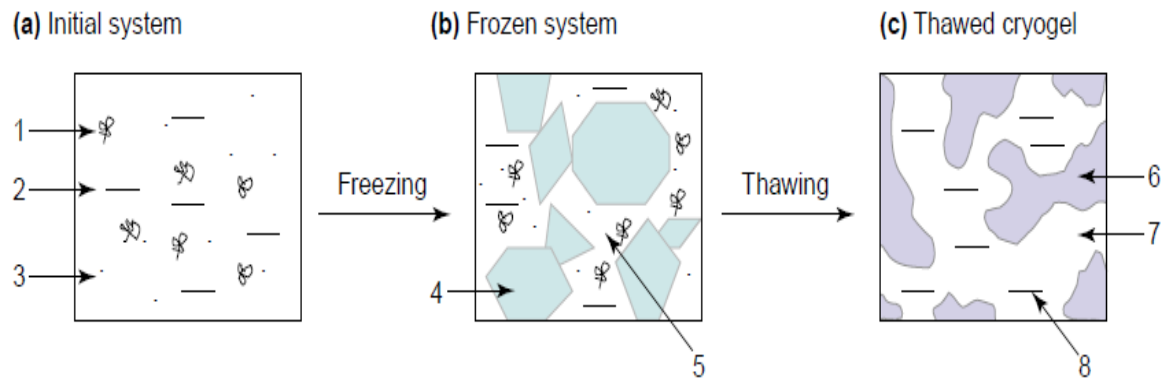

Figure 6.2: *Cryopolymerisation schematic illustrating (a) the initial system containing (1) monomer, (2) solvent (water), (3) low molecular weight solutes such as initiator); (b) the frozen system with (4) ice crystals of solvent (water), (5) unfrozen liquid microphase, and (c) the resulting polymeric gel (6) thawed cryogel framework, (7) macropores and (8) thawing solvent crystals [9].*

The gelation process is initiated by freezing as shown in Figure 6.2 above. In this reaction mixture, the functional monomers (macromolecules) and initiators (low molecular solutes) are components that freeze at a temperature lower than that at which the solvent freezes. This results in an unfrozen liquid microphase that ultimately forms the polymeric gel. In most cases, the solvent is an aqueous based solvent. As Figure 6.2 (b) shows, when the system approaches a suitably low temperature (-8 to -80 °C) the unfrozen liquid microphase polymerises through the interstices of the frozen solvent crystal phase. During freezing, the crystals have grown and joined each other to form interconnected channels. When the solvent crystals are thawed, the polymer morphology is supermacroporous, and the inverse of the frozen solvent system. Micropores can also form on joining polymer chains, therefore cryogels are deemed to be heterophase gels [9].

Cryogels typically have pore sizes ranging from 10-100 m in size [9-13]. Unfortunately another trait these materials share with polyHIPEs, is low surface areas residing within the range of 3-20 m^2/g [14]. The modification of polyHIPEs to increase surface area and tailor selectivity for chromatography can be challenging as demonstrated by the working chapters of this thesis. In particular, modifications undertaken during the emulsion process can cause in phase separation or even extreme change in surface morphology. Cryogels in contrast, have been modified with significant ease throughout the literature. Modifications observed in the previous studies of cryogels have included methods such as grafting reactive groups [12, 15, 16] or metal ligands [17-25] to the final cryogel. More recently, the use of MIPs within cryogels have been observed [25-28]. MIPs are formed by using a polymer template, which an analyte molecule is included in and then is subsequently removed. This leaves behind crevices in the shape of the analyte to which only the analyte can bind [29]. Interestingly MIP cryogels in addition to improving analyte selectivity have also have been reported to increase surface area in some instances [26, 28].

Similarly, to MIPs, another strategy in which cryogels have been modified is by incorporation of nanoparticles within the cryogel [30-32]. However, agglomeration of nanoparticles to the surface of cryogels have not yet been investigated. Therefore, the surface area can be increased in a similar manner to the proposed modification of GMA-*co*-DVB polyHIPEs. Preliminary results of a HEMA-*co*-MBAAm within syringes with 2-(methacryloyloxy) ethyl trimethylammonium chloride (META) groups grafted to its surface are presented below.

6.2.2 Preliminary fabrication and modification of HEMA-*co*-MBAAm cryogels

In Figure 6.3 the cryopolymerisation of HEMA-*co*-MBAAm monoliths at -20 °C is shown via SEM. These images show the cryogel polymerised within a syringe barrel in immersed in water.The cryogel morphology shown in Figure 6.3 (b) which shows no evidence of unpolymerised material on the surface of the cryogel from its smooth surface.

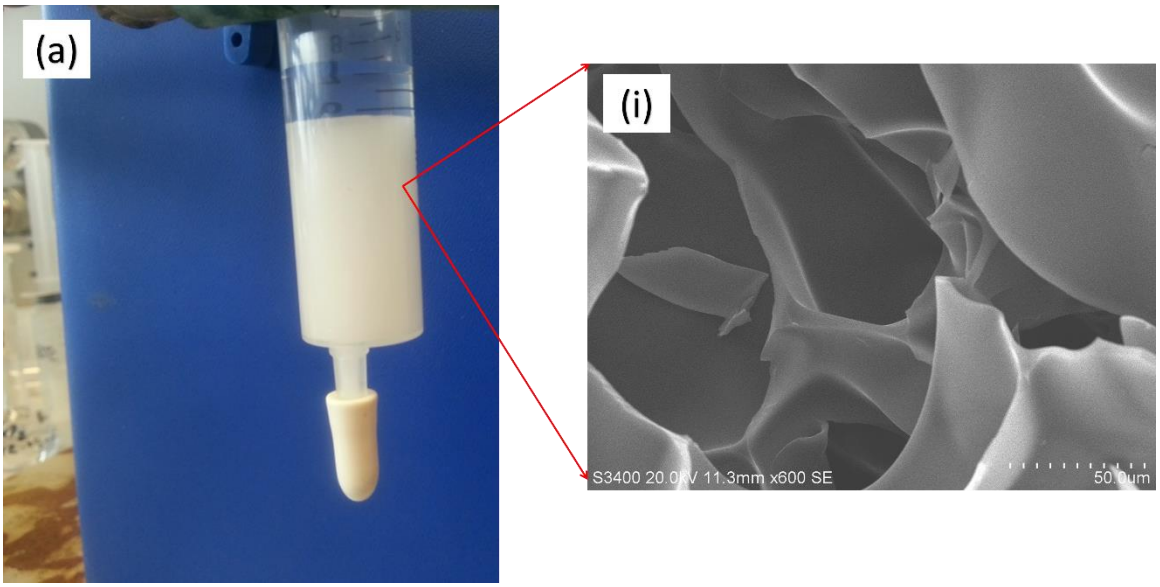

Figure 6.3: *SEM images where (a) Digital photograph of HEMA-co-MBAAm cryogel polymerised at -20 °C within syringe barrel (10 mL total volume) (b) SEM image of HEMA-co-MBAAm cryogel polymerised at -20 °C. Magnification (i) 600x.*

Previous studies achieved good quality cryogel material using elaborate freezing ramps and high freezing temperatures [31, 33, 34]. In the preliminary study here, it was observed that -20 °C for polymerisation was sufficient as the resulting materials had a clean surface and remained swollen against the housing it was formed within.

After fabrication of the cryogel within its housing the cryogel can undergo an addition reaction as shown in Figure 6.4. Here, the addition of [2 (methacryloyloxy) ethyl] - trimethylammonium chloride (META) using cerium nitrate as the initiator. This will render the cryogel with a positive charge allowing the attachment of negatively charged citrate stabilised gold nanoparticles.

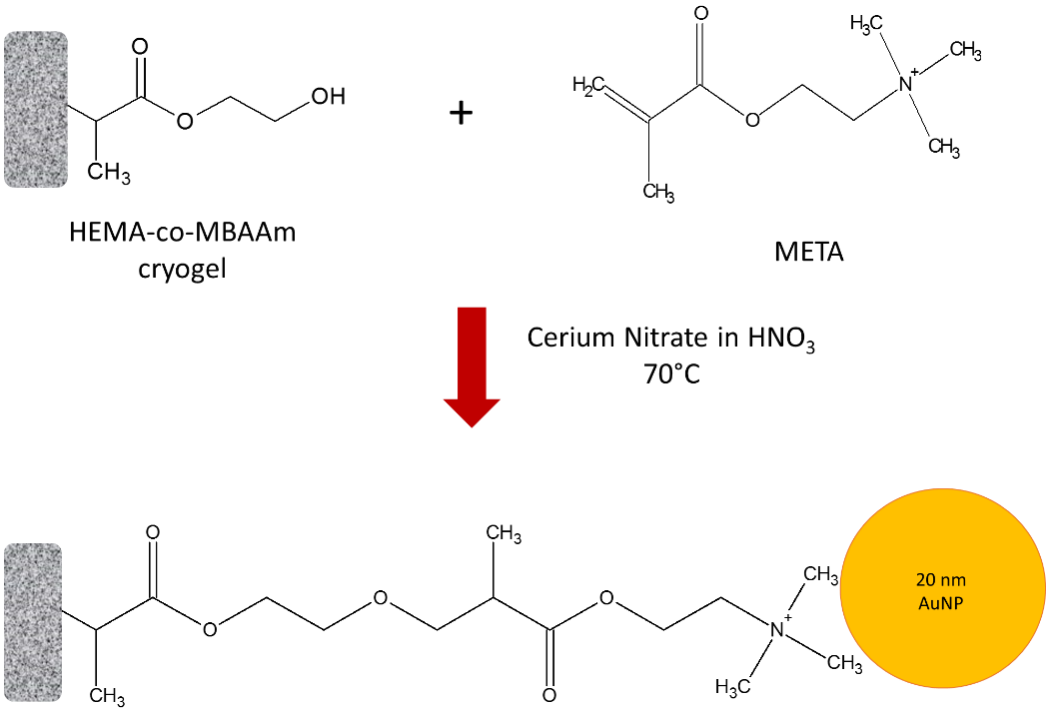

Figure 6.4: *Schematic of the reactive group graft polymerisation procedure used to allow for gold nanoparticle attachment.*

A preliminary modification using gold nanoparticles is shown in Figure 6.5.Here the cryogel was grafted overnight in triplicate In Figure 6.5 (b) (i) and (ii) it can clearly be seen that the gold nanoparticles are attached to the exterior surface of the cryogels. However, upon closer inspection, there was no attachment of gold to the inner region of the cryogel (Figure 6.5 (a) (i)). Imaging via FESEM showed the region where the cryogel was homogenously agglomerated successfully with the gold nanoparticles

illustrated in Figure 6.5 (b) and the area where the grafting solution did not penetrate, Figure 6.5 (a).

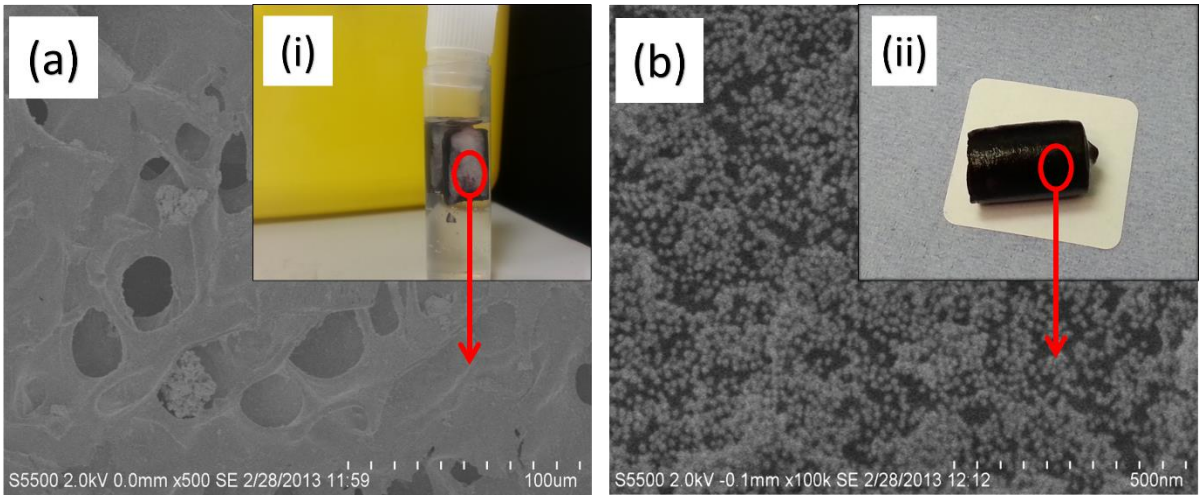

Figure 6.5: *FESEM images (a) unmodified area of HEMA cryogel (b) gold nanoparticle agglomerated area of HEMA cryogel where (i) and (ii) indicate the regions of the cryogel which were imaged.*

Longer graft polymerisation of HEMA for 72 hours produced preliminary results where the first graft attempt gave a cryogel with full gold nanoparticle coverage as shown in Figure 6.6 (a). Nevertheless, when the grafting procedure was repeated the issue of radial homogeneity was observed again Figure 6.6 (b).

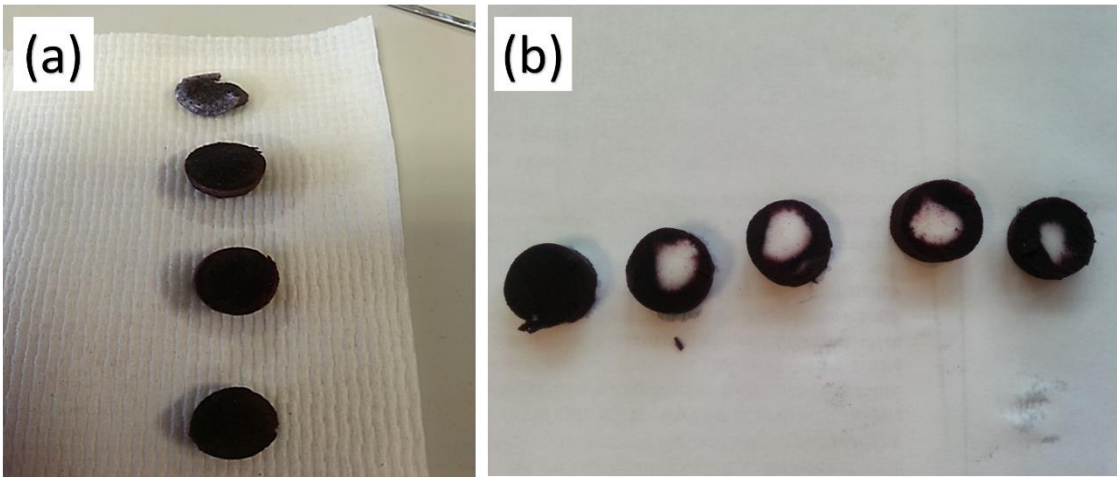

Figure 6.6: *Digital images of 72 h grated HEMA cryogel (a) fully modified using gold nanoparticles (b) replicate of (a) which was unsuccessfully modified.*

It is certain that the META grafting procedure for modification of cryogels using gold nanoparticles requires a significant amount of optimisation. Parameters that could be optimised for this grafting procedure include concentration of grafting agent META, temperature of graft reaction and the effect of the size of the gold nanoparticles upon loading. However, the ease of modification of the materials is demonstrated in the preliminary results. Once the cryogel is modified with gold, the material can be further modified with lectins. The modified cryogels within the syringe barrels could be used in SPE of protein samples. Conversely, the material could be fabricated within fused silica capillaries and then after modification could be used in online separations [33, 34].

6.3 Conclusion

This thesis has advanced the applicability of polyHIPEs in liquid chromatography for analysis of small molecules. RP-HPLC of proteins have been shown to deliver fast protein separations [35-37], however, the underlying issue of low surface area remains. The chromatographic performance of PS-*co*-DVB materials within microbore silcosteel tubing was initially established. Modification of the surface of polyHIPEs by creating gold nanoparticle covered polyHIPEs, and by incorporating graphene oxide nanoparticles during emulsion formulation was then pursued. While surface area did not increase in the addition of GONPs, the increased adsorption mechanism in addition to higher efficiencies was observed. The columns prepared have been utilised with success in HPLC and with less success using OTCEC, however, the chromatographic performance characteristics have been determined readily for all columns. From this study, it is shown that polyHIPEs in their current manner and even after attempted modifications have been shown to give increased diffusion effects. It is likely that their inherent concave void shape causes this. Therefore, where diffusion characteristics are concerned, unless the polyHIPE materials remove their iconic void shape and increase surface area, it is likely that polyHIPEs are inadequate in comparison to other high surface area organic polymer monoliths that can be fabricated. Regardless of having such low surface areas, separations of a small molecule series was possible using these materials. Although large diffusion effects are present upon using these materials as stationary phases, it is likely that their inherent morphology leads to a longer interaction of analytes to the stationary phase at slower flow rates. Despite this large diffusion effect and low efficiencies demonstrated by polyHIPE materials, they have shown immense

capability in terms of superior adsorption when compared to previous polymer monoliths of lower surface area [38-40].

6.4 References

[1] Y. Tunc, C. Golgelioglu, A. Tuncel, K. Ulubayram, Separation Science and Technology, 47 (2012) 2444.

[2] Y. Tunc, C. Golgelioglu, N. Hasirci, K. Ulubayram, A. Tuncel, Journal of Chromatography A, 1217 (2010) 1654.

[3] P. Floris, B. Twamley, P.N. Nesterenko, B. Paull, D. Connolly, Microchimica Acta, 181 (2014) 249.

[4] E.P. Nesterenko, P.N. Nesterenko, D. Connolly, X. He, P. Floris, E. Duffy, B. Paull, Analyst, 138 (2013) 4229.

[5] H. Alwael, D. Connolly, P. Clarke, R. Thompson, B. Twamley, B. O'Connor, B. Paull, Analyst, 136 (2011) 2619.

[6] D. Connolly, B. Twamley, B. Paull, Chemical Communications, 46 (2010) 2109.

[7] K. Schumacher, B. Schneider, G. Reich, T. Stiefel, G. Stoll, P.R. Bock, J. Hanisch, J. Beuth, Anticancer Research, 23 (2003) 5081.

[8] E. Gorelik, U. Galili, A. Raz, Cancer and Metastasis Reviews, 20 (2001) 245.

[9] V.I. Lozinsky, I.Y. Galaev, F.M. Plieva, I.N. Savinal, H. Jungvid, B. Mattiasson, Trends in Biotechnology, 21 (2003) 445.

[10] V.I. Lozinsky, Uspekhi Khimii, 71 (2002) 559.

[11] Z.Y. Chen, L. Xu, Y. Liang, J.B. Wang, M.P. Zhao, Y.Z. Li, Journal of Chromatography A, 1182 (2008) 128.

[12] K.J. Yao, J.X. Yun, S.C. Shen, F. Chen, Journal of Chromatography A, 1157 (2007) 246.

[13] K.J. Yao, S.C. Shen, J.X. Yun, L.H. Wang, X.J. He, X.M. Yu, Chemical Engineering Science, 61 (2006) 6701.

[14] F. Svec, Journal of Chromatography A, 1217 (2010) 902.

[15] J.X. Yun, S.C. Shen, F. Chen, K.J. Yao, Journal of Chromatography B-Analytical Technologies in the Biomedical and Life Sciences, 860 (2007) 57.

[16] C. Yan, S.C. Shen, J.X. Yun, L.H. Wang, K.J. Yao, S.J. Yao, Journal of Separation Science, 31 (2008) 3879.

[17] A. Kumar, V. Bansal, K.S. Nandakumar, I.Y. Galaev, P.K.R. Roychoudhury, R. Holmdahl, B. Mattiasson, Biotechnology and Bioengineering, 93 (2006) 636.

[18] A. Derazshamshir, B. Ergun, G. Pesint, M. Odabasi, Journal of Applied Polymer Science, 109 (2008) 2905.

[19] B. Ergün, G. Baydemir, M. Andaç, H. Yavuz, A. Denizli, Journal of Applied Polymer Science, 125 (2012) 254.

[20] N.S. Bibi, N.K. Singh, R.N. Dsouza, M. Aasim, M. Fernández-Lahore, Journal of Chromatography A, 1272 (2013) 145.

[21] B.M.A. Carvalho, L.H.M. Da Silva, L.M. Carvalho, A.M. Soares, L.A. Minim, S.L. Da Silva, Journal of Chromatography A, 1312 (2013) 1.

[22] Ş. Ceylan, M. Odabaşı, Artificial Cells, Nanomedicine, and Biotechnology, 41 (2013) 376.

[23] N. Ünlü, Ş. Ceylan, M. Erzengin, M. Odabaşı, Journal of Separation Science, 34 (2011) 2173.

[24] Ş.C. Cömert, M. Odabaşı, Materials Science and Engineering: C, 34 (2014) 1.

[25] C. Aydogan, M. Andac, E. Bayram, R. Say, A. Denizli, Biotechnology Progress, 28 (2012) 459.

[26] S. Jobling, M. Nolan, C.R. Tyler, G. Brighty, J.P. Sumpter, Environmental Science & Technology, 32 (1998) 2498.

[27] S. Asliyuce, L. Uzun, A.Y. Rad, S. Unal, R. Say, A. Denizli, Journal of Chromatography B-Analytical Technologies in the Biomedical and Life Sciences, 889 (2012) 95.

[28] M. Le Noir, F. Plieva, T. Hey, B. Guieysse, B. Mattiasson, Journal of Chromatography A, 1154 (2007) 158.

[29] K. Haupt, K. Mosbach, Chemical Reviews, 100 (2000) 2495.

[30] M. Erzengin, N. Ünlü, M. Odabasi, Journal of Chromatography A, 1218 (2011) 484.

[31] K.J. Yao, J.X. Yun, S.C. Shen, L.H. Wang, X.J. He, X.M. Yu, Journal of Chromatography A, 1109 (2006) 103.

[32] J.M. Billakanti, C.J. Fee, Biotechnology and Bioengineering, 103 (2009) 1155.

[33] R.D. Arrua, P.R. Haddad, E.F. Hilder, Journal of Chromatography A, 1311 (2013) 121.

[34] R. Dario Arrua, A. Nordborg, P.R. Haddad, E.F. Hilder, Journal of Chromatography A, 1273 (2013) 26.

[35] C.H. Yao, L. Qi, G.L. Yang, F.Y. Wang, Journal of Separation Science, 33 (2010) 475.

[36] C.H. Yao, L. Qi, H.Y. Jia, P.Y. Xin, G.L. Yang, Y. Chen, Journal of Materials Chemistry, 19 (2009) 767.

[37] P. Krajnc, N. Leber, D. Stefanec, S. Kontrec, A. Podgornik, Journal of Chromatography A, 1065 (2005) 69.

[38] Q.C. Wang, F. Švec, J.M.J. Fréchet, Journal of Chromatography A, 669 (1994) 230.

[39] J. Urban, F. Svec, J.M.J. Frechet, Analytical Chemistry, 82 (2010) 1621.

[40] J. Urban, F. Svec, J.M.J. Frechet, Journal of Chromatography A, 1217 (2010) 8212.